THE UNIVERSITY OF QUEENSLAND

AUSTRALIA

Natural Killer Cells in Hodgkin Lymphoma

Karolina Bednarska

BSc, MSc

A thesis submitted for the degree of Doctor of Philosophy at

The University of Queensland in 2019

Faculty of Medicine

Abstract

Programmed cell death protein 1 (PD-1) blockade has proven clinical utility in relapsed/refractory Hodgkin Lymphoma (HL). Interestingly, a recent study in HL from my laboratory demonstrated that PD-1, aside from T cells, is also expressed on NK cells. In addition, the "missing-self" hypothesis dictates that NK cells have capacity to lyse target cells with lost expression of Major Histocompatibility Complex molecule I (MHC-I). Hence, the frequent absence of MHC-I on Hodgkin-Reed-Sternberg (HRS)-cells, the malignant cells in HL, suggests that manipulation of host NK cells might be a viable strategy to enhance PD-1 blockade therapy outcomes.

The Inositol-requiring enzyme-1-X-box binding protein 1 (IRE1-XBP1) pathway has been demonstrated to play an important role in a range of immune cells, and notably its role varies across tested settings. For instance, in macrophages it is required for the optimal secretion of TNFα, whereas in B cells and eosinophils it is a key factor involved in cell differentiation. The role of this pathway in Natural Killer (NK) cells and in NK cells from patients with HL has not yet been explored.

Here, I outline new data identifying a hitherto unrecognized mechanism that is pivotal to how NK cell function, including the relatively poorly understood processes of NK cell migration, and NK cells Immune Synapse (NKIS) formation.

Firstly, I demonstrate that splicing of the unfolded protein response (UPR)-related transcription factor *XBP1* to its active form XBP1s is induced during NK cell-mediated direct cytotoxicity against various blood cancer cell lines. Notably, the induction of the IRE1-XBP1 pathway was not associated with up-regulation of known XBP1s target molecules implicated in ER stress alleviation, indicating the *XBP1* splicing in NK cells occurs independently from the canonical UPR system.

Then, utilising a small molecule inhibitor, 4-methyl umbelliferone 8-carbaldehyde (4μ8c), I interrogated the role of the IRE1-XBP1 pathway in NK cell function. Inhibition of the IRE1-mediated splicing led to significant decrease in XBP1s expression, which was associated with impaired migration, NKIS formation and secretion of IFNγ and TNFα. These findings further demonstrate the importance of the IRE1-XBP1 pathway in NK cell function.

Next, I show that in pre-therapy HL patient blood samples, there is a ~2-fold reduction in XBP1s in response to activation by a HL line, compared to blood from healthy donors.

Notably, this observation was restricted to the $CD56^{bright}CD16^{-}$ subset of cells that my laboratory has previously shown to be expanded and to display high expression of PD-1 in patients with HL. The cells with suppressed XBP1s activation displayed impaired NKIS formation, degranulation, and secretion of IFNγ and TNFα. Not only did addition of PD-1 blockade enhance IFNγ secretion and NKIS formation to a PD-L1/PD-L2 gene amplified HRS-line, but critically the beneficial impact of PD-1 blockade on IFNγ and NKIS formation was partially reversed by inhibition of the XBP1s-pathway. Manipulation of the IRE1-XBP1 pathway to enhance anti-tumour responses should be further explored as a novel lymphoma treatment strategy to enhance host NK cell immunity.

Declaration by author

This thesis is composed of my original work, and contains no material previously published or written by another person except where due reference has been made in the text. I have clearly stated the contribution by others to jointly-authored works that I have included in my thesis.

I have clearly stated the contribution of others to my thesis as a whole, including statistical assistance, survey design, data analysis, significant technical procedures, professional editorial advice, financial support and any other original research work used or reported in my thesis. The content of my thesis is the result of work I have carried out since the commencement of my higher degree by research candidature and does not include a substantial part of work that has been submitted to qualify for the award of any other degree or diploma in any university or other tertiary institution. I have clearly stated which parts of my thesis, if any, have been submitted to qualify for another award.

I acknowledge that an electronic copy of my thesis must be lodged with the University Library and, subject to the policy and procedures of The University of Queensland, the thesis be made available for research and study in accordance with the Copyright Act 1968 unless a period of embargo has been approved by the Dean of the Graduate School.

I acknowledge that copyright of all material contained in my thesis resides with the copyright holder(s) of that material. Where appropriate I have obtained copyright permission from the copyright holder to reproduce material in this thesis and have sought permission from co-authors for any jointly authored works included in the thesis.

Publications included in this thesis

No publications included

Submitted manuscripts included in this thesis

No manuscripts submitted for publication

Other publications during candidature

Conference abstracts:

Bednarska K, Gunawardana J, Vari F, Cui Q, Thillaiyampalam G, Stehbens S, Mujaj SA, Nourse JP, Cristino AS, Gandhi MK, *The IRE1-XBP1s Pathway Impairment Underpins NK Cell Dysfunction in Hodgkin Lymphoma, That Is Partly Restored By PD-1 Blockade.* **Poster presentation at American Society of Hematology Conference**; Orlando, USA (2019)

Bednarska K, Vari F, Stehbens S, Cui Q, Gunawardana J, Thillaiyampalam G, Mujaj SA, Nourse JP, Cristino AS, Gandhi MK, *Impaired NK cell function and immune synapse formation in Hodgkin Lymphoma.* **Oral presentation at Australasian Society of Medical Research Postgraduate Student Conference**; Brisbane, QLD (2019)

Bednarska K, Vari F, Stehbens S, Cui Q, Gunawardana J, Thillaiyampalam G, Mujaj SA, Nourse JP, Cristino AS, Gandhi MK, *Impaired NK cell function and immune synapse formation in Hodgkin Lymphoma.* **Oral presentation at 47th Annual Scientific Meeting of Australian Society of Immunology Annual Meeting**; Perth, WA (2018)

Bednarska K, Gunawardana J, Stehbens S, Vari F, Cui Q, Thillaiyampalam G, Mujaj SA, Nourse JP, Cristino AS, Gandhi MK, *Impaired NK cell function and immune synapse formation in Hodgkin Lymphoma.* **Poster presentation at EMBL Australia Postgraduate Student Symposium**; Brisbane, QLD (2018)

J. Gunawardana, **K. Bednarska**, S. Law, M. B. Sabdia, S. Birch, J. Tobin, C. Keane and M. K. Gandhi, *The Intratumoral Tumor Microenvironment Of Nodular Lymphocyte Predominant Hodgkin Lymphoma Is A Unique Immunobiological Entity Distinct From Classical Hodgkin Lymphoma.* Poster at American Society of Hematology Conference; San Diego, USA (2018)

J. Lee, J. Tobin, **K. Bednarska**, S. Law, V. Murigneux, M.K. Gandhi and J. Gunawardana, *NLRC5: A novel genetic mechanism that underpins immune evasion in Follicular Lymphoma.* Poster at TRI Poster Symposium; Brisbane, QLD (2018)

Thillaiyampalam G, **Bednarska K**, Cui Q, Vari F, Gandhi MK, Cristino AS, *An integrated systems analysis of miRNA target network associated with Natural Killer cell activation.* Poster at 68th Annual Meeting of the American Society of Human Genetics, San Diego, USA (2018)

Thillaiyampalam G, **Bednarska K**, Cui Q, Vari F, Gandhi MK, Cristino AS, *An integrated systems analysis of miRNA target network associated with Natural Killer cell activation.* Poster at TRI Translational Research symposium, Brisbane, QLD (2018)

Thillaiyampalam G, **Bednarska K**, Cui Q, Vari F, Gandhi MK, Cristino AS, *An integrated systems analysis of miRNA target network associated with Natural Killer cell activation.* Poster at Princess Alexandra Hospital (PAH) Health Symposium, Brisbane, QLD (2018)

Thillaiyampalam G, **Bednarska K**, Cui Q, Vari F, Gandhi MK, Cristino AS, *Developing a systems-based analysis of miRNA target networks.* Oral presentation at EMBL Australia Postgraduate Symposium, Brisbane, QLD (2018)

Contributions by others to the thesis

My supervisors Professor Maher Gandhi, Dr. Alex Cristino, Dr. Frank Vari, and Dr. Qingyan Cui contributed to conception and design of the projects described in this thesis as well as reviewing of the thesis. In addition, Dr. Jay Gunawardana also contributed to the conception of projects. No other significant contributions were made.

Statement of parts of the thesis submitted to qualify for the award of another degree

No works submitted towards another degree have been included in this thesis

Research Involving Human or Animal Subjects

Ethics approval no: HREC/07/QPAH/035

Project Title: “Biomarkers as Tools to Assist Clinical Outcome in Patients with Lymphomas”

Approving committee: Metro South Human Research Ethics Committee

Acknowledgements

First and foremost, I would like to express my gratitude to my principal supervisor Prof. Maher Gandhi, and my co-supervisory team: Dr. Alexandre Cristino, Dr. Frank Vari, and Dr. Qingyan Cui. Maher, thank you for the continuous support of my PhD study, your insightful comments, sharing your immense knowledge and time, and steering me in a good direction whenever I needed it. Frank, I would like to thank you for your advice and guidance on experiments involving NK cells. You were not only my co-supervisor but a friend who was always there with a helping hand and a smile (on a tough day) to ease my way through this journey. Alex, thank you for encouragement, motivation, but also for letting me see science from a different perspective. Qingyan, thank you for your advice, sharing your expertise, and insightful discussions (both scientific and otherwise) over a cup of coffee.

I would like to convey sincere gratitude to my committee panel (Dr. James Wells, Dr. Chris Slape, and Dr. Stephen Mattarollo) for their advice, guidance, and keeping me focused on this project.

My thanks are extended to both current and former lab members of Blood Cancer Research Group for their advice and support. In particular, I would like to thank our Development Fellow Dr. Jay Gunawardana. Jay, you were always there to troubleshoot my experiments and bounce my ideas off you, and you always did it with a friendly smile (maybe not first thing in the morning but still!). You made my time in the lab enjoyable and I could not have asked for a better colleague.

I would also like to express my deepest appreciation to my family for their love, understanding, and continuous support. I am also grateful to my partner, Wojtek, thank you for travelling across the world to be by my side during this (roller-coaster) journey (and I did not mean the flight but my candidature!). I am profoundly grateful to you all, for providing me with unfailing support and continuous encouragement throughout my years of study and through the process of researching and writing this thesis. This accomplishment would not have been possible without them.

I would also like to thank one of my close friends Sandra Brosda, who was working on her thesis in parallel. Despite being a bioinformatician I believe that Sandra has gained a deep knowledge of flow cytometry and NK cell biology through her unwavering support during my long lab hours. Sandra, your constructive, at times very “German”, critique made me a better

scientist who pays attention to the tiniest details. After many failed experiments your encouragement and belief in me kept me from giving up.

My research would have been impossible without the aid and support of my scholarship funded by the University of Queensland International Scholarship and a University of Queensland Diamantina Institute Postgraduate Scholarship. In addition, I would like to acknowledge the Translational Research Institute (TRI), including state-of-the-art facilities i.e. flow cytometry and microscopy, where I carried out my research.

Financial support

This research was supported by a University of Queensland International Scholarship and a University of Queensland Diamantina Institute Postgraduate Scholarship.

Keywords

natural killer cells, x-box binding protein 1, unfolded protein response, direct cytotoxicity, cytokine, innate immunity, hodgkin lymphoma, pd-1 blockade, immune synapse

Australian and New Zealand Standard Research Classifications (ANZSRC)

ANZSRC code: 110707 Innate Immunity, 40%

ANZSRC code: 110709 Tumour Immunology, 30%

ANZSRC code: 111206 Haematological Tumours, 30%

Fields of Research (FoR) Classification

FoR code: 1107, Immunology, 40%

FoR code: 1112, Oncology and Carcinogenesis, 60%

Table of Content

Abstract I

Table of Content XII

List of Figures XVII

List of Tables XX

List of Abbreviations XXI

CHAPTER 1: General Introduction 1

1.1 NK CELL SUBSETS 2

1.2 NATURAL KILLER CELL FUNCTION 3

1.2.1 Direct Cytotoxicity 3

1.2.2 Antibody-Dependent Cell-mediated Cytotoxicity 4

1.2.3 Cytokine Secretion 4

1.3 NATURAL KILLER CELL RECEPTORS 5

1.3.1 Killer Cell Immunoglobulin-like Receptors 6

1.3.2 C-type Lectin Receptors 7

1.3.3 Natural Cytotoxicity Receptors 8

1.3.4 The NK cell immunological synapse 9

1.4 NK CELL BASED THERAPIES IN CANCER 10

1.4.1 Monoclonal antibody therapies 11

1.4.2 Adoptive NK cell transfer 12

1.5 THE UNFOLDED PROTEIN RESPONSE 13

1.5.1 The IRE1-XBP1 pathway 14

1.5.2 A role of IRE1-XBP1 pathway in immunity 15

1.6 HODGKIN LYMPHOMA 16

1.6.1 The Tumour Microenvironment in HL 18

1.6.2 Immune evasion mechanisms in HL 19

1.7 AIMS AND HYPOTHESIS 22
1.7.1 Hypothesis 22
1.7.2 Aims 22
CHAPTER 2: Materials and Methods 23
2.1 ETHICS 24
2.2 STUDY POPULATION 24
2.3 MEDIA AND BUFFERS 24
2.4 CELL CULTURE AND STORAGE 26
2.4.1 Expansion of SNK10 cell line 26
2.4.2 Expansion of KHYG-1 cell line 26
2.4.3 Expansion of NK-92 cell line 26
2.4.1 Expansion of NK-92 cell line 26
2.4.2 Culture of target cell lines 26
2.4.3 Cryopreservation of Cells and Thawing of Cryopreserved cells 27
2.4.4 Thawing of Cryopreserved cells 27
2.5 PERIPHERAL BLOOD MONONUCLEAR CELLS SAMPLES PROCESSING 27
2.6 INHIBITION OF IRE1-XBP1 PATHWAY 28
2.6.1 Inhibition of IRE1-mediated splicing of *XBP1* 28
2.6.2 Induction of the Endoplasmic Reticulum stress 28
2.6.3 CHECKPOINT BLOCKADE 28
2.6.4 PD-1 blockade assay 28
2.7 STIMULATION OF NK CELLS 29
2.7.1 Stimulation with target cells – Direct cytotoxicity 29
2.8 GENE EXPRESSION PROFILING 30
2.8.1 RNA extraction – RNeasy Mini Kit 30
2.8.2 Random Primed First Strand cDNA Synthesis 31
2.8.3 Primers used for PCR analysis 31

2.8.4 Real Time RT-PCR 32
2.9 PRIMARY NK CELL EXPANSION 33
2.9.1 Expansion of NK cells from Peripheral Blood Mononuclear Cells 33
2.9.2 Isolation of Expanded NK Cells 34
2.9.3 FACS-sorting of the primary NK cells 34
2.10 NK CELL ABSOLUTE COUNTS 35
2.11 FLOW CYTOMETRY 36
2.11.1 Table of Antibodies 36
2.11.2 Assessment of cell viability staining 36
2.11.3 NK Cell-Mediated Killing Assay 37
2.11.4 Surface Staining 38
2.11.5 CD107a Staining 38
2.11.6 Intracellular staining 39
2.11.7 Intranuclear staining 39
2.11.8 CFSE staining 40
2.11.9 Cell trace dyes 41
2.12 NK CELL MOTILITY AND IMMUNE SYNAPSE FORMATION 41
2.12.1 Conjugate formation assay 41
2.12.2 Actin accumulation assay 42
2.12.3 NK-cell immune synapse formation analysis 43
2.12.4 NK cell migration 43
2.13 STATISTICAL ANALYSIS 44
CHAPTER 3: XBP1s activation is associated with appropriate function of NK cells 45
3.1 INTRODUCTION 46
3.1.1 NK cell effector function 46
3.1.2 The NK cell immunological synapse 46
3.2 AIMS 48

3.3 RESULTS 49
3.3.1 *XBP1* splicing occurs upon stimulation of NK cells with K562 49
3.3.2 *XBP1* splicing is a common marker of NK cell-mediated cytotoxicity 51
3.3.3 The IRE1-XBP1 pathway is activated during NK cell-mediated cytotoxicity in a non-canonical manner 53
3.3.4 XBP1 splicing is effectively blocked in the presence of IRE1 inhibitor 56
3.3.5 IRE1 inhibitor does not affect cell viability 58
3.3.6 Concomitant with *XBP1* splicing, expression of selected NK cell effector RNA molecules is increased 59
3.3.7 Inhibition of IRE1 impairs cytokine protein secretion 63
3.3.8 Activation of the IRE1-XBP1 pathway is associated with increased expression of cytokine proteins 67
3.3.9 Inhibition of *XBP1* splicing does not affect NK cell-target cell conjugate formation 71
3.3.10 Inhibition of *XBP1* splicing impairs actin polarization at the NK cell immune synapse interface 73
3.3.11 Inhibition of IRE1 impairs NK cell migration 74
3.3.12 Summary of results 76
3.4 DISCUSSION 77
3.4.1 *XBP1* splicing occurs following NK cell activation 77
3.4.2 XBP1s is required for NK cell effector function 78
3.4.3 Conclusion 78
CHAPTER 4: The IRE1-XBP1 pathway is dysregulated in NK cells from Hodgkin lymphoma 80
4.1 INTRODUCTION 81
4.1.1 The IRE1-XBP1 pathway in blood cancers 81
4.1.2 NK cells in Hodgkin lymphoma 82
4.1.3 PD-1 blockade in HL 83

4.2 AIMS 85
4.3 RESULTS 86
4.3.1 The IRE1-XBP1 pathway is not activated in the $CD56^{bright}CD16^{-}$ subset of NK cells from HL patients 86
4.3.2 The absolute NK cell count is reduced in patients with Hodgkin lymphoma 88
4.3.3 XBP1s suppression is associated with impaired NK cell immune synapse formation 89
4.3.4 PD-1 blockade rescues immune synapse formation 90
4.3.5 PD-1 blockade improves NK cell migration 92
4.3.6 Suppression of XBP1s is associated with impaired IFNγ secretion 93
4.3.7 PD-1 blockade partially reverses IFNγ secretion 96
4.3.8 The impact of IRE1 inhibition on TNFα secretion by pNK cells 99
4.3.9 The impact of PD-1 blockade on TNFα secretion by pNK cells 102
4.3.10 Suppression of the IRE1-XBP1 pathway is associated with impaired degranulation 105
4.3.11 PD-1 blockade does not significantly enhance NK cell degranulation 108
4.3.12 Thapsigargin enhances NK cell degranulation and cytotoxicity 110
4.3.13 Summary of results 111
4.4 DISCUSSION 112
4.4.1 The IRE1-XBP1 pathway is impaired in NK cells from HL patients 112
4.4.2 PD-1 blockade enhances NK cell function 113
4.4.3 The interplay between IRE1-XBP1 pathway and PD-1 in HL 114
4.4.4 Conclusion 114
CHAPTER 5: Final Discussion 116
5.1 INTRODUCTION 117
5.2 *XBP1* SPLICING IN NK CELLS 118
5.3 PD-1 BLOCKADE EFFECT ON NK CELL FUNCTION 119

5.4 CLINICAL IMPLICATIONS 121
5.5 CONCLUSION 123
List of References 124
Appendix 1. Ethics approval letter 135

List of Figures

Figure 1.1: The conventional subsets of human NK cells. 2
Figure 1.2: NK cell mediated direct cytotoxicity 3
Figure 1.3: NK cell-mediated ADDC. 4
Figure 1.4: The "missing-self" hypothesis. 6
Figure 1.5: Schematic of NK cell immune synapse formation process. 9
Figure 1.6: A schematic representation of the IRE1-XBP1 pathway. 15
Figure 1.7: The tumour microenvironment in HL. 18
Figure 2.1: Isolation of Stimulated NK cells using MACS. 30
Figure 2.2: Primary NK cell expansion assay. 33
Figure 2.3: A gating strategy of FACS sorted pNK cells. 35
Figure 2.4: Live/dead cells gating strategy. 37
Figure 2.5: Intracellular staining of IFNγ. 39
Figure 2.6: Intranuclear staining of XBP1s. 40
Figure 2.7: Gating strategy of NK cell-HRS cell conjugates. 42
Figure 2.8: A schematic of migration assay. 44
Figure 3.1: Stimulation of various NK cell lines induces XBP1 splicing. 50
Figure 3.2: The XBP1 splicing occurs in an IL-2-independant NK-92.MI cell line. 51
Figure 3.3: XBP1 splicing occurs in SNK10 cells following the stimulation with Hodgkin Lymphoma target cells. 52

Figure 3.4: XBP1s expression increases following the SNK10 cells stimulation with different HL cell lines. 53

Figure 3.5: The UPR is not activated during SNK10 cell-mediated cytotoxicity..... 54

Figure 3.6: The UPR is not activated during KHYG-1 cell-mediated cytotoxicity..... 55

Figure 3.7: The UPR is not activated during NK-92 cell-mediated cytotoxicity. 55

Figure 3.8: Production of XBP1s RNA is inhibited by 4μ8c. 56

Figure 3.9: Production of XBP1s protein is inhibited in the presence of IRE1 inhibitor 4μ8c. 57

Figure 3.10: IRE1 inhibitor, 4μ8c, does not significantly impair NK cell viability. 58

Figure 3.11: IRE1 inhibitor, 4μ8c, does not significantly impair target cells viability. 59

Figure 3.12: Inhibition of IRE1 reduces *IFNγ* expression. 60

Figure 3.13: Inhibition of IRE1 reduces *TNFα* expression. 60

Figure 3.14: Inhibition of IRE1 reduces *FASL* expression. 61

Figure 3.15: Inhibition of IRE1 reduces *GZMB* expression. 61

Figure 3.16: Inhibition of IRE1 reduces *NKG2D* expression. 62

Figure 3.17: The expression of selected genes is affected upon inhibition of IRE1..... 63

Figure 3.18: Inhibition of IRE1 impairs expression of selected effector molecules in SNK10 cells.65

Figure 3.19: Inhibition of IRE1 impairs expression of selected effector molecules in KHYG-1 cells. 66

Figure 3.20: Inhibition of IRE1 impairs expression of selected effector molecules in NK-92 cells. 67

Figure 3.21: Inhibition of the IRE1 impairs IFNγ secretion by NK cells stimulated with different target cells. 69

Figure 3.22: Inhibition of the IRE1 impairs TNFα secretion by NK cells stimulated with different target cells. 70

Figure 3.23: The number of NK cells-HRS cells conjugates is not affected by IRE1 blockade. 72

Figure 3.24: Inhibition of IRE1 does not affect the adhesion of NK cells to target cells is not affected. 73

Figure 3.25: IRE1 blockade impairs NK cell immune synapse formation with HRS cells. 74

Figure 3.26: IRE1 blockade impairs migration of NK cells. 75

Figure 4.1: A time-course of XBP1s expression in different subsets of pNK cells from healthy individuals in response to HRS cells-stimulation. 86

Figure 4.2 : Gating strategy of different pNK cell subsets and XBP1s. 87

Figure 4.3: XBP1s is not activated in primary NK cells from HL patients. 88

Figure 4.4: NK cell compartment in Hodgkin lymphoma is contracted. 89

Figure 4.5: IRE1 blockade impairs NK cell immune synapse formation with HRS cells. 90

Figure 4.6: Expression of PD-1/PD-L1/PD-L2 axis molecules on pNK cells and HDLM-2 cells. Following the expansion of pNK cells the PD-1 expression was tested on $CD3^{-}CD56^{+}$ pNK cells of each patient's sample (A, B, C). 91

Figure 4.7: PD-1 blockade enhances pNK cell immune synapse formation with HRS cells and rescues. 92

Figure 4.8: PD-1 blockade improves NK cell migration. 93

Figure 4.9: Gating strategy of IFNγ in NK cell subset. 94

Figure 4.10: In patients with HL, expanded pNK cells with IRE1-XBP1 pathway blockade have impaired secretion of IFNγ. 95

Figure 4.11: Gating strategy of IFNγ in distinct NK cell subsets. 95

Figure 4.12: In patients with HL, distinct subsets of expanded pNK cells have impaired secretion of IFNγ upon the IRE1 blockade. 96

Figure 4.13: PD-1 blockade partially reverses IFNγ secretion by pNK cells from HL patients. 97

Figure 4.14: PD-1 blockade partially reverses IFNγ secretion by $CD56^{bright}CD16^{-}$ cells from HL patients. 98

Figure 4.15: Gating strategy for TNFα in NK cells. 100

Figure 4.16: In patients with HL, expanded pNK cells with IRE1 blockade display impaired secretion of TNFα. 101

Figure 4.17: Gating strategy of TNFα in distinct NK cell subsets. 101

Figure 4.18: In patients with HL, both subsets of expanded pNK cells have impaired secretion of TNFα upon the IRE1 blockade. 102

Figure 4.19: PD-1 blockade partially reverses TNFα secretion by pNK cells from patients with HL. 103

Figure 4.20: PD-1 blockade partially reverses TNFα secretion in both $CD56^{bright}CD16^{-}$ and $CD56^{dim}CD16^{+}$ cells with suppressed IRE1-XBP1 pathway. 104

Figure 4.21: In HL, pNK cells with suppressed XBP1s exert impaired degranulation. 105

Figure 4.22: Gating strategy of CD107a in NK cell subset. 106

Figure 4.23: Gating strategy of CD107a in distinct NK cell subsets. 107

Figure 4.24: In HL, both NK cell subsets display impaired degranulation in the presence of IRE1 blockade. 107

Figure 4.25: PD-1 blockade does not significantly improve degranulation of pNK cells in patients with HL. 108

Figure 4.26: PD-1 blockade does not improve degranulation by CD56brightCD16- or CD56dimCD16+ cells in patients with HL. 109

Figure 4.27: Thapsigargin reverses impaired target cell lysis mediated by pNK cells with suppressed expression of XBP1s. 110

Figure 5.1: The IRE1-XBP1 pathway is required for the optimal NK cell function. 120

List of Tables

Table 2.1: Demographic information on Hodgkin lymphoma patients tested in the study. 24

Table 2.2: Primers used for Real Time PCR. 32

Table 2.3: List of antibodies used for flow cytometry. 36

Table 2.4: P values summary. 44

List of Abbreviations

4-HNE	4-Hydroxy-Trans-2-Nonenal
ACT	Adoptive Cell Transfer
ADCC	Antibody-Dependent Cell-Mediated Cytotoxicity
AICL	Activation-Induced C-Type Lectin
AML	Acute Myeloid Leukaemia
APC	Antigen Presenting Cells
ATF4	Activating Transcription Factor 4
ATF6	Activating Transcription Factor 6
B2M	Beta-2-Microglobulin (Protein)
B2M	Beta-2-Microglobulin (Gene)
BAT-3	HLA-B Associated Transcript 3
BCR	B Cell Receptor
BiP	Binding Immunoglobulin Protein
CCL5	Chemokine (C-C Motif) Ligand 5
CCR7	CC-Chemokine Receptor 7
CD4+ Th1	CD4+ T Helper Type 1 Cell
cDNA	Complementary DNA
cFLIP	Cellular FADD-Like Interleukin 1β-Converting Enzyme-Inhibitory Protein
cHL	Classical Hodgkin Lymphoma
CIITA	MHC Class II Transactivator (Gene)
CLL	Chronic Myeloid Leukaemia
CR	Complete Response
CRISPR	Clustered Regularly Interspaced Short Palindromic Repeats
cSMAC	Central Supramolecular Activation Cluster
CTL	Cytotoxic T Lymphocyte
CTLR	C-Type Lectin Like Receptor
DC	Dendritic Cell
DLBCL	diffuse large b cell lymphoma
DMSO	Dimethyl Sulfoxide
DNA	Deoxyribonucleic Acid

dNTP	Deoxyribonucleotide Triphosphate
EBNA1	EBV Nuclear Antigen 1
EBV	Epstein-Barr Virus
EC	Endothelial Cell
EDTA	Ethylenediaminetetraacetic Acid
EMA	European Medicines Agency
eNOS	endothelial Nitric Oxide Synthase
ER	Endoplasmic Reticulum
ERAD	ER Associated Degradation
ERK	Extracellular signal–Regulated Kinases
FACS	Fluorescence Activated Cell Sorting
Fas	Fas (Tnf Receptor Superfamily, Member 6)
FasL	Fas Ligand (Tnf Superfamily, Member 6)
FASLG	Fas Ligand (Tnf Superfamily, Member 6) (Gene)
FBS	Foetal Bovine Serum
FC	Fold Change
FDA	Food And Drug Administration
FL	Follicular Lymphoma
FSC	Forward Scatter
GCB cell	Germinal Centre B Cell
GM-CSF	Granulocyte-Macrophage Colony-Stimulating Factor
GvHD	Graft Vs Host Disease
GZMB	Granzyme B (Gene)
HA	Hemagglutinins
HCMV-pp65	Human Cytomegalovirus Tegument Protein-pp65
HCV	Hepatitis C Virus
HIV	Human Immunodeficiency Virus
HL	Hodgkin Lymphoma
HLA	Human Leukocyte Antigen
HN	Hemagglutinin Neuraminidases
HRS	Hodgkin And Reed-Sternberg Cells
HSPG	Heparan Sulfate Proteoglycan
ICAM-1	Intracellular Adhesion Molecule-I
IFNγ	Interferon Gamma
Ig V	Immunoglobulin V Genes
IgSF	Immunoglobulin Superfamily

IL	Interleukin
IL-2	Interleukin 2
IL-6	Interleukin 6
IL-8	Interleukin 8
IRE1-LD	IRE1 Luminal Domain
IRE1α	Inositol Requiring Kinase 1α
IS	Immunological Synapse
ITAM	Immune Tyrosine-Based Activating Motifs
ITIM	Immunoreceptor Tyrosine-Based Inhibitory Motif
JAK-STAT	Janus Kinase Stat Pathway
KIR	Killer Cell Immunoglobulin-Like Receptor
KIR2D	KIR With 2 Domains
KIR3D	KIR With 3 Domains
LD	Luminal Domain
LDHL	Lymphocyte-Depleted Hodgkin Lymphoma
LFA-1	Lymphocyte Function-Associated Antigen 1
LFA-1	Lymphocyte Function-associated Antigen 1
LMP1	Latent Membrane Protein 1
LMP2a	Latent Membrane Protein 2a
LRCHL	Lymphocyte-Rich Classical Hodgkin's Lymphoma
mAb	Monoclonal Antibody
MACS	Magnetic-Activated Cell Sorter
MCHL	Mixed Cellularity Hodgkin Lymphoma
MDSC	Myeloid Derived Suppressor Cell
MFI	Mean Fluorescence Intensity
MHC	Major Histocompatibility Complex
MIC	MHC Class I Chain-Related Peptides
MM	Multiple Myeloma
mRNA	Messenger RNA
MTOC	Microtubule Organising Centre
NCAM-1	Neural Cell Adhesion Molecule 1, CD56
NCR	Natural Cytotoxicity Receptor
NF-κB	Nuclear Factor-Kb
NHL	Non-Hodgkin Lymphoma
NK Cell	Natural Killer Cell
NKIS	NK-Cell Immune Synapse

NKR	NK-Cell Receptor
NLPHL	Nodular Lymphocyte-Predominant Hodgkin Lymphoma
NSHL	Nodular Sclerosis Hodgkin Lymphoma
ORR	Overall Response Rate
PBMC	Peripheral Blood Mononuclear Cells
PBS	Phosphate Buffered Saline
PCNA	Proliferating Cell Nuclear Antigen
PCR	Polymerase Chain Reaction
PD-1	Programmed Cell Death Protein 1
PD-L1	Anti-Programmed Cell Death-1 Ligand
PD-L2	Anti-Programmed Cell Death-2 Ligand
PERK	Pancreatic Er Kinase
PfEM-1	Plasmodium Falciparum Erythrocyte Membrane Protein-1
PI3K	Phosphatidylinositol (PI)-3 Kinase
PIPKIγ	type Iγ phosphatidylinositol 4-phosphate 5-kinase
pNK	Primary Nk Cells
pSMAC	Peripheral Supramolecular Activation Cluster
PTLD	Post-Transplant Lymphoproliferative Disorder
RANTES	Regulated On Activation, Normal T Cell Expressed And Secreted, CCL5
RIDD	Regulated IRE1-Dependent Decay
RNA	Ribonucleic Acid
RNase activity	Endoribonuclease Activity
RPMI	Roswell Park Memorial Institute
RS	Reed-Sternberg Cell
RTK	Receptor Tyrosine Kinase
RT-PCR	Reverse Transcription Polymerase Chain Reaction
SYK	Spleen Associated Tyrosine Kinase
T2D	Type 2 Diabetes
TAMs	Tumour-Associated Monocytes
tDC	Tumour Associated Dendritic Cell
TG	Thapsigargin
TGFβ	Transforming Growth Factor Beta
Th	T Helper Cell
Th1	CD4+ T Helper Type 1 Cell
TLR	Toll Like Receptors
TME	Tumour Microenvironment

TNFα	Tumour Necrosis Factor A
TRAIL	TNF-Related Apoptosis Inducing Ligand
TRAIL-R	TNF-Related Apoptosis Inducing Ligand-Receptor
Treg	T Regulatory Cell
ULBPs	UL16 Binding Protein
UPR	Unfolded Protein Response
WASP	Wiskott Aldrich Syndrome protein
XBP1	X-Box Binding Protein 1 (Gene)
XBP1	X-Box Binding Protein 1 (Protein)
XBP1s	X-Box Binding Protein 1, Spliced Variant (Protein)
XBP1U	X-Box Binding Protein 1, Unspliced Variant (Gene)
ZAP-70	Zeta-Chain-Associated Protein Kinase 70

CHAPTER 1:

General Introduction

1.1 NK CELL SUBSETS

Human Natural Killer (NK) cells are a heterogeneous population phenotypically defined as $CD3^-$ $CD56^+$ lymphocytes. NK cells can be divided into two sub-populations based on differential expression of the neural cell adhesion molecule 1 (NCAM-1, CD56), namely: $CD56^{bright}$ and $CD56^{dim}$ (Figure 1.1). Most NK cells belong to the $CD56^{dim}CD16^+$ population, which dominates in the peripheral blood (90%) and exhibits high level of cytotoxicity and is capable of antibody-dependent cell-mediated cytotoxicity (ADCC) [1]. The minority subset (10%) within the peripheral blood is the $CD56^{bright}CD16^-$, which generally resides in secondary lymphoid organs and produces cytokines following stimulation but is only weakly cytotoxic before activation. One theory is that the cells of this subset are precursors of the $CD56^{dim}$ $CD16^+$ NK cells [2].

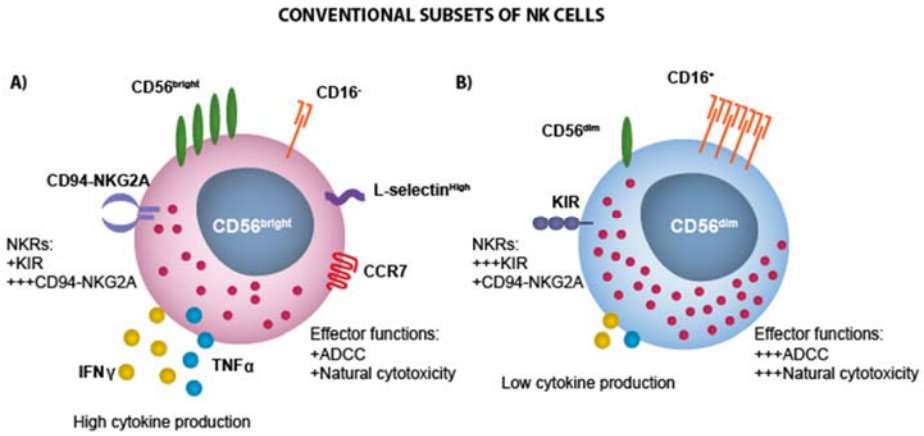

Figure 1.1: The conventional subsets of human NK cells. The $CD56^{brigh}CD16^-$ subset produces high levels of cytokines following stimulation (A). These cells exert a high capacity to perform lymphokine-activated killing, but only limited ability to instigate ADCC due to low expression of CD16, and natural cytotoxicity. Both adhesion molecules, CCR7 and L-selectin, are responsible for homing properties of these cells to lymph nodes. In contrast, $CD56^{dim}CD16^+$ cells produce modest amount of cytokines, but are potent mediator of ADCC and natural cytotoxicity (B). These cells express a high level of KIRs and have more granular morphology.

NK cell subsets express various chemokine receptors and adhesion molecules that affect their homing preferences. In the contrary to $CD56^{dim}$ NK cells, $CD56^{bright}$ NK cells express CC-chemokine receptor 7 (CCR7) - a lymph node homing receptor and L-selectin (CD62L) – a molecule that enables members of this subset to adhere to the lymph node's high endothelial venules. Therefore, these factors may play a critical role in trafficking of the $CD56^{bright}$ cells to lymph nodes [3] [4].

Over twenty years ago, the third subset of NK cells, $CD56^{neg}CD16^+$, was identified in patients with chronic viral infections such as HIV or HCV [5] [6] [7]. Later, it was shown that these cells also exist in healthy people but represent only few percent of total NK cells in the blood. In HIV-infected individuals $CD56^{neg}CD16^+$ cells are characterized by decreased expression of activating receptors

and elevated expression of inhibitory receptors. Generally, they exhibit lower capacity to perform cytolysis, proliferate and produce cytokines [8] [9].

1.2 NATURAL KILLER CELL FUNCTION

1.2.1 Direct Cytotoxicity

NK cells are important innate effector cells that possess the unique ability to lyse abnormal cells without previous sensitization (Figure 1.2) [10] [11]. Target cell death can be executed by various mechanisms, including degranulation and death receptor engagement [12]. The principal mechanism of NK cell mediated direct cytotoxicity involves recognition of a target cell and formation of an immunological synapse (IS), followed by the exocytosis of lytic granules, which leads to a target cell lysis [13]. The content of lytic granules includes: perforin - a membrane-disrupting protein, proteolytic enzymes known as granzymes, Fas ligand (FasL), TNF-related apoptosis inducing ligand (TRAIL), and granulysin [14] [15] [16]. Of the various granzymes present in the lytic granule, granzyme B is a critical molecule that triggers apoptotic target cell death via caspase-dependent and independent mechanisms [17] [18].

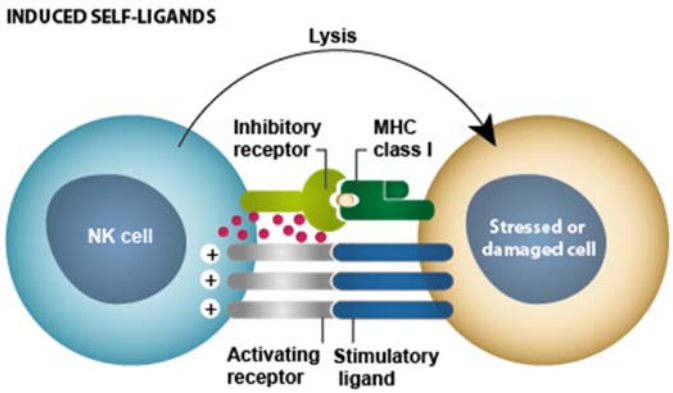

Figure 1.2: NK cell mediated direct cytotoxicity. The increased expression of activating ligands at the surface of malignant cells induces NK cell activation and subsequent target cell lysis.

Another mechanism initiates extrinsic apoptotic pathway through activation of death receptors, Fas or TRAIL receptor (TRAIL-R), present on target cells [19]. These molecules engage with cognate ligands expressed on NK cells (FasL and TRAIL) what activates a caspase enzymatic cascade that triggers apoptosis. Moreover, engagement of activating receptors of NK cells causes release of chemokines and cytokines, which further modulate the immune response. Among these molecules are tumour necrosis factor α (TNFα), interferon γ (IFNγ) or granulocyte-macrophage colony-

stimulating factor (GM-CSF). Additionally, IFNγ may induce expression of death receptors on target cells, thereby making them more prone to TRAIL/FasL-mediated cytotoxicity [14].

1.2.2 Antibody-Dependent Cell-mediated Cytotoxicity

As mentioned previously, another type of NK cell-mediated cytotoxicity is ADCC (Figure 1.3). In this case, antibody-coated target cells are recognized by NK cells through engagement of their CD16 (FcγRIIIA) receptor with Fc portion of IgG antibody [20] [21]. CD16 is present within the cell membrane and associates with homo- or heterodimers of FcϵRI-γ and CD3-ζ chains, which possess immune tyrosine-based activating motifs (ITAM) that are crucial for the rapid generation of intracellular messengers. Following FcγR engagement, ITAMs undergo phosphorylation what results in activation of tyrosine kinases such as ZAP-70 and SYK, as well as phosphatidylinositol (PI)-3 kinase (PI3K), nuclear factor-κB (NF-κB) and ERK pathways. Collectively, these mechanisms trigger NK cell degranulation, TNF family death receptor signalling and secretion of cytokines such as IFNγ, which consequently leads to the opsonised cell death [14] [22].

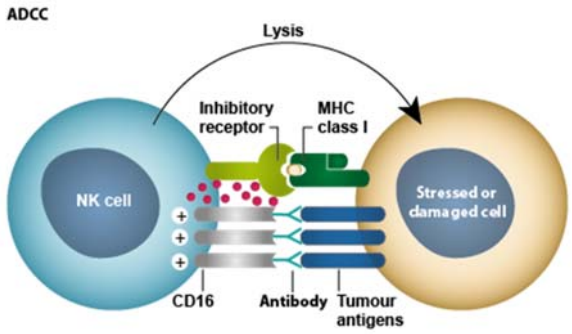

Figure 1.3: NK cell-mediated ADDC. Tumour cell coated with monoclonal antibody is recognized by NK cell through binding of its CD16 receptor with Fc portion of IgG antibody that induces Antibody-Dependent Cell-mediated Cytotoxicity.

1.2.3 Cytokine Secretion

Apart from the ability to kill malignant or infected cells, NK cells have the capacity to rapidly produce a variety of cytokines and chemokines in response to stimulation [3]. NK cells, mainly the $CD56^{bright}CD16^{-}$ population, are the primary source of TNF-α, IFNγ and GM-CSF. Secretion of these cytokines significantly shapes responses mediated by other immune cells such as T cells, dendritic cells (DC), macrophages, and neutrophils [12]. For example, IFNγ released by NK cells can increase expression of the major histocompatibility complex class I (MHC-I) molecule on antigen presenting cells (APC) [23]. Moreover, IFNγ secreted by NK cells primes responses mediated by the $CD4^{+}$ T

helper type 1 (Th1) cells [10]. These responses are further enhanced by DCs, which mature in response to IFNγ secreted by NK cells [24]. Equally important is TNFα, a powerful cytokine with pleiotropic functions including tumour killing or immune response editing. As an illustration of its function, TNFα is known to augment B cell proliferation and induce monocyte and macrophage differentiation [25] [26] [27] [28]. NK cells are also known to secrete several other factors, including immunoregulatory cytokines such as IL-5, IL-10, IL-13 and the chemokines MIP-1α, MIP-1β, IL-8, and RANTES (CCL5). The latter facilitates recruitment of other effector cells to the inflammation site [29] [30].

Thus, NK cells are not only the cytotoxic cells but also immunoregulatory cells that can orchestrate anti-cancer responses by shaping the responses of other immune cells [31].

1.3 NATURAL KILLER CELL RECEPTORS

NK cells harbour a variety of transmembrane receptors [32]. Their effector functions, such as cytotoxicity, cytokine production or proliferation depend on the balance between inhibitory and activating signals received by these receptors [22] [33]. NK cell receptors possess various adaptor molecules which facilitate signal transduction. These adaptor molecules include: DAP12, CD3ζ or FcRγ, which further transduce signals via cytoplasmic domain motif: ITAM or immunoreceptor tyrosine-based inhibitory motif (ITIM), activating or inhibiting signals respectively [34] [35]. Whereas DAP10, another adaptor molecule, uses alternative signalling via YINAM motif [34] [12, 35].

Interaction between activating receptors and their ligands induces phosphorylation of tyrosine residue and activates downstream kinases (SYK or ZAP70), which leads to a signalling cascade, NK cell degranulation and cytokine secretion. In case of inhibitory receptors, following the phosphorylation, phosphatases deactivate signalling kinases, what results in inhibition of NK cell function [22] [33].

According to the “missing-self” hypothesis, introduced by Karre, target cells with reduced or lost MHC-I molecule expression, which under normal circumstances is expressed by each healthy cell, are recognized by NK cells as “missing-self” and if activating signals are unopposed by inhibitory signals NK cell kills target cell (Figure 1.4) [36] [37]. Individual types of NK cell receptors (NKRs) will be discussed in turn.

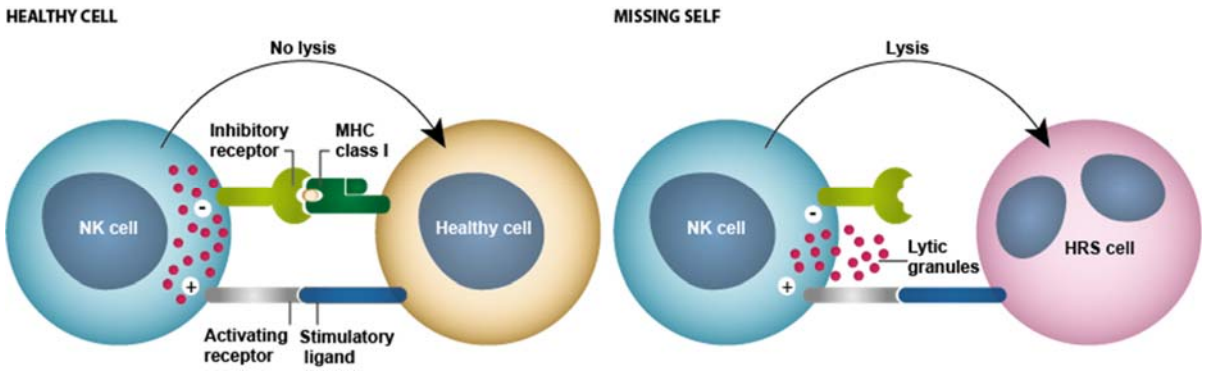

Figure 1.4: The "missing-self" hypothesis. The loss of MHC-I molecule on malignant cell renders them sensitive to NK cell-mediated cytotoxicity. A balance between activating and inhibitory signals received by the receptors at NK cell surface regulates the recognition of healthy cell by NK cells. Malignant cells with lost MHC-I molecule expression, such as HRS cells (malignant cells in Hodgkin lymphoma), are recognized as "missing-self" and induce NK cell-mediated cytotoxicity.

1.3.1 Killer Cell Immunoglobulin-like Receptors

Killer cell immunoglobulin-like receptors (KIRs) are part of the immunoglobulin superfamily (IgSF) [2]. These receptors prevent NK cell-mediated killing of normal cells but promote lysis of cancerous or virally infected cells, with reduced or lost expression of the MHC-I [22] [36] [38] [39].

KIRs family includes both activating and inhibitory receptors, which signal through ITAM or ITIM associated with DAP-12 or FcεRI-γ adaptor molecules [40] [39]. Structurally, they are characterized by the presence of type I transmembrane glycoproteins with two (KIR2D) or three (KIR3D) Ig-like domains, with either short or long cytoplasmic tail. The latter determines their functional properties, and hence the long tail associated with ITIM mediates inhibitory signals, while the short tail associated with ITAM mediates activating ones. Primarily, KIRs are known to recognize MHC-I molecules, such as human leukocyte antigen (HLA)-A, -B, and -C, what provides NK cells with inhibitory signals. Specificity for HLA-C or HLA-A/B allotypes is dictated by the extracellular Ig-domains, precisely KIR2DL recognizes HLA-A and KIR3DL recognizes HLA-A/B. Likewise, selected HLA molecules are also ligands for the activating KIRs. So far, it has been established that KIR2DS1 recognizes HLA-C and HLA-A, KIR2DS4 can recognize HLA-C2, and KIRDL4 recognizes HLA-G (Figure 1.4) [41] [39].

The expression of KIR on individual NK cells is regulated by the methylation of the *KIR* gene [34]. Each individual has a unique repertoire of KIRs, with the exception for KIR2DL4 which is expressed universally by all NK cells [32] [34]. Interestingly, this receptor, despite having a long cytoplasmic tail, acts as activating receptor responsible for induction of IFNγ secretion without triggering NK cell mediated killing [32].

Inhibitory KIRs are an attractive target for immunotherapy targeting NK cell activity. These receptors play a critical role in allotransplantation, where KIR-MHC-I mismatch between donor and recipient ensures NK cell activity upon transplantation, which leads to elimination of cancer cells, despite the expression of the MHC-I on their surface. This approach has clinical utility in both acute myeloid leukaemia (AML) and multiple myeloma (MM) patients. Another strategy utilizes monoclonal antibodies (mAbs) blocking KIR receptors, specifically KIR2DL1/L2/L3, which represent half of the total NK cell repertoire. Blockade of these KIRs prevents engagement of inhibitory ligands (HLA-C) that normally inhibit NK cell function [41]. The interaction of KIRs and self-HLA class I molecules leads to inhibition of NK cell mediated cytotoxicity [42].

1.3.2 C-type Lectin Receptors

The C-type lectin like receptors (CTLR) family is a heterogeneous group of NK cell receptors. Members of this family are heterodimers that possess common subunit CD94 bound to the NKG2 molecule. The latter ensures signalling via extracellular and cytoplasmic domains that are responsible for the functional specificity of CTLRs. The CD94:NKG2 family comprises of four closely related members: NKG2A, NKG2C, NKG2E and NKG2F [32]. Within this family, NKG2A is the only inhibitory receptor. It contains a long intracytoplasmic tail bearing ITIM. The remaining receptors transduce activating signals with the use of short cytoplasmic tails associated with ITAM [43]. The ligand for these activating receptors, CD94:NKG2A, C and E, is the non-classical MHC-I molecule HLA-E [44] [45] [46] [47].

Although not capable of forming complexes with CD94; the homodimer NKG2D is grouped within the CTLR family [48]. NKG2D is expressed by all NK cells and its intracellular domain associates with adaptor protein DAP10 to transduce signals via recruitment of PI3K that leads to cytotoxicity and cytokines release [49] [50]. The ligands for NKG2D include the MHC-I chain-related peptides (MIC) A (MICA) and B (MICB), and UL16 binding proteins (ULBPs) [48] [51] [52]. These ligands are abundantly expressed on “stressed” cells or cells which undergo a malignant transformation [53]. Moreover, many tumour cells release NKG2D ligands in a soluble form to prevent NK cell activation and subsequent NK cell mediated killing of target cells. Furthermore, these soluble ligands contribute to down-regulation of NKG2D expression on effector cells. Multiple studies have shown that sera from cancer patients exert increased levels of soluble NKG2D ligands what correlates with disease severity [2].

Another member of this family NKp80, nearly universally expressed by NK cells, contains an unusual hemi-ITAM-like cytoplasmic domain triggering NK cell mediated cytotoxicity [54]. Almost all NK

cells express this activating receptor. Interestingly, ligand for NKp80, activation-induced C-type lectin (AICL), is stored intracellularly and surfaces upon NK cell stimulation. This ligand is expressed by haematopoietic cells, particularly myeloid cells in AML and chronic myeloid leukaemia (CML). It is also found in non-haematopoietic cells of carcinoma and melanoma cells. Engagement of AICL expressed on these cells with NKp80 increases their susceptibility to NK cell mediated cytotoxicity [54] [55] [56].

1.3.3 Natural Cytotoxicity Receptors

Natural Cytotoxicity Receptors (NCRs) belong to activating receptors from the IgSF and are able to trigger direct cytotoxicity upon engagement with ligands such as: non-MHC-I molecules or pathogen-derived molecules [57] [58]. The signals received by these receptors are transduced via adaptor molecules associated with ITAM. Interestingly, NKp44 receptor is the only member of this family that also contains adaptor molecules bearing ITIM, a motif usually transducing inhibitory signalling [Hudspeth, 2013]. NKp46 and NKp30 receptors are constitutively expressed by resting NK cells and their expression increases upon NK cell stimulation. Conversely, expression of NKp44 is detected solely upon activation of NK cells [59, 60]. Recent studies indicate that each of the NCR genes can undergo alternative splicing what results in generation of multiple splice variants. Each of these variants may exert different functionality [61]. Apparently, alternative splicing of NCR genes is driven by cytokines present in particular tumour microenvironment.

NKp46, identified as the first NCR family member, is the leading receptor mediating cell death of tumour cells that lack MHC-I [62]. Multiple studies have shown a negative correlation between absence of NKp46 expression and efficient clearance of tumours, such as lymphoma or melanoma [58]. NKp46 engages with a range of ligands including: heparan sulfate proteoglycan (HSPG) – present on many tumour cells, as well as bacterial proteins such as vimentin, *Plasmodium falciparum* erythrocyte membrane protein-1 (PfEM-1), or viral proteins - hemagglutinins (HA) and hemagglutinin neuraminidases (HN) expressed by a range of virally-infected cells [63]. After engaging its ligands NKp46, endowed with two extracellular domains, transduces signals via ITAM, what leads to target cell lysis and release of cytokines [64] [65].

NKp44 has a single extracellular domain that likely transmits signals through the ITAM-bearing adapter molecule DAP-12. NKp44 cytotoxic activity towards target cells decreases following its blockade with specific mAbs; notably this is decreased further by a co-blockade of NKp46 suggesting that these two receptors cooperate towards clearance of target cells [66]. Ligands for this receptor are: NKp44L, proliferating cell nuclear antigen (PCNA), and various virus-derived proteins [63].

Wherein, ligation of PCNA potently inhibits either NK cell mediated cytotoxicity of tumour cells and IFN-γ secretion. PCNA-mediated inhibition of NK cell function perhaps occurs through the inhibitory ITIM motif present in the structure of the splice variant NKp44-1.

Another receptor within this family NKp30 is endowed with one extracellular domain [67] [62]. Its expression on NK cells is down-regulated in the presence of TGF-β, a cytokine often found to be extensively secreted in a tumour microenvironment [62]. Currently, there are several known ligands for NKp30: HSPG, HLA-B associated transcript 3 (BAT-3), B7-H6 (expressed on many tumour cell lines), and human cytomegalovirus tegument protein (HCMV-pp65) [63] [68]. Both ligands, BAT-3 and B7-H7, are expressed by multiple tumour cells what implicates NKp30 involvement in tumour clearance. However, NKp30 appears to also mediate NK cell interactions with DCs, what has significant impact on shaping the overall immune responses [68].

1.3.4 The NK cell immunological synapse

The NK cell immune synapse (NKIS) formation is a finely-tuned, stepwise process of which key components include: adhesion to a target cell, actin polymerization and rearrangement at the IS, lytic granule convergence, microtubule-organizing centre (MTOC) and lytic granule polarization toward the synapse, granule secretion, and detachment of NK cell following target cell destruction (Figure 1.5) [69, 70].

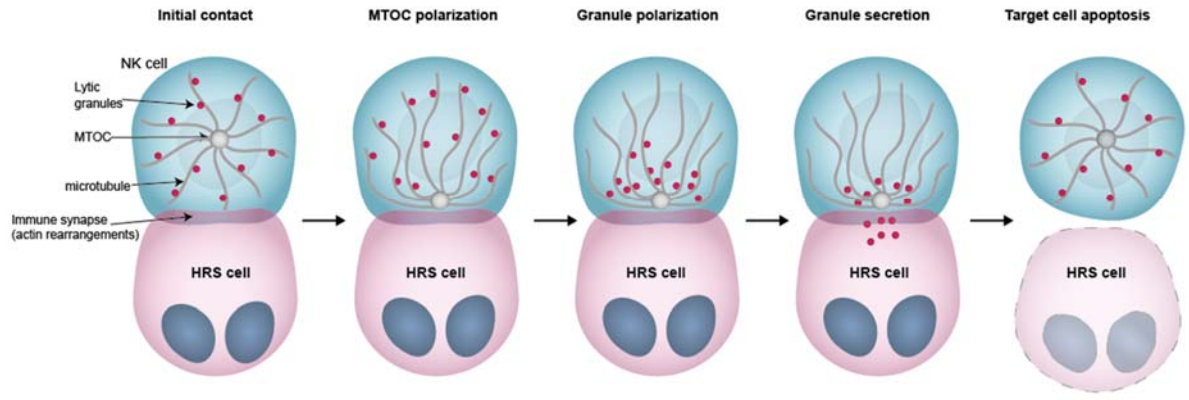

Figure 1.5: Schematic of NK cell immune synapse formation process. The NKIS formation is a multiple step process that initiates by conjugate formation between NK cell and a target cell. At the interphase of the IS actin undergoes rearrangements to form a stable synapse. In the next step, MTOC polarization occurs, followed by the lytic granule polarization, which leads to granule secretion at the IS and eventually target cell apoptosis.

Adhesion of NK cell to a target cell is an indispensable checkpoint to establish a stable connection and subsequent immune synapse. Within the NKIS interface we can distinguish two sections referred

to as peripheral supramolecular activation cluster (pSMAC) and the central SMAC (cSMAC). The first section is a ring-shaped structure comprised of adhesion molecules, such as lymphocyte function-associated antigen 1 (LFA-1), that cluster at the contact point of NK cell and target cell. As follows, LFA-1 induces actin polymerization and subsequent accumulation of F-actin filaments within the pSMAC [71] [72] [73]. Conversely, activating receptors, responsible for the cytotoxic response i.e. NKG2D, NKp30, or NKp46, cluster in the cSMAC [72]. In the aftermath of signalling transduced via activating receptors NK cell can either mediate target cell lysis or secrete cytokines [74] [75] [70].

To deliver a lethal hit to a target cell, further rearrangements of the NK cell cytoskeleton are required. In particular, the MTOC, a structure that organizes the microtubule cytoskeleton, undergoes dynamic changes and is polarized toward the target cell to ensure transport of lytic granules to the IS [70]. Concomitant rearrangement of F-actin at the synapse interface leads to formation of granule-sized pores, which enable lytic granules secretion [76] [77] [78]. It has been reported that myosin IIA may facilitate lytic granules passage through the F-actin network of the IS or be involved in induction of confined changes in the F-actin structure to allow polarized lytic granules access to the membrane [70] [79] [80] [81]. As the lytic granules reach a target cell, perforin disrupts its membrane to enable entry of granzymes into the cell and subsequent target cell death [82]. In the final step, the NK cell detaches from the target cell and is able to engage with the next target [83].

1.4 NK CELL BASED THERAPIES IN CANCER

The fact that NK cells can recognize and kill an array of tumour cells without prior sensitization renders them a promising tool for anti-cancer therapy [84]. As mentioned previously, NK cell function is tightly regulated by a balance between activating and inhibitory signals received by a mosaic of receptors expressed at the cell surface. These receptors enable NK cells to engage with and eliminate abnormal cells. Each abnormal cell has a unique suite of ligands, which upon binding to specific receptors on NK cell will induce a response, such as cytokine secretion, cytotoxicity or proliferation. [42]. NK cells are known to attack tumour cells with lost or down-regulated expression of MHC-I molecules, which is often a case in hematopoietic malignancies [85] [84]. Moreover, given that NK cells are “ready to kill”, as oppose to T cells that require a certain time to acquire anti-tumour activity, makes them an attractive tool for immunotherapy [42] [32]. Indeed, an 11-year follow up study of healthy participants demonstrated that low NK cell activity is associated with the increased cancer risk [86] [42] [37].

Recent progress in the field of NK cell biology and concomitant improved understanding of their function allowed for the development of novel immunotherapeutic strategies [32]. Generally, NK cell

immunotherapy can be achieved either by activating endogenous NK cell response or using exogenous NK cells via adoptive cell transfer. So far, several strategies for NK cell immunotherapies for human cancer have been proposed and selected therapies will be discussed further [84].

1.4.1 Monoclonal antibody therapies

NK cell function can be modulated by targeting specific receptors expressed at the cell surface. Of importance among activating receptors is CD16, a molecule that enables ADCC of antibody-coated tumour cells. Specifically, the Fc portion of antibody coating a tumour cell is bound by CD16 receptor present on NK cell, what initiates NK cell mediated killing of malignant cell [87]. One such antibody, with a proven clinical success in patients with various lymphoid malignancies (follicular lymphoma - FL, diffuse large B-cell lymphoma - DLBCL), is rituximab, a molecule targeting CD20 antigen expressed on the malignant cells [88]. Moreover, the ADCC activity of NK cells can be enhanced by means of bispecific or trispecific antibodies. This type of antibodies combines the binding avidity and biologic activity of two or three antibodies into one molecule, targeting at least one tumour antigen and at least one surface antigen on NK cell. By crosslinking these epitopes, the antibody facilitates the interaction between a tumour cell and NK cell. For instance, in MM patients, a recombinant bispecific protein (ULBP2-BB4) promotes ULBP2 interaction with NKG2D receptor present on NK cells, and BB4 moiety binding to CD138 receptor expressed by the neoplastic cells. This bispecific antibody showed enhanced NK cell-mediated killing of malignant plasma cells both in the allogeneic and autologous setting [89] [90].

Further, NK cells express also an array of inhibitory receptors, and blockade of these receptors, which serve as checkpoints in NK cell activation, emerges as a promising tool for immunotherapy. Recently, anti-PD-1 mAb has been the focus of multiple studies due to the great success in unleashing the anti-tumour efficacy of immune cells with a proven clinical efficacy [87]. Anti-PD-1 mAb targets programmed cell death protein-1 (PD-1), which is expressed on a range of activated immune cells, including NK cells. Conversely, its cognate ligands PD-ligand 1 (PD-L1, CD274) or PD-ligand 2 (PD-L2, CD273) are expressed on a variety of tumour cells [90]. A large body of evidence suggests that the PD-1/PD-L1/PD-L2 axis is implicated in tumour immune escape in many solid cancers, as well as haematological malignancies, including Hodgkin lymphoma (HL), non-Hodgkin lymphoma (NHL), and MM [91]. In fact, PD-1 and PD-L1 blockade was found to trigger a robust NK cell response, what orchestrates that not only T cells but also NK cells mediate the effects of PD-1/PD-L1 blockade. Shaping the anti-tumour response via NK cells may be of importance in cases where tumour cells express low levels of MHC-I and high levels of PD-1 ligands [92]. In a recent study of HL, it was demonstrated that PD-1/PD-L1 axis plays a critical role in tumour immune evasion due to

expansion of the $CD3^{-}CD56^{bright}CD16^{-}CCR7^{+}PD\text{-}1^{+}$ subset of NK cells, which function was inhibited directly by malignant cells, as well as the $CD163^{+}PD\text{-}L1^{+}/PD\text{-}L2^{+}$ tumour-associated monocytes (TAMs). Upon PD-1 blockade NK cells orchestrated enhanced degranulation which was consistent with increased killing of malignant cells [93]. Another study on patients with MM, has also shown PD-1 expansion within NK cell compartment. Additionally, *in vitro* experiments demonstrated that a blockade of PD-1 boosted NK cell mediated cytotoxicity of autologous malignant cells. However, the exact mechanism of PD-1 blockade effect on NK cell function remains to be elucidated [90] [42].

Normally, all nucleated cells in the host express MHC-I molecules, which once recognized by inhibitory KIRs on NK cells protect them from NK cell-mediated lysis. Hence, disruption of inhibitory KIRs through mAb-mediated blockade could enhance NK cell-mediated killing of tumour cells, and therefore, KIRs have become a target for immune checkpoint blockade to unleash NK cell killing potential against tumour cells that still express MHC-I molecules. A monoclonal antibody, known as lirilumab, blocks three inhibitory KIRs: KIR2DL1, KIR2DL2 and KIR2DL3; its application has been shown to enhance NK cell activity against tumour cells *in vitro* and in the phase I clinical trials in AML patients [94] [95] [42] [96] [97].

NKG2A is another inhibitory receptor on NK cells, which recognizes MHC-I ligand HLA-E, and it was shown that signalling via this receptor inhibits NK cell-mediated anti-tumour activity in a range of malignancies. Thus, NKG2A is a potential target for checkpoint blockade therapy. Currently, several clinical trials utilizing a monalizumab, a mAb blocking NKG2A receptor, are ongoing. In the future, the combinatorial approach targeting a different aspect of NK cell function might prove beneficial for the treatment of cancer [89] [42] [92].

1.4.2 Adoptive NK cell transfer

Alternative way to modulate the host's immune system to fight cancer is adoptive cell transfer (ACT) therapy. Either autologous or allogeneic cells transfer can be considered to replace, repair, or enhance the function of the immune system. Several strategies can be pursued with regards to ACT therapy, such as: depletion or enrichment of specific cell subsets, expansion of selected hematopoietic cell subsets, activation of lymphocytes for immunotherapy, and genetic modification of lymphoid cells [87]. Particularly attractive strategy for immunotherapy is the transfer of NK cells, as they do not require prior sensitization to eliminate malignant cells and can induce a potent cytokine response [87]. NK cell products for adoptive transfer can be prepared from: umbilical cord blood, cell lines, and adult donor leukapheresis products. The benefit of using adoptively transferred adult NK cells is that

these cells are educated in healthy hosts and have the potential to have greater anti-tumour activity [98].

Initially, the therapeutic potential of NK cells was explored by adoptive transfer of Interleukine-2 (IL-2) activated NK cells. However, the outcomes of this approach were disappointing due to high toxicity of IL-2 and the inhibition of NK cell function by engagement of their inhibitory receptors KIRs with self-MHC-I molecules expressed on malignant cells [85] [98] [99].

Subsequently, trials encompassing allogeneic NK cell transfer were investigated. The revolutionary study by Ruggeri *et al*., demonstrated that alloreactive NK cells transfer to patients with AML not only could eliminate relapse and graft rejection, but also protect them against graft vs host disease (GvHD). The great advantage of allogeneic NK cells is that they are derived from healthy donors, therefore they govern more powerful killing activity, and unlike T cells, they do not induce GvHD [100]. The observations in AML patients indicated that allogeneic transfer of NK cells with KIR mismatch is associated with anti-tumour activity, thereby specific selection criteria for KIR-mismatched donors have been established. This in turn, led to clinical studies of the allogeneic transfer of NK cells with promising results [101] [102] [103]. Further, Miller *et al.* have established safety and efficacy of alloreactive NK cells transfer in patients with meta-static melanoma, renal cell carcinoma, refractory HL and refractory AML [104]. A recent study by Bachanova *et al.*, indicates that allogeneic transfer of NK cells promotes remission in NHL patients with low level of immunosuppressive cells, such as regulatory T cells (Treg) and myeloid derived suppressor cells (MDSC) [105]. This clinical evidence strongly supports a therapeutic role for allogeneic NK cells in controlling human malignancies [106] [107] [37] [90].

Another alternative is the use of pre-established clinical grade NK cell lines expanded to high numbers and cryopreserved as an “off-the-shelf” therapy. Importantly, prior modulation of these cells might be used to further enhance their effector functions [42] [37] [108]. Moreover, combination of NK cell transfer with checkpoint inhibitors or immunomodulatory drugs may provide enhanced efficacy [42] [1] [90].

1.5 THE UNFOLDED PROTEIN RESPONSE

The Unfolded Protein Response (UPR) system is responsible for maintenance of protein homeostasis. Once cells are exposed to endoplasmic reticulum (ER) stress, signalling pathways within the UPR system are initiated to reduce protein translation, upregulate expression of the ER enzymes and

chaperones involved in protein folding, and degrade the misfolded proteins. Nonetheless, if the ER stress cannot be resolved the UPR triggers cell death through apoptosis [109] [110].

Three arms of the UPR system operate in parallel with the use of different signal transduction mechanisms. Each pathway is initiated with an ER membrane-bound sensor component, specifically: Inositol Requiring Kinase 1α (IRE1α) and X-Box binding Protein 1 (XBP1); Pancreatic ER Kinase (PERK) and Activating Transcription Factor 4 (ATF4); and ATF6 [111].

1.5.1 The IRE1-XBP1 pathway

The IRE1 is a type I ER transmembrane protein with both kinase and endoribonuclease (RNase) activity. The serine/threonine kinase domain is located on N-terminal of the ER luminal domain (LD), while the C-terminal endoribonuclease domain resides in the cytosol. Out of two mammalian isoforms of IRE1, IRE1α and IRE1β, only IRE1α is ubiquitously expressed, while the other isoform is expressed exclusively by the intestinal epithelial cells [112] [113].

In the absence of unfolded proteins, Binding immunoglobulin Protein (BiP) associates with IRE1-luminal domain (IRE1-LD) to keep it inactive. With the increase of unfolded proteins in the ER, BiP releases IRE1-LD and binds the unfolded proteins, whereas IRE1 undergoes dimerization, followed by auto phosphorylation, what leads to its activation [114] [115] [116]. The activated IRE1 processes the *XBP1U* mRNA by splicing out a 26-nucleotide-long intron, what in turn shifts the open reading frame of *XBP1* mRNA. In the aftermath, a stable form of XBP1 is expressed – spliced XBP1 (XBP1s). The latter is an active transcription factor that translocates to the nucleus to induce the upregulation of specific target genes involved in ER-associated degradation (ERAD) and protein folding (Figure 1.6) [117-119].

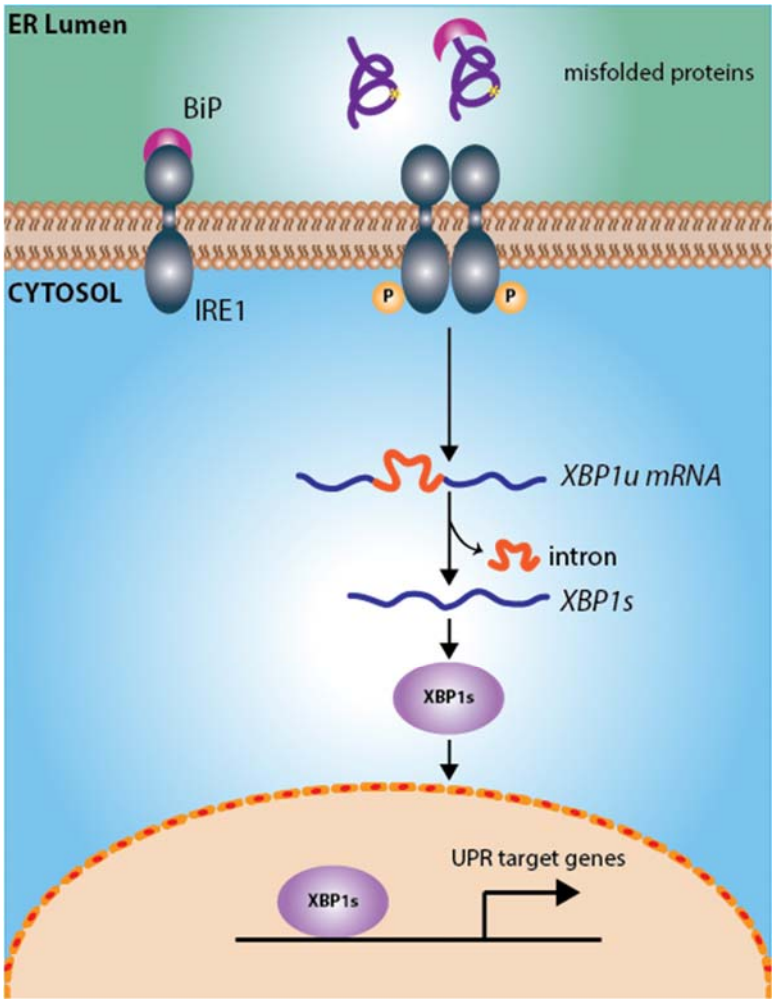

Figure 1.6: A schematic representation of the IRE1-XBP1 pathway. In the absence of unfolded proteins BiP associates with IRE1 and maintains it in a monomeric inactive form. In a stressed cell, BiP associates to misfolded proteins, while IRE1 undergoes dimerization followed by autophosphorylation, which ultimately leads to its activation. Activated IRE1 mediates the splicing of *XBP1* mRNA by excision of the intron from the *XBP1* transcript, which results in the production of a potent transcription factor, XBP1s. The latter regulates many UPR target genes to promote protein folding in the ER lumen, ER-associated degradation (ERAD) of misfolded proteins and ER biogenesis.

1.5.2 A role of IRE1-XBP1 pathway in immunity

XBP1s is a transcription factor that plays an important role in several immune cell types. First, it was shown to be involved in terminal differentiation of B lymphocytes to plasma cells, as well as in the production of antibodies and interleukin 6 (IL-6), a cytokine essential for plasma cell differentiation [120] [121]. Subsequently, it was found that stimulation of macrophages via Toll Like Receptors (TLRs) leads to the activation of IRE1 and subsequent upregulation of XBP1s. Interestingly, activation of the IRE1-XBP1 pathway occurred independently of the two other branches of the UPR and was required for the optimal secretion of specific cytokines, such as IL-6, TNFβ, and IFNβ [122].

Again, XBP1s was shown to be a prerequisite for DCs differentiation and survival [123]. Conversely, in ovarian cancer patients, XBP1s was found to cause tumour-associated DCs (tDC) dysfunction. Specifically, the tumour microenvironment generates metabolic by-products, such as unsaturated aldehyde 4-hydroxy-trans-2-nonenal (4-HNE), which induces a sustained ER stress in tDCs. In other words, constitutive activation of the IRE1-XBP1 pathway driven by 4-HNE, leads to the accumulation of lipids in tDCs, and as a result disrupts their homeostasis and impairs the antigen presentation. In this case, tumour cells hamper the normal activity of tDCs to eliminate T cell-mediated anti-tumour responses. Accordingly, therapeutic silencing of XBP1 in tDCs enhances anti-tumoural responses against ovarian cancer cells [124]. Apart from this, induction of XBP1s was shown to be essential for differentiation of the $CD8^+$ T cells into effector cells during an acute infection, however the exact mechanism of this process remains unknown [125]. In the recent study of ovarian cancer, tumour-infiltrating $CD4^+$ and $CD8^+$ T cells were found to have increased level of XBP1s. Notably, the increase of XBP1s was associated with decreased production of IFNγ [126].

1.6 HODGKIN LYMPHOMA

Several cases of HL were described for the first time by Thomas Hodgkin in 1832 [127]. Initially, it was referred to as Hodgkin's disease and only after it was realized it is a type of lymphoma the name was changed to Hodgkin lymphoma [128]. HL occurs in 3 cases per 100.000 people, and accounts for 10% of all lymphomas [127] [129]. HL is characterized by a unique bimodal distribution of age-specific incidence rates with two peaks in the age groups of 15-34 years, and older than 55 years. Moreover, it affects men more frequently than women [130]. Based on the histological picture and phenotype of malignant cells, HL is divided into classical HL (cHL), and nodular lymphocyte-predominant Hodgkin lymphoma (NLPHL) that accounts for 5% of cases. The HL can be further divided into 4 different subtypes: nodular sclerosis (NSHL), mixed cellularity MCHL), lymphocyte-depleted (LDHL), and lymphocyte-rich classical Hodgkin's lymphoma (LRCHL) [129] [131]. The hallmark of HL is a presence of malignant cells known as mononucleated Hodgkin cells and multinucleated Reed-Sternberg (RS) cells. The latter population of cells stems from Hodgkin cells that undergo a process similar to endomitosis, a nuclear division without cellular one, which in turn leads to formation of bi- and multinuclear RS cells [132] [129].

A typical malignant lymph node in HL contains a scarce number (0.1-2%) of Hodgkin and Reed-Sternberg (HRS) cells, which are embedded into a rich infiltrate of variegated immune cells. The presence of an inflammatory microenvironment promotes survival of HRS cells and facilitates an immune attack evasion [128] [129]. HRS cells constitutively express CD30, and CD15 (70-80%), but

only in minority of cases they express CD20 [133] [128]. Interestingly, HRS cells show decreased expression of B cell markers but they frequently express markers typical for other haematopoietic cell lineages, such as T cells (CD3, CD4), dendritic cells (fascin, CCL17), myeloid cells (colony-stimulating factor 1 receptor and α1-antitrypsin), or cytotoxic molecules (granzyme B, perforin) [128]. The reason why HRS cells express such diverse markers is a global dysregulation of signalling pathways, which either suppress the expression of B cell markers or support expression of other immune cell phenotypes. Pathways that are frequently affected in HRS cells include: NF-κB, janus kinase (JAK)–STAT, PI3K–AKT, ERK, AP-1, NOTCH 1 and receptor tyrosine kinases [128].

The expression of such a unique compilation of markers and restricted number of malignant cells in the tumour microenvironment made it challenging to establish HRS cell origin [132]. However, the advent of new technologies enabled precise analysis of HRS cells, which allowed for cell origin determination. Detection of rearranged and somatically mutated *immunoglobulin (Ig) V* genes in dissected HRS cells eventually revealed their B-cell origin, as these genes are highly specific for the germinal centre (GC) B cells. Under normal circumstances, the GCB cells that acquire unfavourable mutations, rendering *Ig V* genes non-functional, undergo immediate apoptosis. Even though, HRS cells harbour similar mutations they manage to avoid apoptosis and initiate lymphomagenesis. Hence, majority of HL cases are of GCB cell origin, and only limited cases (1-2%) with T cell receptor rearrangement are of T cell origin [128] [129] [132].

In almost 40% of HL cases, the HRS cells are latently infected by Epstein-Barr virus (EBV) [132] [128]. Generally, EBV can cause different types of latency, but HRS cells show EBV latency II, which is demonstrated by the expression of a set of viral proteins, such as: EBV nuclear antigen 1 (EBNA1) and latent membrane proteins 1 and 2a (LMP1 and LMP2a). EBNA1 is a prerequisite of viral genome replication and is expressed by all EBV-positive cells. It's been shown that EBNA1 not only can down-regulate tumour-suppressor genes, but also upregulate CCL20 to attract Treg cells into the HL microenvironment [127]. LMP1 clusters in the cell membrane and acts as CD40 receptor which triggers the stimulation of NF-κB and PI3K/AKT pathways. Finally, LMP2a is endowed with a cytoplasmic motif, which mimics the ITAM motif of B cell receptor (BCR). As CD40 and BCR signalling are critical survival signals for GCB cells, it is speculated that LMP1 and LMP2a can rescue B cells with unfavourable mutations from apoptosis by mimicking these signals. Hence, EBV infection of GCB cells may provide an explanation as to why and how these crippled B cells survive and initiate lymphomagenesis [129] [132] [127].

1.6.1 The Tumour Microenvironment in HL

HRS cells represent a small fraction (0.1-2%) of cells found in a typical lymph node of HL patient. These malignant cells are embedded into an inflammatory tissue, which consists of different immune cell types, including: T cells, macrophages, B cells, mast cells, eosinophils, macrophages, plasma cells, and broad connective tissue encompassing fibroblasts and collagen fibres (Figure 1.7).

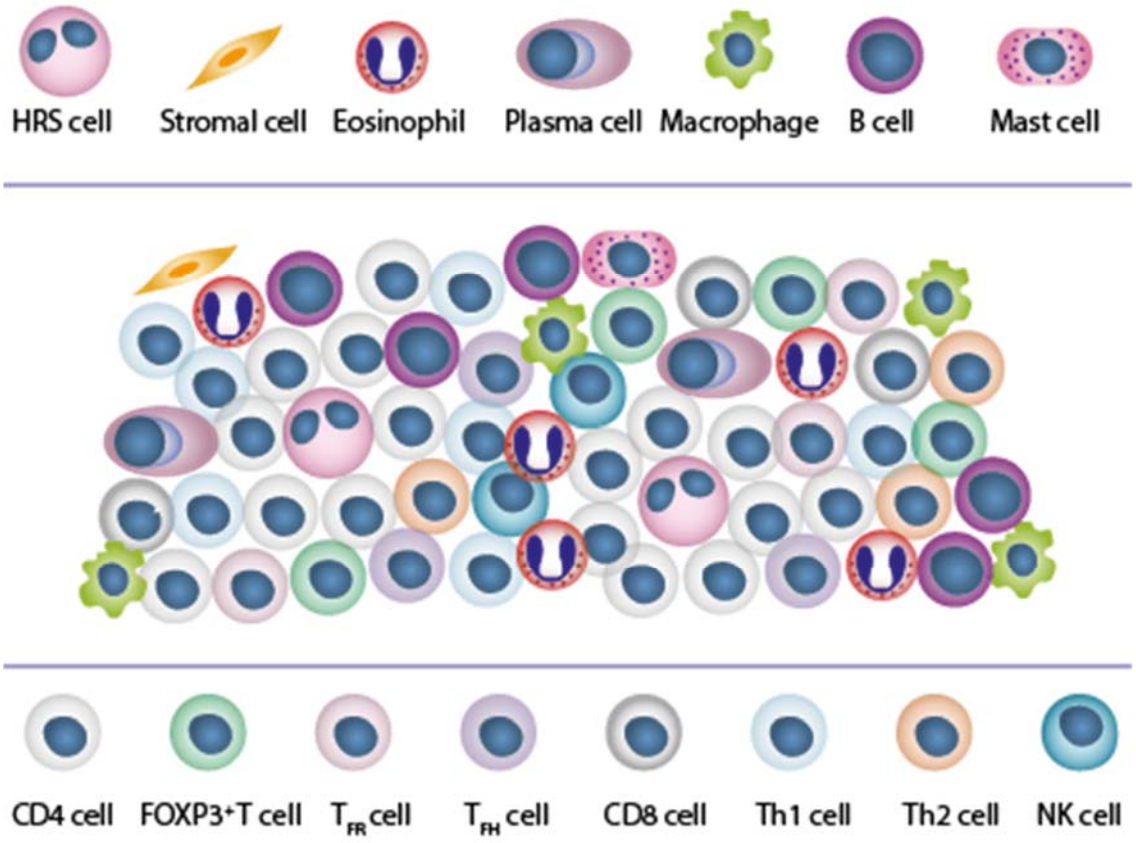

Figure 1.7: The tumour microenvironment in HL. Figure illustrates a typical tumour microenvironment of the Hodgkin lymphoma with scarce number of malignant cells ~2% infiltrated by recruited cells.

The predominant population in such a lymph node is T cell family, which encompasses different subsets, specifically T helper (Th) cells, T reg, and cytotoxic T lymphocytes (CTLs). The first two groups promote HRS cells survival and protect them from the anti-tumour immune responses [127] [133] [134]. The immune cells are attracted to the tumour microenvironment (TME) by a range of cytokines that are secreted by the HRS cells. Specifically, chemokines such as CCL5, CCL17/TARC, CCL22/MDC, and IL-5 facilitate recruitment of $CD4^+$ T cells into the tumour milieu. The histological sections often show that HRS cells are surrounded by a rosette of T cells, which not only form a physical barrier against cytotoxic cells, but also promote the HRS cells survival by various ligand-receptor interactions, including CD80 and CD40-CD40L. These interactions provide pro-survival

signals for HRS cells and protect them from elimination by the immune system [135] [133] [127] [134]. Further, secreted by HRS cells CCL5 attracts mast cells and macrophages which are immunosuppressive. Importantly, the number of tumour infiltrating macrophages correlates with HL patient's prognosis, as these cells might support the growth of HRS cells and prevent an effective immune response towards HRS cells [131] [132].

Moreover, fibroblasts are a substantial component of the malignant lymph node, and they form typical for HL scar tissue. The recruitment of fibroblasts and subsequent formation of fibrosis in the neoplastic tissue is driven by the presence of cytokines, such as IL-13, TNFα, TGFβ, and fibroblast growth factors. As follows, fibroblasts activated with these cytokines and CD40/CD40L interaction contribute to production of diverse cytokines/chemokines including eotaxin and RANTES that attract eosinophils or Treg cells and promote proliferation of HRS cells. Furthermore, fibroblasts in the HL microenvironment are a source of collagen type I. The interaction between HRS cells and collagen has been shown to activate DDR1, a receptor tyrosine kinase (RTK) that is frequently expressed in HL and renders malignant cells resistant to apoptosis [132] [129] [136].

The eosinophils attracted to the tumour microenvironment stimulate CD30L/CD30 interaction with HRS cells. A recent study implicates the exosome vesicles in delivering the CD30 molecule to CD30L positive cells to stimulate interleukin 8 (IL-8) production. This interleukin, secreted also by HRS cells, facilitates attraction of neutrophils [127].

The microenvironment in HL represents a unique niche of reactive immune cells, with the malignant cells accounting for up to 2% of cells in the affected lymph node. These inflammatory cells are recruited to the lymph node to enable interactions with HRS cells, which in turn provides prerequisite signals for HRS cells survival and proliferation. The fact that HRS cells thrive in the malignant lymph node, while are typically not present in the peripheral blood circulation, further supports the importance of the interplay between malignant cells and the tumour infiltrating cells.

1.6.2 Immune evasion mechanisms in HL

As discussed in previous sections, HRS cells rely on the rich inflammatory microenvironment and employ a multitude of signalling pathways to support their growth and anti-apoptotic phenotype. These malignant cells have also developed an array of immune evasion mechanisms to thrive in the tumour microenvironment and avoid an immune attack.

Over the past years, a range of strategies utilised by HRS cells to suppress anti-tumour activity of surrounding immune cell infiltrate were identified. The major component of the malignant lymph node – T cells, along with HRS cells secrete immunosuppressive cytokines, such as IL-10 and TGFβ,

which inhibit cytotoxic T cell function [128]. The latter molecule is also known to dampen NK cell proliferation and cytotoxic activity by down-regulation of activating receptors NKG2D and NKp30 [137]. Further, HRS cells shape the immunosuppressive microenvironment by direct interactions with immune cells. Indeed, HRS cells overexpress a surface molecule FasL that binds to a cognate receptor on cytotoxic T cells and induces their apoptosis. Although, HRS cells express Fas receptors on their surface, they manage to avoid Fas-induced apoptosis due to overexpression of cellular FADD-like interleukin 1β –converting enzyme-inhibitory protein (cFLIP) that inhibits death receptor signalling [138].

Similarly, galectin-1 is overexpressed on the surface of HRS cells, which can induce apoptosis of activated T cells in HL and promote Treg cells mediated suppression [139, 140]. Moreover, galectin-1 overexpression is associated with reduced infiltration of T cells, whereas blockade of galectin-1 enhances T cell mediated responses [141]. Furthermore, HRS cells were found to express high level of PD-1 ligands, namely PD-L1, and PD-L2. Signalling mediated via PD-1/PD-L1/PD-L2 axis leads to T cell exhaustion, which is a reversible state of T cell activation and proliferation inhibition. The large body of evidence indicates that upregulation of PD-1 ligands on HRS cells is attributable to the amplification of *9p24.1* gene locus. The expression of these ligands is further intensified by the enhanced JAK2 signalling typical for HL. Likewise, EBV upregulates expression of PD-L1 through LMP1, a molecule that induces JAK-STAT and AP-1 pathways [142] [135] [134]. It has also been demonstrated that HRS cells induce PD-L1 expression on TAMs to further enhance the immunosuppressive environment [142].

Frequent loss of MHC-I molecule is another mechanism that enables HRS cells to escape CD8+ T cell surveillance. Several lines of evidence indicate that lack of MHC-I expression and β2-microglobulin (B2M) at the surface of HRS cells pertains to 80% of HL cases. The gene for *B2M*, a component of the MHC-I complex, carries inactivating mutations in a proportion of cases, which explains why the immunohistochemistry stains have shown either a complete loss of MHC-I or intracellular accumulation of MHC-I heavy chains. The retention of the MHC-I heavy chains may result from the loss of β2-microglobulin expression, which normally assembles the MHC-I molecule and transports it to the cell surface. Similarly, the MHC-II molecule expression is also reduced at the surface of HRS cells, which is caused by a recurrent chromosomal translocation of the MHC-II transactivator (*CIITA*). Inactive *CIITA* gene leads to reduced expression of the MHC-II molecule and hampered antigen presentation to $CD4^+$ T cells [134] [132] [143] [144] [145].

Conversely, almost 60% of HL cases with the loss of MHC-I expression were found to overexpress the non-classical MHC-I molecule HLA-G. The latter is the ligand for inhibitory receptors present on

a range of immune cells including NK cells or T cells, and the engagement of these receptors with HLA-G may lead to the immune evasion [146, 147].

Another immune evasion mechanism employed by HRS cells involves a high expression level of the disulphide-isomerase ERp5 and the disintegrin-metalloproteinase ADAM10. These enzymes are capable of shedding the ligands for NKG2D, such as MICA and ULBP3, from the cell membrane. As a result, HRS cells manage to escape T cell or NK cell mediated cytotoxicity due to the lack of cognate ligands for NKG2D. In fact, high levels of soluble NKG2D ligands, in patient's serum are correlated with disease progression in a range of blood cancers, including MM, CLL, NHL, and AML [148].

Collectively, HRS cells are able to efficiently escape from the host immune attack through various mechanisms, including release of chemokines modulating an immunosuppressive microenvironment as well as the expression of surface molecules gaining immune privilege through the reduction of HRS cell immunogenicity.

1.7 AIMS AND HYPOTHESIS

1.7.1 Hypothesis

I. NK cell stimulation involves activation of the IRE1-XBP1 pathway (***Aims A and B - Chapter 3***).

II. Activation of the IRE1-XBP1 pathway is impaired in NK cells of HL patients (***Aims C, D, and E - Chapter 4***).

1.7.2 Aims

The primary aim of this thesis is to determine if and how the IRE1-XBP1 pathway activation is associated with NK cell function in the context of HL.

Aim of chapter 3:

A. To determine if the IRE1-XBP1 pathway is activated following NK cell stimulation by target cell lines representing a range of blood cancers.

B. To investigate if blockade of the IRE1-XBP1 pathway is relevant for NK cell effector function.

Aim of chapter 4:

C. To determine if the IRE1-XBP1 pathway is impaired in circulating pNK of pre-therapy HL patients.

D. To characterise in detail, the nature of NK-cell dysfunction and its relationship with the IRE1-XBP1 pathway in HL.

E. To test the ability of PD-1 blockade to reverse IRE1-XBP1 pathway associated pNK cell dysfunction.

CHAPTER 2:

Materials and Methods

2.1 ETHICS

The study protocols used in this thesis were approved by The Translational Research Institute (TRI) Human Research Ethics Committee (Brisbane, Australia) and the Princess Alexandra Hospital Human Research Ethics Committee (Brisbane, Australia). Informed consent was obtained from all subjects prior to sample collection.

2.2 STUDY POPULATION

Table 2.1: Demographic information on Hodgkin lymphoma patients tested in the study.

Pre-therapy Hodgkin lymphoma study population			
Age (range)	**Sex**	**Histology**	**Stage I/IIA vs IIB/III/IV**
Median 31 years (16-73)	60% F: 40% M	60 % Nodular Sclerosing; 10 % Lymphocyte Rich; 30% Nodular Lymphocyte Predominant;	40% vs 60%

2.3 MEDIA AND BUFFERS

Foetal Bovine Serum (FBS) (*Life Technologies)**:***

Prior to aliquoting and storage at -20°C, the FBS was heat inactivated at 56°C for 60 minutes.

Donor Equine Serum (ES) (*Hyclone, ThermoFisher Scientific):*

Prior to aliquoting and storage at -20°C, the ES was heat inactivated at 56°C for 60 minutes.

Roswell Park Memorial Institute (RPMI) 1640 medium *(Life Technologies):*

Medium was supplemented with 100U/mL of Penicillin (*Bristol-Myers Squibb)*, 100µg/ml Streptomycin (*Bristol-Myers Squibb)*, and 292µg/ml L-glutamine (*Life Technologies*) before use.

R10 Medium

RPMI (with penicillin/streptomycin/L-glutamine) supplemented with 10% FBS.

Recombinant human Interleukin-2 (IL-2) (*Promega):*

Solution of IL-2 resuspended in RPMI medium at a concentration of 60U/µl.

Recombinant human Interleukin-15 (IL-15) (*PeproTech*):

Solution of IL-15 at a concentration of 100ng/µl. Stored at -20°C until use.

Freezing Medium

80% FBS and 20% dimethyl sulfoxide (DMSO) (*Sigma-Aldrich*)

TBE (10×)

108g Tris, 55g boric acid (*Sigma-Aldrich*), 40ml 0.5 M Ethylenediaminetetraacetic acid (EDTA) pH 8 (*Sigma-Aldrich)*, 800ml of MilliQ H_2O. Heat and stir with a magnetic stirrer. Use 1X working solution (diluted in MilliQ H_2O).

FACS Buffer

PBS (*Life Technologies*) supplemented with 2% FBS

MACS Buffer

PBS (*Life Technologies*) supplemented with 0.5% FBS and 2mM EDTA (*Sigma-Aldrich*)

Nuclease-Free Water:

UltraPure™ DNase/RNase-Free Distilled Water (*Life Technologies)*

Agarose Gel

Appropriate amount of Agarose powder (*Sigma-Aldrich*) is added to 100mL 1x TBE depending on the required percentage of gel. For instance, 2 g is added to 100ml 1x TBE to obtain 2% agarose gel. This is then heated in a microwave to dissolve powder. After cooling down the liquid to ~60C, 5µL of SYBR safe DNA gel stain (*Life Technologies, Grand Island, USA*) is added to 100mL of gel.

0.5% Paraformaldehyde

A 1ml of 16% paraformaldehyde (*EMS*) is added to 31 ml of PBS (*Life Technologies*) to obtain 0.5% paraformaldehyde.

Buffered glycerol with anti-fade

A 10ml of 0.2M TRIS buffer (pH 8.0) and 500mg of n-propyl gallate is added to 90ml of 90% glycerol.

2.4 CELL CULTURE AND STORAGE

2.4.1 Expansion of SNK10 cell line

SNK10 cells, kindly provided by Prof Martin Rowe at the Institute for Cancer Studies, Birmingham, UK following permission from Dr Norio Shimizu [149]. Cells were cultured at 3×10^5 cells/mL in R10 medium with 120U/mL IL-2. Fresh medium and IL-2 was added to cultures twice a week and cells were expanded when confluent.

2.4.2 Expansion of KHYG-1 cell line

KHYG-1 cells, purchased from Japan Collection of Research Bioresources (JCBR) cell bank, were cultured at 3×10^5 cells/mL in R10 medium with 100U/mL IL-2. Fresh medium and IL-2 was added to cultures twice a week and cells were expanded when confluent.

2.4.3 Expansion of NK-92 cell line

NK-92 cells, purchased from American Type Culture Collection (ATCC), were cultured at 3×10^5 cells/mL in RPMI medium supplemented with 12.5% of FBS, 12.5% ES, and 200U/mL IL-2. Fresh medium and IL-2 was added to cultures twice a week and cells were expanded when confluent.

2.4.1 Expansion of NK-92 cell line

NK-92.MI cells, purchased from ATCC, were cultured at 3×10^5 cells/mL in RPMI medium supplemented with 12.5% of FBS, 12.5% ES. Fresh medium was added to cultures twice a week and cells were expanded when confluent.

2.4.2 Culture of target cell lines

To assess NK cell effector function the cell lines K562, KM-H2 and HDLM-2 were used. K562 cell line was grown in R10 medium which was changed twice a week. KM-H2 and HDLM-2 cell lines were grown in R20 medium which was changed twice a week. Cells were expanded when confluent.

2.4.3 Cryopreservation of Cells and Thawing of Cryopreserved cells

Cells to be cryopreserved were counted and assessed for viability with the use of Trypan Blue stain (*Sigma-Aldrich*). Subsequently, cells were pelleted at 1500 rpm for 5 min and resuspended at 1×10^7 cells/mL in freshly made Freezing Medium. 1mL aliquots were added to cryovials (*Thermo Fisher Scientific*) and transferred into a cryo-freezing container (Mr Frosty™; *Nalgene, NalgeNunc*) that was stored at $^{-}80^{o}$C for 24 hours before being transferred to Liquid Nitrogen for long term storage.

2.4.4 Thawing of Cryopreserved cells

Cryovials containing the frozen cells were removed from liquid nitrogen and transported on dry ice. Vials were then immediately placed into a 37^{o}C water bath. Thawed cells were transferred to a 10mL tube (*BD Biosciences*) containing 9ml of warmed R10 medium. Cells were then centrifuged at 1500rpm for 5min to wash away DMSO. Afterwards, cells were resuspended in an appropriate amount of culture medium and transferred into the appropriate culture vessel.

2.5 PERIPHERAL BLOOD MONONUCLEAR CELLS SAMPLES PROCESSING

Cryovials containing the frozen cells were removed from liquid nitrogen and transported on dry ice. Vials were then immediately placed into a 37^{o}C water bath. Once 60-70% of vial content is thawed, cells were mixed by pipetting up and down, and transferred to a 10mL tube (*BD Biosciences*) containing 9ml of warmed RPMI medium. Cells were then centrifuged at 1500rpm for 5min to wash away DMSO. The washing step was performed twice. Afterwards, cells were resuspended in an appropriate amount of culture medium and counted. To break down clumps present in thawed samples cells were treated with 200 Kunitz of DNase I (*Sigma*) for 15 min at 37°C. If clumps persist in the sample, cells were then passed through a 70µM mesh cell strainer (*Miltenyi Biotec, Germany*) into a fresh conical tube. The cell suspension was then ready for cell counting and for downstream applications.

2.6 INHIBITION OF IRE1-XBP1 PATHWAY

2.6.1 Inhibition of IRE1-mediated splicing of *XBP1*

During ER stress, IRE1 undergoes phosphorylation and excises a 26-nucleotide intron out of *XBP1* mRNA. This leads to a frame shift in the protein's code and results in a production of the active protein XBP1s. To interrogate the importance of *XBP1* splicing during NK cell-mediated cytotoxicity, IRE1-mediated splicing of *XBP1* was inhibited with 8-formyl-7-hydroxy-4-methylcoumarin (4μ8c, *Sigma-Aldrich*), a potent and selective IRE1α inhibitor. 4μ8C blocks substrate access to the active site of IRE1 and selectively inactivates both XBP1 splicing and IRE1-mediated mRNA degradation [150]. For inhibition in NK cells, 60μM of 4μ8c was added to cultures at the same time as target cells.

2.6.2 Induction of the Endoplasmic Reticulum stress

Thapsigargin (TG) is a highly potent and selective inhibitor of calcium dependent ATPases. It depletes calcium storage in the ER that leads to subsequent reduction of calcium dependent chaperones activity, and in turn contributes to accumulation of unfolded proteins and activation of the UPR [151] [152]. NK cells were treated with this molecule at a final concentration of 100nM/ml for 2 or 6 hours depending on the assay. For this, cells were cultured in the RPMI medium supplemented with appropriate amount of IL-2 (refer to section 2.3).

2.6.3 CHECKPOINT BLOCKADE

2.6.4 PD-1 blockade assay

Pembrolizumab is a humanized IgG_{4K} isotype antibody that targets PD-1, a checkpoint inhibitor expressed on immune effector cells and implicated in tumour immune-escape mechanisms. Pembrolizumab has distinctive immunomodulatory activity and is used in the immunotherapy of cancer to enhance cytotoxic activity of effector cells toward cancer cells [153]. For blocking assay, NK cells were pre-incubated for 72hrs with this antibody at the final concentration of 10μg/ml. In parallel, a batch of NK cells was pre-incubated with human IgG_{4K} isotype control antibody (*BioLegend*) to control for the non-specific binding affinity to cells.

2.7 STIMULATION OF NK CELLS

2.7.1 Stimulation with target cells – Direct cytotoxicity

To stimulate SNK10 cells to kill by direct cytotoxicity, NK cells were incubated at a 1:1 ratio with K562 target cells. This ratio was used based on the established protocols within the laboratory. This ratio triggers a powerful NK cell stimulation that allows detection of effector molecules. Stimulation was performed in NK cell culture medium as described in section 2.3. NK cells were stimulated for 2 hours for RNA extraction unless stated otherwise. For RNA extractions, 3×10^5 NK cells were incubated with the same number of target cells.

Following stimulation with target cells, NK cells were separated from target cells using the NK cell isolation kit (*Miltenyi Biotec, Germany*), as per the manufacturer's instructions, prior to RNA extraction. Briefly, cells were centrifuged at 1500rpm for 10min and then resuspended in 40µL of MACS buffer and 10µL if NK cell biotin-antibody cocktail. To allow for binding it was incubated for 10 min at 4^{o}C prior to addition of a further 30µL of MACS buffer and 20µL of NK cell micro-bead cocktail. This was incubated for 15 min at 4^{o}C and after this time, cells were washed in 1mL of MACS buffer and centrifuged at 1500rpm for 10 min. During this spin, LS columns were rinsed with 3ml of MACS buffer. Pelleted cells were resuspended in 500µL of MACS buffer and applied on the prepared column flow through into collection tubes. Columns were washed with 3ml of MACS buffer. After collection of the flow through, isolated NK cells were centrifuged, supernatant removed, and RNA was then extracted. For RNA extraction protocol refer to section 2.8.1. An aliquot of cells before and after isolation was collected and NK cell purity was assessed using the flow cytometry. On average, the NK cells were demonstrated to be more than 90% pure (Figure 2.1).

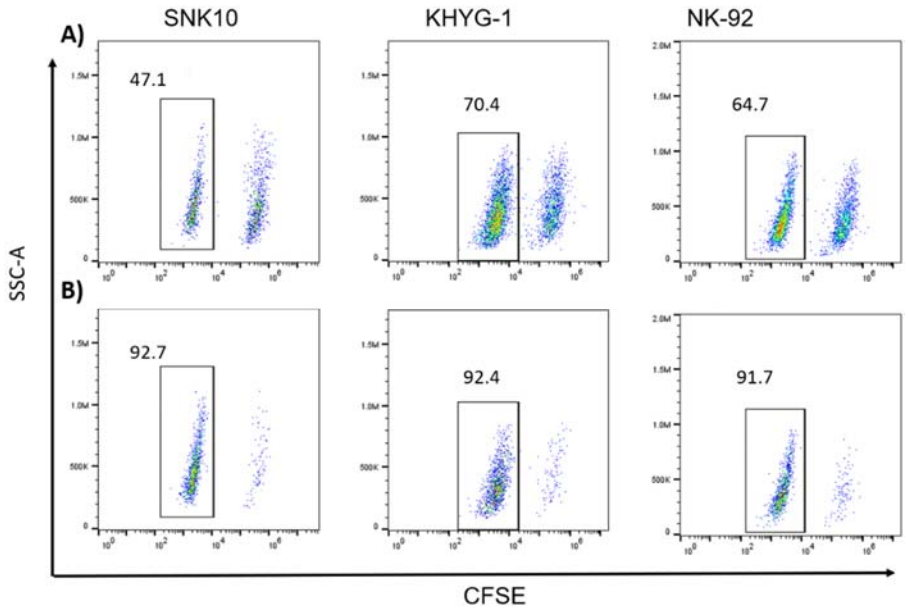

Figure 2.1: Isolation of Stimulated NK cells using MACS. SNK10 cells, KHYG-1 cells and NK-92 cells were separated from target cells following stimulation using MACS. Purity of isolated NK cells was more than 90% as presented on the graph showing NK cell purity before (A) and after isolation (B).

2.8 GENE EXPRESSION PROFILING

2.8.1 RNA extraction – RNeasy Mini Kit

Total RNA from NK-cells was extracted using the miRNeasy Mini Kit (*Qiagen*) according to the manufacturer's protocol. Briefly, cell pellets (3×10^5 cells) were lysed by addition of 700µL of QIAzol lysis reagent. The cell suspension was vortexed for 1 min to homogenize the cells and then left on the benchtop for 5 min to facilitate dissociation of nucleoprotein complexes. 140µL of chloroform was then added to this homogenised lysate and mixed by vigorous shaking. The homogenate was left at the benchtop for another 3 min and then centrifuged for 15 min at 12.000 x g at 4°C to separate out the RNA phase. The latter was then transferred to a new tube and admixed with 1.5 volume of 100% ethanol. The sample was then transferred into a RNeasy Mini spin column and centrifuged at 8.000 x g for 15 sec at RT, the flow through was discarded and this was repeated with remaining sample. The column was then washed with 350µl of RWT buffer and centrifuged for 15sec at 8.000 x g. Then the RNA bound to the membrane underwent DNase treatment by application of 80µl of DNase I incubation mix (10µl of DNase I diluted with 70µl RDD buffer, *Qiagen*) directly on the RNeasy Mini Spin Column membrane and incubation for 15 min at RT. After this time the column was washed with 350µL of RW1 buffer and twice with 500µL of RPE buffer, centrifuged at 8000×g

for 15 sec each time except for the last wash when the column was centrifuged for 2 min to dry out the membrane and eliminate the residual ethanol. Dried columns were then placed in a new 1.5mL eppendorf tube and RNA eluted by centrifugation for 2 min at 8000×g to 14µL of RNase-free water. RNA quantification was performed using the NanoDrop 2000 spectrophotometer (*ThermoFisher Scientific*). All RNA samples were stored at -80ºC.

2.8.2 Random Primed First Strand cDNA Synthesis

RNA templates were reverse-transcribed to cDNA using SuperScript® III Reverse Transcriptase (*Life Technologies*). For this, 300-1000ng of RNA diluted to 12µl in ultra-pure water (*Life Technologies*), 0.5µl of random hexamers (500µg/mL; *Promega, Madison, USA*) and 1µL of 10mM dNTPs (500µM final concentration; *Promega*) were incubated for 5min at 65ºC and then placed on ice for 2 min. Afterwards, the mix was combined with 0.5µL RNasin (40U/mL; *Promega*), 4µL of 5X first-strand buffer, 1µL of 0.1M DTT, and 1µl of Super Script® III Reverse Transcriptase (200U/mL). This sample was subjected to the following RT-PCR program: 25˚C 10 min, 50˚C 1hr and 70˚C 15 min using the Applied Biosystems 2720 thermocycler. Samples were diluted to receive the final concentration of cDNA 2.5 ng/µl.

2.8.3 Primers used for PCR analysis

Primers used for Real Time RT-PCR were designed using Primer3 software (http://primer3.wi.mit.edu/). Primers were designed to amplify 100- 150bp regions within the open reading frame of selected genes. Default settings within the Primer3 software were used. All primers were ordered from *Integrated DNA Technologies* and arrived as lyophilizate. Primers were resuspended in Ultra-pure water (*Life Technologies*) to obtain a stock concentration of 100µM and working concentration of 10µM. A list of primers used can be found in Table 1.

Table 2.2: Primers used for Real Time PCR.

Gene	Sequence Forward (5' to 3')	Sequence Reverse (5' to 3')
IFNG	GAGTGTGGAGACCATCAAGGA	CAGCTTTTCGAAGTCATCTCG
GZMB	CCCTGGGAAAACACTCACAC	TTCGCACTTTCGATCTTCCT
TNF	TCTGGGCAGGTCTACTTTGG	GGTTGAGGGTGTCTGAAGGA
FASLG	ATCCTGAGCCATCGGTGAAA	ACCCCTACAATTGCACTGGA
NKG2D	ATCGCTGTAGCCATGGGAAT	GGAATACAGCACTCCATATTGTT
CD16	TGAGGTGTCACAGCTGGAAG	TGAGTGTGGCTTTTGGAATG
XBP1u	CGCAGCACTCAGACTACG	GAAGGGCATTTGAAGAACAT
XBP1s	GAGTCCGCAGCAGGTGC	CAAAAGGATATCAGACTCAGAATCTGAA
B2M	ACTCTCTCTTTCTGGCCTGGAG	CATTCTCTGCTGGATGACGTGAG
GAPDH	AATCCCATCACCATCTTCCA	TGGACTCCACGACGTACTCA

2.8.4 Real Time RT-PCR

Gene expression profiling was performed by qPCR using the Roche Light Cycler 480 System. 10µl reaction containing 5µl of PowerUp SYBR Green Master Mix (*Applied Biosystems by Life Technologies*), RNase-free H_2O, 0.2µM forward and 0.2µM reverse primers, and 5ng of DNA per well. Each sample was analysed in triplicate. Samples were then subjected to an initialization step (1 cycle at 95°C for 10 min), followed by 45 cycles of amplification: denaturation at 95°C for 15sec, annealing along with elongation at 60°C for 60sec. Finally, the reaction ended with Melting Curve analysis to assess whether SYBR green has produced single, specific products.

Quantification of samples was determined using the Light Cycler 480 software (*Roche*) relative quantification analysis. Relative quantification analysis provides the relative expression of samples compared to a control sample. For all real time analysis in this thesis untreated SNK10 cells were used as the control sample.

Relative expression values given using comparative quantification analysis were normalised to the expression of the house-keeping gene *B2M* to account for slight variations in cDNA concentrations. Experiments were repeated three times as indicated in results with technical triplicates and water negative controls.

2.9 PRIMARY NK CELL EXPANSION

2.9.1 Expansion of NK cells from Peripheral Blood Mononuclear Cells

Primary NK (pNK) cells were expanded from cryopreserved PBMCs. For this, NK-cells were stimulated with irradiated feeder lymphoblastoid cell lines (LCL) on day 1 (effector: stimulator ratio 1:5) and cultured in 24-well flat bottom plates at 1.0 x 10^6 cells/mL in RPMI 1640 (*Gibco, Life Technologies*) with 10% fetal bovine serum (*Gibco, Life Technologies*), 100U/mL penicillin/streptomycin (*Bristol-Myers Squibb*), and 100 U/ml IL-2 (*Promega*), and 10ng/ml IL-15 (*PeproTech*) at 37°C in a 5% CO_2 incubator. Then every 2-3 days, cultures were supplemented with IL-2/IL-15 and re-stimulated with LCL (on day 7-10) at an effector: stimulator ratio 1:5. Expansion was typically for 14 days.

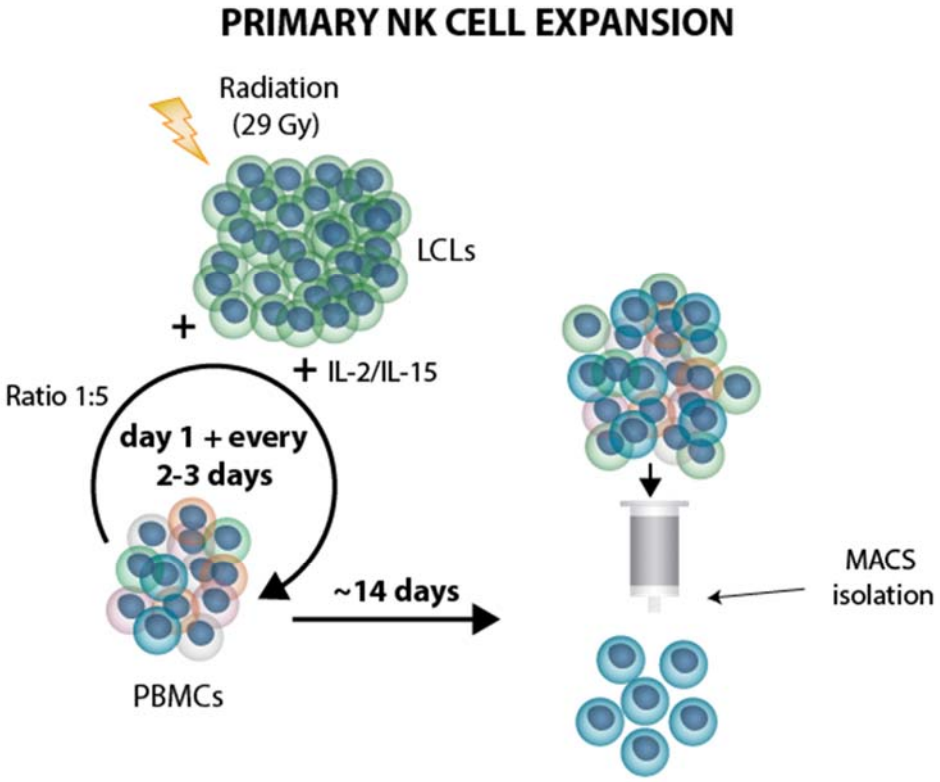

Figure 2.2: Primary NK cell expansion assay. On day 1 and then every 2-3 days PBMCs from HL patients were stimulated with irradiated LCLs (ratio 1:5) as well as IL-2 and IL-15 to ensure optimal expansion of pNK cells. At the end of expansion process, typically on day 14, expanded pNK cells were isolated using NK cell isolation kit and MACS column-based system for downstream applications.

2.9.2 Isolation of Expanded NK Cells

Following expansion of primary NK cells, untouched NK cells were purified using the NK cell isolation kit (*Miltenyi Biotec, Germany*) as per the manufacturer's instructions. Briefly, 10^8 PBMCs were centrifuged at 1500rpm for 10min and then resuspended in 400µl MACS buffer and 100µl NK cell biotin-Antibody cocktail was added and incubated for 10 min at 4°C. To allow for binding it was incubated for 10 min at 4°C prior to addition of a further 300µl of MACS buffer and 200µl of NK cell micro-bead cocktail. This was incubated for 15 min at 4°C and after this time, cells were washed with MACS buffer and centrifuged at 1500rpm for 10 min. During this spin, LS columns were rinsed with 3ml of MACS buffer. Pelleted cells were resuspended in MACS buffer and applied on the prepared column flow through into collection tubes. Columns were washed with 3ml of MACS buffer.

After collection of the flow through the purity of isolated NK cells was assessed by expression of CD3, CD56 and CD16 using the flow cytometry. On average, the $CD3^-CD56^+$ NK cells were demonstrated to be more than 85% pure. Primary NK cells were then incubated with the anti-PD-1 or isotype control antibodies prior to the functional assays.

2.9.3 FACS-sorting of the primary NK cells

Following expansion of primary NK cells, NK cells were purified for downstream application (actin accumulation assay) by FACS-sorting.

For this, expanded cells were collected, centrifuged at 1500rpm for 5 min, resuspended in medium and counted. Prior the staining, cells were washed with PBS. Cells were stained at density $2x10^6$ cells/ml. To sort only viable cells, Zombie NIR dye was used to exclude dead cells. Further cells were washed with FACS buffer, and a surface staining antibody cocktail containing CD3, CD14, CD19, CD16, and CD56 was applied. Prior to sorting, cells were washed twice with FACS buffer and resuspended at cell density $1x10^7$ cells/ml in PBS containing 10% FBS. Example of gating strategy of pNK cells is presented below on Figure 2.3.

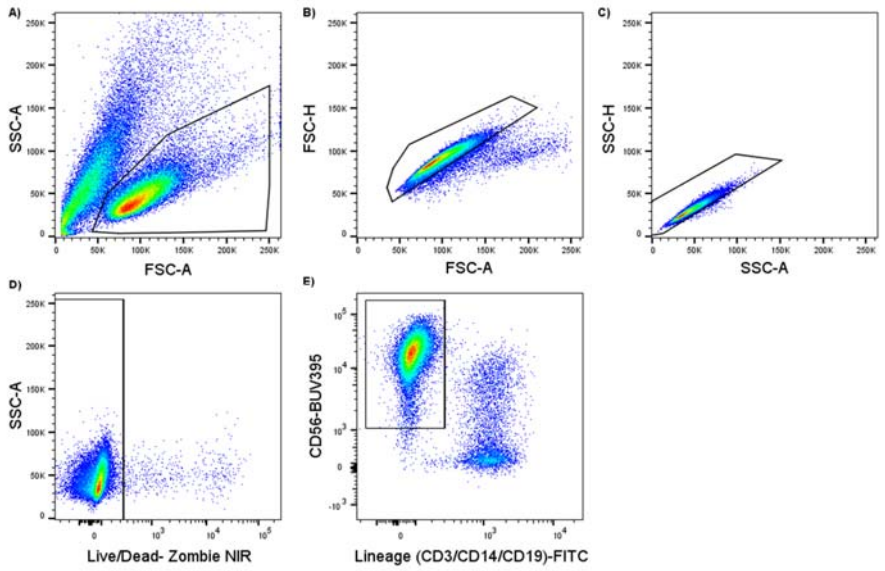

Figure 2.3: A gating strategy of FACS sorted pNK cells. Fluorochrome-conjugated surface markers used for the surface characterization of the subsets are shown in the respective plot. The initial gate was defined based on forward- and site-scatter (A), followed by discrimination of doublets using FSC-A and FSC-H (B), as well as SSC-A and SSC-H (C). Further dead cells were removed from the analysis using Zombie NIR stain (D). Finally, lineage negative (CD3/CD14/CD19) but CD56+ cells were sorted for downstream applications (E).

2.10 NK CELL ABSOLUTE COUNTS

To determine the size of NK cell compartment within PBMCs of healthy participants and HL patients, the absolute counts of NK cells were calculated. For HL patients, NK cell numbers were back-calculated by cross-referencing clinical data on the number of lymphocytes and monocytes within patient's peripheral blood at the time of diagnosis with the flow cytometry data obtained for each patient. For healthy participants, a set value of 2500 was used as an average number of lymphocytes and monocytes in healthy individuals and cross-referenced with the flow cytometry results.

Briefly, based on flow cytometry data ***NK cell percentage*** was calculated as follows:

$$NK\ cell\ percentage = (Counts\ of\ CD3^{-}CD56^{+}\ cells / Counts\ of\ Live\ cells) \times 100.$$

Then to establish the ***NK cell counts per µl***, flow cytometry data was cross referenced with clinical data:

$$NK\ cell\ counts\ per\ \mu l = (NK\ cell\ percentage \times Counts\ of\ Lymphocytes\ and\ Monocytes).$$

To calculate counts of specific NK cell subsets, information on the percentage of respective subset from flow cytometry data was cross referenced with ***NK cell counts per µl.***

2.11 FLOW CYTOMETRY

2.11.1 Table of Antibodies

All antibodies used were specific to humans and they are all listed in Table 2.3.

Table 2.3: List of antibodies used for flow cytometry.

Marker	Clone	Fluorophore	Dilution	Supplier
CD3	UCHT1	FITC	1:100	BD Pharmingen
CD14	MϕP9	FITC	1:200	BD Biosciences
CD19	HIB19	FITC	1:100	BD Biosciences
CD56	NCAM16.2	BUV395	1:400	BD Biosciences
CD16	3G8	PE-Cy7	1:400	BD Biosciences
CD107a	H4A3	APC	1:200	BD Biosciences
IFNϒ	B27	APC	1:100	Biolegend
NKG2D	1D11	APC	1:50	BD Pharmingen
FASL	DX2	BV711	1:100	BD Biosciences
TNFα	Mab11	FITC	1:30	Biolegend
Granzyme B	GB11	Alexa Fluor 700	1:20	BD Biosciences
PD-1	PD1.3.1.3	PE	1:200	Miltenyi
PD-L1	MIH1	PE-Cy7	1:30	BD Biosciences
PD-L2	MIH18	BV711	1:50	BD Biosciences
XBP1s	Q3-695	PE	1:20	BD Biosciences
CD3	SK7	APC-Cy7	1:50	BD Biosciences
CD14	MϕP9	APC-H7	1:400	BD Biosciences
CD19	SJ25C1	APC-H7	1:200	BD Biosciences

2.11.2 Assessment of cell viability staining

Cell viability was assessed with the use of Zombie NIR™ Fixable Viability kit (*Biolegend*). For this, cells were washed in PBS buffer and then resuspended in Zombie NIR™ dye diluted 1 in 2000 in PBS buffer (*Life Technology*). Cells subjected to high temperature by microwaving for 4 sec were used as a positive control. Cells were then incubated in the dark for 15 min at RT and then washed with PBS buffer prior to the next staining step. At the end, samples were acquired on the Fortessa

X20 (*BD Biosciences*) and analysed using FlowJo_v10 software (*Tree Star Inc., Ashland, USA*). Gating strategy is presented in Figure 2.4.

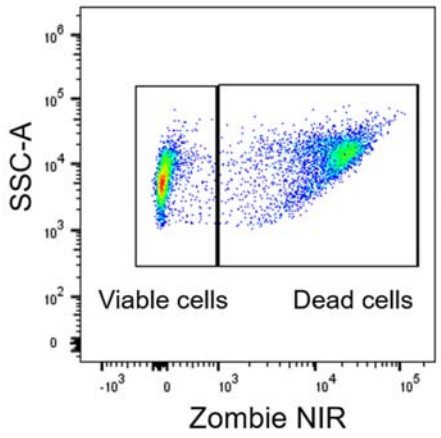

Figure 2.4: Live/dead cells gating strategy. Zombie NIR™ Fixable Viability kit was used to distinguish viable cells from dead cells. Shown are KHYG-1 cells that were subjected to high temperature to induce cell death.

2.11.3 NK Cell-Mediated Killing Assay

To determine NK cell-mediated killing of target cells, a flow cytometry-based method was used. Briefly, pNK cells were enumerated and resuspended at a concentration of 0.5 x 10^6 cells/ml. 100 µL of pNK cells were added to wells of 96-well plate. CTV-labelled target cells were also resuspended at 0.5 x 10^6 cells/ml and 100 µL were added to appropriate wells to obtain a 1:1 effector: target cell ratio. For each experiment target controls without effector cells were also seeded. In addition, 5 000 CountBright counting beads (*ThermoFisher*) were added to each well to allow for cell number calibration. Each experimental condition was performed in triplicate. After 6 hours of incubation at 37°C, cells were washed with PBS and stained for markers of interest. Flow cytometry was performed using the Fortessa X-20 and a minimum of 1 000 events were collected in the beads gate.

The number of cells in each gate was determined using FlowJo software (*Tree Star Inc.*). Briefly, beads (B) and cells were gated based on forward scatter (FSC) and side scatter (SSC). The cells were then further divided into CTV positive target cells (T) and CTV negative effector cells (E). These raw values were then analysed to determine the effectiveness of NK cell-mediated cytotoxicity. Initially this involved calibrating each cell value to the number of beads: for calibrated targets (T') T was divided by B. To determine the level of NK cell-mediated killing of target cells, the T' value of each experimental well was divided by the average T' value of target control wells. This value gave the percentage of surviving target cells and the number of cells killed was determined by subtracting this value from 1. The reduction in absolute numbers of targets by NK cells was determined by

comparison to control wells (targets without effectors) and expressed as a percentage. To determine if any observed differences were statistically significant analysis was performed as described in section 2.13.

2.11.4 Surface Staining

Flow cytometry was utilised to assess the size of various populations of cells in a sample and expression level of diverse markers by specific cell subsets. To identify different populations based on expression of various surface markers, cells (1×10^5 to 1×10^6 depending on assay) were washed in FACS buffers and resuspended in antibody cocktail diluted with FACS buffer to a total volume of 100 µl (refer to Table 2) and incubated at 4^{o}C for 20 min in the dark. The optimal antibody amount was determined based on titration. Following incubation, cells were washed twice with FACS buffer, pelleted (1500rpm/5min), and subjected to the subsequent staining step or resuspended with 300µL of FACS buffer prior the acquisition on the flow cytometer. Flow cytometry was performed using the Fortessa 20X (*BD Biosciences*) and analysed using FlowJo_v10 software (*Tree Star Inc., Ashland, USA*).

2.11.5 CD107a Staining

This staining allows for detection of the surface expression of CD107a (LAMP-1) that occurs during NK cell degranulation following stimulation. NK cells contain pre-formed cytolytic granules in their cytoplasm and these lytic vesicles consisting of perforin and granzymes are contained in lysosomes coated with lysosomal-associated membrane proteins (LAMPs). During the process of degranulation, the membrane of secretory lysosomes fuses with the plasma membrane of the activated NK cell and the lytic granules content is then released at the immunological synapse inducing death of the target cells [154].

To detect CD107a surface expression during NK cell-mediated cytotoxicity, NK cells were incubated with target cells at a 1:1 ratio for 1 hour. After this time, CD107a-APC antibody (1/200 dilution) and GolgiSTOP (1/1500 dilution, monesin, *BD Biosciences*) were added to each well. Addition of the antibody this early during NK cell activation assay allows for the cumulative amount of CD107a to be detected, whereas monensin prevents the re-internalization of the secretory vesicles from the surface and allows for the visualization of this marker. Cells were then incubated for a further 5 hours and washed twice with FACS buffer prior to being subjected to the next staining step or acquisition on the Fortessa X-20 (*BD Biosciences*). Flow cytometry data were analysed using FlowJo_10

software (*Tree Star Inc., Ashland, USA*). Statistical analysis of changes in CD107a expression was done using GraphPad Prism 7 software.

2.11.6 Intracellular staining

Flow cytometry was also used to assess the production of IFNγ, TNFα, Granzyme B (see table 2). For this, cells were resuspended in culture media appropriate for tested cells and stimulated with target cells at a 1:1 ratio for 1 hour. After this time GolgiPLUG (Brefeldin A, *BD Biosciences*) was added to each well at a 1:1000 final dilution as its component, brefeldin A, prevents the exocytosis of cytokines and allows for the visualization of cytokine production following NK cell stimulation. Then cells were incubated for further 3 hours (unless stated otherwise).

At the end of incubation, cells were washed in FACS buffer and subsequently fixed and permeabilised by incubating in 100µl of Cytofix/Cytoperm solution (*BD Biosciences*) for 20 min at 4°C. Cells were then washed twice with BD Perm/Wash™ buffer (*BD Biosciences*), pelleted and resuspended in antibody cocktail diluted with BD Perm/Wash™ buffer and left to stain for 30 min at 4°C. After this time cells were washed twice in BD Perm/Wash™ buffer prior to acquisition on the Fortessa-X20 (*BD Biosciences*) and analysed using FlowJo_v10 software (*Tree Star Inc., Ashland, USA*). Example of IFNγ gating strategy can be found in Figure 2.5. Statistical analysis of changes in expression of these proteins was done using GraphPad Prism 7 software.

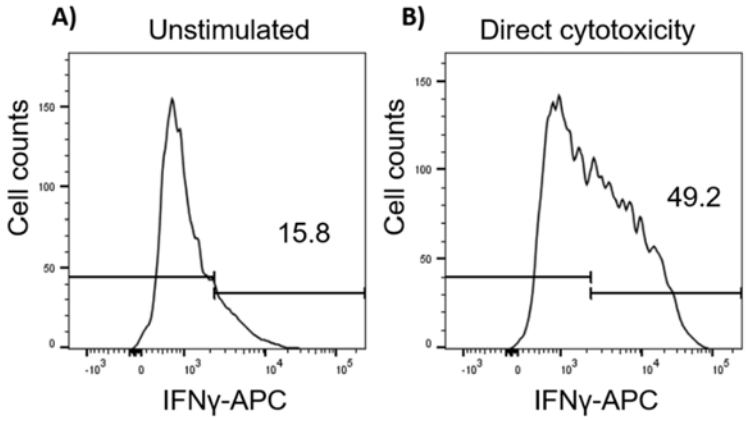

Figure 2.5: Intracellular staining of IFNγ. Intracellular staining was used to detect any changes in the secretion of IFNγ in unstimulated SNK10 cells (A) and during direct cytotoxicity (B).

2.11.7 Intranuclear staining

Upon activation IRE1 excises a 26-nucleotide fragment out of *XBP1* mRNA what leads to generation of an active transcription factor XBP1s that operates in the nucleus. To detect XBP1s protein in NK

cells the BD Pharmingen™ Transcription Factor Buffer Set was utilised as it allows for staining of intracellular and intranuclear proteins. For this, NK cells were cultured in appropriate medium with target cells in a 1:1 ratio for 2 hours (unless stated otherwise). Cells then underwent live/dead staining (refer to section 2.11.1) and/or surface staining (refer to section 2.11.2).

After the cell surface staining procedure was completed, cells were pelleted and resuspended in 150µl of freshly prepared 1x Fix/Perm Buffer working solution and incubated at 4°C for 50 min in the dark. Then cells were topped up with 100µl of 1x Perm/Wash buffer and centrifuged at 2000rpm at 4°C for 5min. After decanting the supernatant cells were washed with 150µl of 1x Perm/Wash buffer and pelleted prior to the intracellular staining with 100µl of anti-XBP1s antibody diluted with of 1x Perm/Wash buffer at 4°C for 50min in the dark. Cell were then washed twice with 150µl of 1x Perm/Wash buffer and pelleted. Prior to acquisition on Fortessa-X20 cells were resuspended in 300µl of FACS buffer. Collected data was analysed in the FlowJo_v10 software (*Tree Star Inc., Ashland, USA*). Gating strategy is shown in Figure 2.6. Statistical analysis of changes in XBP1s expression was done using GraphPad Prism 7 software.

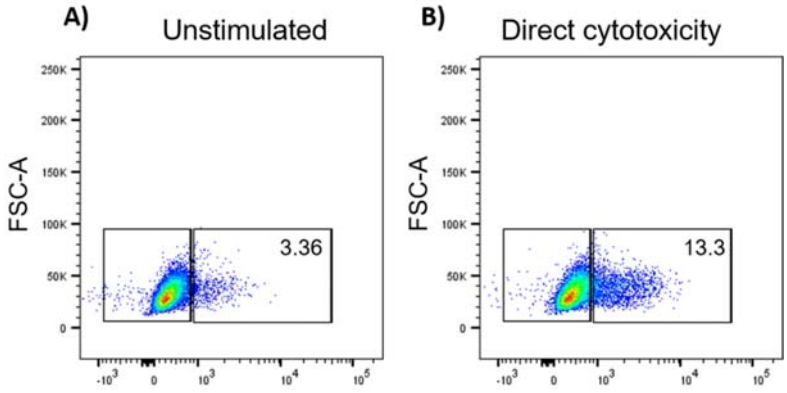

Figure 2.6: Intranuclear staining of XBP1s. Intranuclear staining was used to detect changes in XBP1s expression in unstimulated NK cells (NK-92, A) and during direct cytotoxicity (B).

2.11.8 CFSE staining

To distinguish NK cells from target cells prior to RNA extraction, target cells were pre-stained with CFSE dye (*Sigma-Aldrich*). For this, K562 target cells were pelleted at 1500rpm for 5 min and resuspended in 5 ml of RPMI. An equal volume of CFSE diluted in RPMI (final dilution 1:10000) was then added and incubated for 1 min at room temperature. After 1 min cells were pelleted at 1500rpm for 5 min and washed twice with 5ml of R10 to remove non-incorporated dye. Stained cells were then resuspended in R10 and recounted prior to being used for the assay.

2.11.9 Cell trace dyes

To distinguish NK cells from target cells during the flow cytometry, the CellTrace™ Violet (*Life Technologies*) dye was utilised. Target cells were pre-stained with CellTrace™ Violet dye prior to being added to NK cells, since the CellTrace™ dye easily binds to intracellular amines and ensures a stable fluorescent staining, cells could be fixed with aldehyde-based fixatives. Prior to the staining target cells were counted, pelleted and resuspended at 1x 10^6 cells/ml in PBS. The CellTrace™ dye was then added to cells with the optimal dilution for K562 cell line being 1:5000 and for HDLM-2 or KM-H2 cell lines 1:10000. Cells were then incubated for 20 min at 37°C, in the dark. After that time, five volumes of R10 medium was added to the cells and incubated for 5 min to remove any free dye remaining in the solution. Cells were then pelleted by centrifugation at 15000rpm for 5 min, supernatant decanted and pellets were resuspended in fresh medium. Cells were re-counted prior to being used in the assay.

2.12 NK CELL MOTILITY AND IMMUNE SYNAPSE FORMATION

2.12.1 Conjugate formation assay

Formation of a stable conjugate between NK cell and target cell is a prerequisite for their executive function as it facilitates signal transduction at the contact site. To substantiate a stable connection between NK cell and a target cell the interaction mediated by the integrin LFA-1 on NK cell and ICAM on target cell has to occur. The initial interaction between these cells allows for subsequent signalling that involves other molecules and ultimately leads to formation of a stable intercellular conjugate [155].

The cell populations to be tested were pre-stained using nonspecific fluorescent dyes, specifically HDLM-2 cells with CellTrace™ Violet at dilution 1:10.000, and KHYG-1 cells with CellTrace™ deep red at dilution 1:5.000. Once labelled, 100µl of target cells resuspended to a density of 2x10^6 cells/ml is aliquot into FACS tubes, and admixed with a 100µl of NK cells at a density of 1x10^6 cells/ml. The E:T ratio of 1:2 was selected as it resulted in optimal number of conjugates. Cells were then spun down cells at 20 × g for 1 min and incubated at 37°C in a water bath for 5, 15, and 30 min to allow for conjugation. At the end of each time point, cells were vortexed at high speed for 3sec to disperse loosely associated cells, and immediately fixed by adding 300µl of ice-cold 0.5% paraformaldehyde. Finally, the conjugates were analysed by flow cytometry to quantitatively measure the degree of conjugation. Gating strategy is shown in Figure 2.7

The percent of conjugated NK cells was calculated as follows:

$$\%\ of\ conjugated\ NK\ cells = \frac{\text{double positive counts}}{(\text{double positive counts} + \text{NK cell counts})}\ x\ 100\%$$

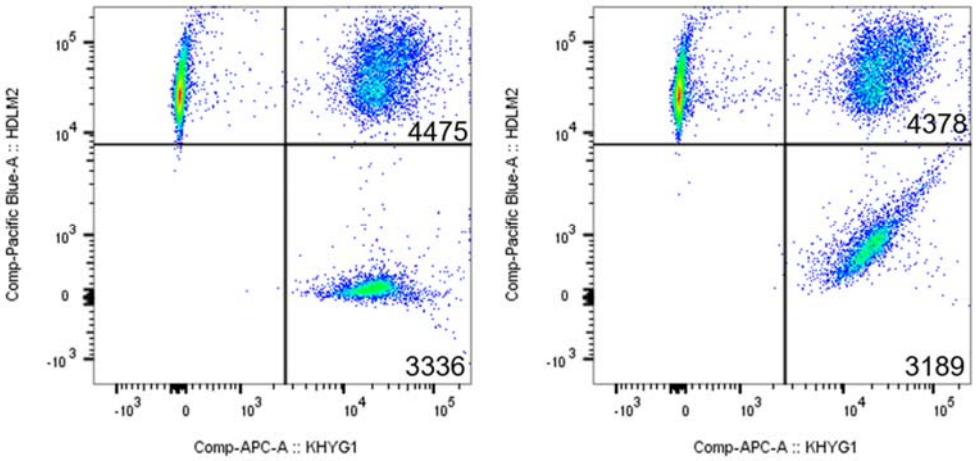

Figure 2.7: Gating strategy of NK cell-HRS cell conjugates. KHYG-1 cells were labelled with APC dye and HDLM-2 cells with CTV dye. The panel shows conjugate formation in the absence (A) or presence of IRE1 blockade (B) upon 5 mins incubation. The cell counts presented in the top and bottom right quadrants are used to calculate the % of KHYG-1 cells in conjugates. For instance, 4475/(3336+4475)*100% = 57.3 % and upon IRE1 blockade 4378/(3189+4378)*100% = 57.8 %.

2.12.2 Actin accumulation assay

KHYG-1 or FACS-sorted $CD3^{-}CD56^{+}$ pNK cells ($1.5x10^5$) were mixed with HDLM-2 cells ($1.5x10^5$, pre-stained with cell tracker red, *Thermofisher Scientific*) and incubated in FACS tubes at 37 °C and 5% CO_2 for 15 min. Conjugates were then transferred to silane-coated microscope slides (*Electron Microscopy Sciences*) and incubated for another 15 min at 37 °C. After a final incubation of 30 min., cells were washed with PBS (Life Technologies) and fixed and permeabilized using 4% Para-Formaldehyde for 20 min at room temperature. After fixation, coverslips were permeabilized in 0.25% Triton-X-100 for 5 min. Blocking and antibody dilution were performed in PBS/0.2% NaAzide/0.25% BSA. F-actin was stained with Alexa Fluor 488 phalloidin (*Life Technologies*) for 30 min. At final stage cells were stained with DAPI for 10 min. Cells were mounted using Menzel-Glaser 22 mm x 40 mm coverslips (*Fisher Scientific*) and buffered glycerol with anti-fade mountant (*Harvard OMX*). Between the staining repetitive washing steps were performed with PBS.

2.12.3 NK-cell immune synapse formation analysis

Confocal microscopy was performed using the Nikon spinning disc confocal microscope. Images were collected using the Nikon Plan Fluor 40X objective (NA = 1.3). The NIS-Elements software was used for image acquisition. Image sets to be compared were acquired during the same session and using the same acquisition settings.

Quantitative image analyses of conjugates were performed using ImageJ analysis software. Quantification of F-actin polarization at the immune synapse was based by random selection of 30 conjugate images containing an APC–stained HDLM-2 cell in contact with a NK cell. To quantitate recruitment of F-actin to the immunological synapse, polarization of actin at the NK cell contact site was measured and then scored based on the median thickness of actin for untreated cells. Conjugates were thereby stratified into three groups with strong (score=1), moderate (score=0.5), or weak (score=0) actin polymerization at the immune synapse site. An overall score for each condition was presented as the percentage of conjugates with actin accumulation. Data were plotted using the GraphPad Prism 7.0 software. Statistical significance was determined using a Student's t-test (two-tailed).

2.12.4 NK cell migration

Transwell assay was used to examine NK cell random migration. Briefly, 1 x 10^5 KHYG-1 cells with pembrolizumab or isotype control in the presence or absence of 60µM of 6-Bromo-2-hydroxy-3-methoxybenzaldehyde (6-bromo, *Sigma-Aldrich*) were seeded into 6.5mm transwells with 5.0µM pores (*Corning*) placed in a 24-well tissue culture plate (*Corning*) and incubated for 5 hours at 37°C (Figure 2.8). Cells were collected and transferred to FACS tubes, spun down, and stained with Zombie NIR dye to exclude dead cells from analysis. Prior to acquisition on Fortessa-X20, 10µl of counting beads was added to each tube to normalize the number of migrant NK cells to the number of beads.

Transwell assay was also used to examine NK cell migration. Briefly, 1 x 10^5 KHYG-1 cells pre-cultured with pembrolizumab or isotype control in the presence or absence of 60µM of 4µ8c or 6-bromo were seeded into 6.5mm transwells with 5.0µM pores (*Corning*) placed in a well, of 24-well plate, and incubated for 5 hours at 37°C (Figure 2.8). Cells were then collected and transferred to FACS tubes, spun down and stained with Zombie NIR dye to eliminate dead cells from analysis. Prior to acquisition on Fortessa-X20, 10µl of counting beads was added to each tube to normalize the number of migrant NK cells to the number of acquired beads.

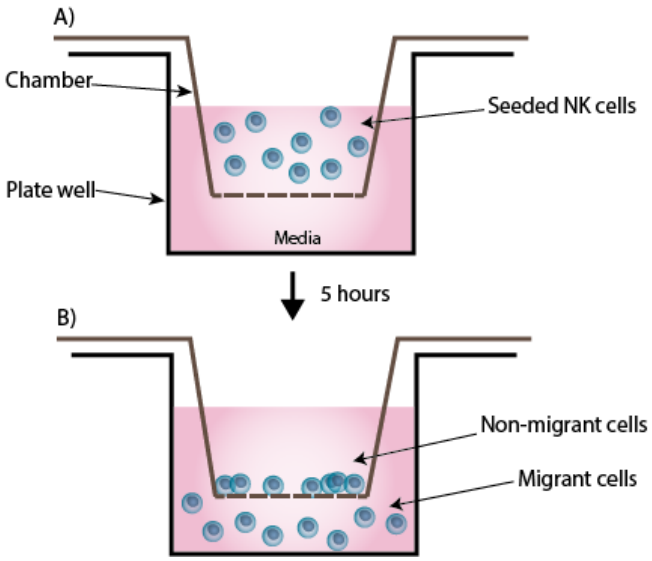

Figure 2.8: A schematic of migration assay. NK cells (KHYG-1 cell line) were seeded at the transwell chamber (A) and allowed to migrate within 5 hours to the bottom chamber (B). The number of migrant NK cells was assessed with the use of flow cytometry.

2.13 STATISTICAL ANALYSIS

All statistical analysis was done using GraphPad Prism 7.00 (*GraphPad Software, San Diego, California, USA*). Comparison of measurements was done using paired 2-tailed T-tests (except where stated otherwise in results). The P values were interpreted as presented in Table 2.4**.**

Table 2.4: P values summary.

P Value	Wording	Summary
< 0.001	Extremely significant	***
0.001 to 0.01	Very significant	**
0.01 to 0.05	Significant	*
>0.05	Not significant	ns

CHAPTER 3:

XBP1s activation is associated with appropriate function of NK cells

3.1 INTRODUCTION

3.1.1 NK cell effector function

Over the last several decades, the importance of NK cells in mediating anti-tumour responses has become increasingly recognized [31]. However, limited understanding of the molecular signalling and intercellular interactions that control NK cell function hinders development of therapies that modulate their function.

NK cells are a component of the innate arm of the immune system that have the capacity to directly kill target cells without prior sensitization [10] [3]. The recognition of target cells by NK cells is regulated by the balance between activating and inhibitory signals. Once the balance is tilted towards NK cell activation the signalling cascades leading to the target cell lysis and cytokine secretion are triggered [23]. The IRE1-XBP1 pathway has important and highly diverse contributions to the function of various immune effector cells. It is unknown whether the IRE1-XBP1 pathway is a part of these signalling cascades involved in NK cell activation. I sought to investigate the role of this pathway in NK cell-mediated anti-tumour responses.

3.1.2 The NK cell immunological synapse

NK cell function involves cytoskeleton integrity and capacity to migrate, recognize, and kill target cells. A pre-requirement for NK cell-mediated responses is direct contact between NK cell and target cells. Upon this interaction, dynamic rearrangements of cellular molecules occur that ultimately lead to formation of an organized interface termed the immunological synapse [156]. This structure is the site that regulates NK cell functions and allows for direct secretion of the lytic granule content onto the target cell to facilitate target cell lysis. However, these functions are regulated by a complex network of interactions between membrane proteins, cytoskeleton, and signalling pathways. Specifically, the contact between the NK cell and a target cell initiates the interactions between various NK cell receptors and adhesion molecules. Of importance are integrins that ensure the communication between the intracellular and extracellular microenvironments. These molecules transmit “outside-in” signals (such as chemokines) received by the surface receptors to mediate cell polarization and chemotaxis. Whereas the signals generated in the cytoplasm are transmitted by integrins to the cell surface in a process termed “inside-out signalling” that regulates adhesiveness and migration [157].

Lymphocyte function-associated antigen 1 (LFA-1), known also as α, β-integrin or CD11a/CD18, plays a fundamental role in NK cell activation, as it mediates binding of NK cell to target cell upon engagement of its ligand, intracellular adhesion molecule I (ICAM-1), on target cells [158] [159]. Formation of a stable conjugate between NK cell and target cells is a key step prior to establishing the immunological synapse and subsequent NK cell-mediated cytotoxicity [158]. Cell adhesion, mediated by LFA-1, initiates conformational changes, such as actin rearrangements, that are critical for the formation of the immunological synapse. Then, to trigger integrin functions, talin which contains binding sites for F-actin, type I phosphatidylinositol 4-phosphate 5-kinase (PIPKIγ), and vinculin, is recruited to the IS. In turn, talin, through association with vinculin and PIPKIγ, mediates two signalling pathways that recruit Arp2/3 and Wiskott Aldrich Syndrome protein (WASP) to the site of LFA-1 ligation and induces localized actin polymerization. The actin nucleating protein complex Arp2/3, which is responsible for the formation of branched filaments by actin, must be first activated by a nucleation promoting factor, and the primary nucleation promoting factor in haematopoietic cells is WASP. The latter molecule is polarized to the IS due to localized increase of phosphatidylinositol (4,5)-bisphosphate (PIP2) mediated by LFA-1/ICAM-1 signalling [159]. Actin-regulatory protein WASP is expressed in human NK cells and is required for actin accumulation at the immunological synapse [160] [156]. Accumulation of F-actin in NK cells at the interface of the NK cell and its target cell is an early step denoting the formation of an immunological synapse [155].

Collectively, signals emanating from activating receptors regulate the affinity and avidity of LFA-1 binding of ICAM-1. Also, the interaction between LFA-1 and ICAM-1 stabilizes the intercellular adhesion between cytotoxic cells and their targets promoting the delivery of cytotoxic granule contents toward susceptible targets [161]. These processes are essential for the initiation of NK cell–mediated cytotoxicity [160]. I interrogated the IRE1-XBP1 pathway to establish its relevance in the formation of a stable immunological synapse and the downstream effector functions mediated by NK cells.

3.2 AIMS

Based on studies in other immune cells, and pre-existing data on NK cells generated in my supervisor's laboratory, I hypothesised that stimulation of NK cells with various blood cancer target cells will lead to activation of IRE1-XBP1 pathway.

The over-arching aim of this chapter was to determine whether activation of the IRE1-XBP1 pathway occurs, and if so to establish the role of the pathway in specific components of NK cell effector function.

The specific aims of this chapter are:

1. To determine if the IRE1-XBP1 pathway is activated following NK cell stimulation by target cell lines representing a range of blood cancers.
2. To investigate if blockade of the IRE1-XBP1 pathway is relevant for NK cell effector function.

3.3 RESULTS

3.3.1 *XBP1* splicing occurs upon stimulation of NK cells with K562

As described earlier, the IRE1-XBP1 pathway has been shown to play an important role in a range of immune cells [121] [123] [122] [125] [162]. I hypothesized that activation of this pathway, defined by increase in the expression of *XBP1* spliced isoform, occurs in NK cells in response to stimulation with target cells. Based on the previous results from our laboratory, *XBP1* splicing occurs in SNK10 cells in response to the target cell line K562; the latter is a MHC-I-negative erythroleukaemia cell line that is known to be a highly NK cell-sensitive target [163]. To confirm as well as extend these data, I compared two additional NK cell lines, KHYG-1 and NK-92, with SNK10. The latter line was isolated from a patient with chronic active EBV infection [149], while the KHYG-1 cell line was derived from a patient with aggressive NK cell leukaemia carrying p53 mutation [164], and the NK-92 cell line was derived from a patient with rapidly progressive non-Hodgkin's lymphoma; these cells demonstrate characteristics of activated NK cells and have potential use in adoptive immunotherapy [165] [166] [167].

To interrogate *XBP1* splicing, NK cells were stimulated with the target cell line K562 in a 1:1 ratio for 2 hours and then the mRNA or protein expression of XBP1s was assessed (Figure 3.1). The mRNA fold change of *XBP1s* in stimulated SNK10 cells was three times higher than in unstimulated SNK10 cells, and the protein has increased two-fold. Furthermore, the *XBP1* splicing also occurred in the other two NK cell lines stimulated with K562 cells. Unexpectedly, the increase in the *XBP1s* mRNA expression was not as prominent in these two cell lines, whereas the XBP1s protein expression was significantly higher for KHYG-1 and NK-92 cells (11.93% ±0.74; 12.4% ±1.23) than SNK10 cells (4.1% ±0.35). Collectively, these results demonstrate that stimulation of NK cells with K562 cells induces *XBP1* splicing across different NK cell lines. Furthermore, these results suggest a role for the IRE1-XBP-1 pathway in NK cell function.

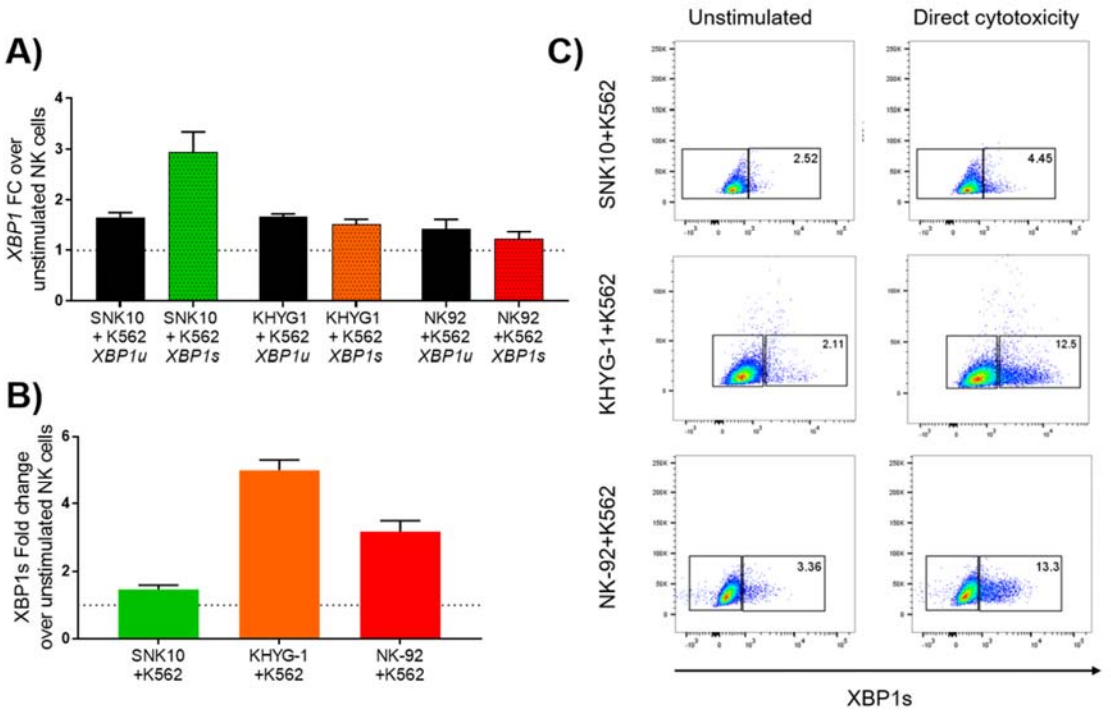

Figure 3.1: Stimulation of various NK cell lines induces XBP1 splicing. RT qPCR was utilised to determine changes in the XBP1 splicing in unstimulated NK cells and those stimulated with K562 targets (direct cytotoxicity) for 2 hours. The expression was normalised to the housekeeping gene *B2M* and presented as relative to expression in unstimulated NK cells (dotted line) (A). Flow cytometry was employed to interrogate changes in the protein expression of XBP1s in the same set of unstimulated and simulated NK cell lines (B). A representative FACS plot presents changes in the protein expression of XBP1s across different NK cell lines (C). Analysis: paired two-tailed Student's t-test (n=3), $*P<0.05$, $**P<0.01$.

Typically, to ensure successful expansion of NK cell lines *in vitro,* the culture is supplemented with IL-2. To investigate whether the *XBP1* splicing is induced by this cytokine, I utilised a cell line (NK-92.MI, purchased from *ATCC*) that is independent of IL-2 supplementation because it has been stably transfected with the human IL-2 cDNA retroviral MFG-hIL-2 vector. The results indicate that stimulation of these cells with K562 targets induces the *XBP1* splicing further suggesting that it is not restricted to the presence of exogenous IL-2 (Figure 3.2).

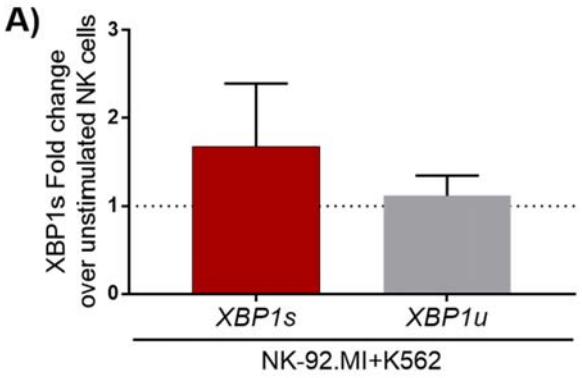

Figure 3.2: The XBP1 splicing occurs in an IL-2-independant NK-92.MI cell line. RT qPCR was utilised to determine changes in the XBP1u and XBP1s expression in unstimulated NK-92.MI cells and those stimulated with K562 targets (direct cytotoxicity) for 2 hours. Real time expression was normalised to the housekeeping gene *B2M* and presented as relative to expression to unstimulated NK-92.MI cells (dotted line).

3.3.2 *XBP1* splicing is a common marker of NK cell-mediated cytotoxicity

Next, I sought to determine whether *XBP1* splicing occurs following NK cell stimulation irrespective of the target cell type. In these experiments, the SNK10 cell line was selected as a model NK cell line, whereas target cells were represented by HDLM-2 and KM-H2 lines, both HL cell lines. While HDLM-2 cell line does not express MHC-I molecules, the KM-H2 cell line expresses following MHC-I molecules: HLA-A, HLA-B, and HLA-C [168]. Given that NK cell function is restricted by MHC-I molecules, comparing both HL cell lines enabled me to establish whether the presence of MHC-I on target cells imposes any differences in terms of the IRE1-XBP1 pathway activation. Initially, SNK10 cells were stimulated with target cells in a 1:1 ratio for 2, 4 or 8 hours to determine the optimal stimulation time with HL lines. A time-course experiment was done to interrogate the transcript expression level. Based on the RT qPCR results, *XBP1* splicing was optimal at the 8 hours' time-point, which resulted in an almost three-fold increase of *XBP1s* expression when compared to unstimulated SNK10 cells (Figure 3.3).

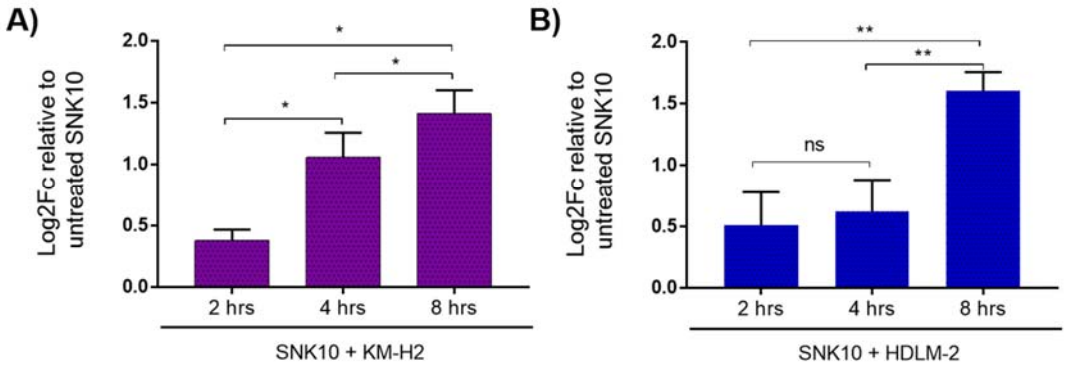

Figure 3.3: XBP1 splicing occurs in SNK10 cells following the stimulation with Hodgkin Lymphoma target cells. Real time PCR was utilised to determine changes in the XBP1s expression in unstimulated SNK10 cells and those stimulated with K562 targets (direct cytotoxicity) for 2, 4, and 8 hours. Real time expression was normalised to the housekeeping gene *GAPDH* and presented relative to expression in unstimulated SNK10 cells (Log2Fc=0). Analysis: paired two-tailed Student's t-test (n=3), ns - not significant, *$P<0.05$, **$P<0.01$.

Next, to evaluate the protein expression, SNK10 cells were stimulated with each target cell type in a 1:1 ratio for 8 hours. The stimulation of NK cells with HDLM-2 resulted in significant increase of XBP1s protein expression (SKN10: 3.15±1.38%, SNK10+HDLM-2: 14.94±0.49%; Figure 4.B/C). Similarly, stimulation of NK cells with KM-H2 cells also induced the *XBP1* splicing (SKN10: 3.15±1.38%, SNK10+HDLM-2: 17.36±1.07%; Figure 3.4.B and C). These results indicate that *XBP1* splicing occurs in NK cells in a variety of blood cancer (lymphoid and leukaemia) lines.

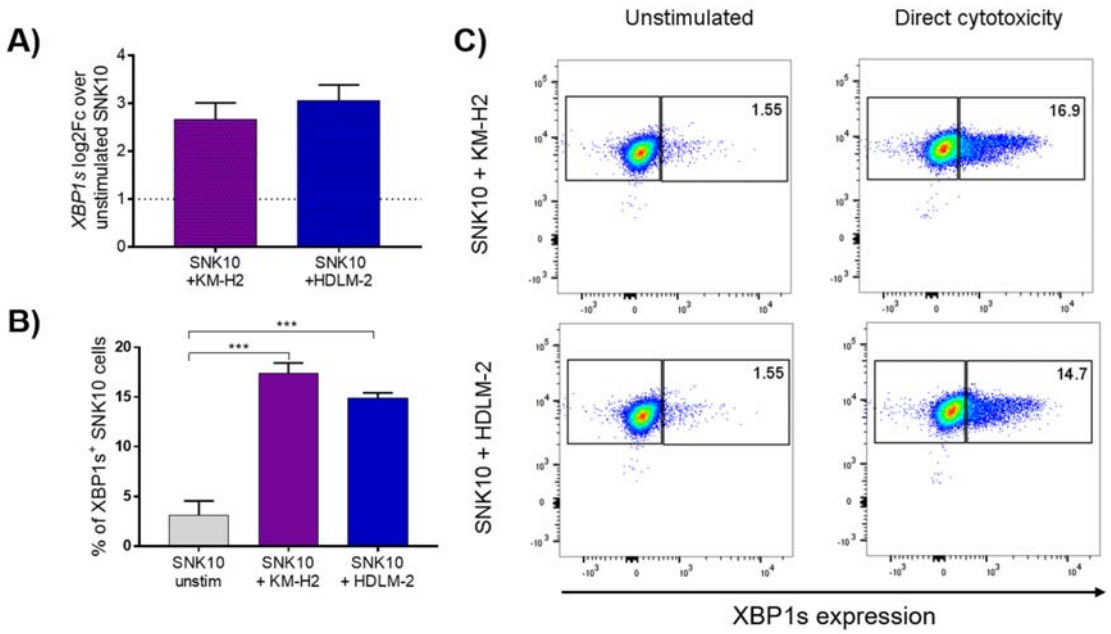

Figure 3.4: XBP1s expression increases following the SNK10 cells stimulation with different HL cell lines. Real time PCR was utilised to determine changes in the XBP1 splicing in unstimulated NK cells and those stimulated with K562 targets (direct cytotoxicity) for 2 hours. The expression is normalised to the housekeeping gene *GAPDH* and presented relative to expression NK cells (dotted line) (A). Flow cytometry was employed to interrogate changes in the protein expression of XBP1s in the same set of unstimulated and simulated NK cell lines (B). A representative FACS plot presents changes in the protein expression of XBP1s in SNK10 cells in response to different target cells (C). Analysis: paired two-tailed Student's t-test (n=3),****P<0.001*.

3.3.3 The IRE1-XBP1 pathway is activated during NK cell-mediated cytotoxicity in a non-canonical manner

Typically, the ER stress response including activation of the UPR system is initiated by the accumulation of unfolded or misfolded proteins in the cell [169]. The UPR system regulates the expression of multiple chaperones and molecules involved in the protein folding to alleviate the ER stress and restore a cellular homeostasis. These responses are mediated through three distinct downstream effector molecules encompassing PERK, ATF6 or IRE1, with the IRE1-XBP1 pathway representing the most evolutionary conserved branch of the UPR system [170] [171]. As demonstrated in the previous section of this chapter, the engagement of target cells by NK cells induces *XBP1* splicing and leads to the increased expression of XBP1s in NK cells.

To test whether stimulation of NK cells with target cells activates the canonical IRE1-XBP1 pathway ER stress response, I evaluated the expression of known *XBP1* target genes. For this RT qPCR was utilised and the transcript expression of *DNAJB9, DNAJB11, DNAJC3, PDIA6*, and *DERL1* genes, involved in increased protein folding capacity, were interrogated [150]. To do so, the NK cell lines were stimulated with either target cells (K562) or TG, a known inducer of ER stress via the canonical IRE1-XBP1 pathway, to establish whether the expression of these genes increases along with the induction of *XBP1* splicing. Then NK cells were separated from target cells, subjected to RNA extraction, followed by RT-PCR. As expected, TG alone induced activation of the ER-stress response, as shown by the induced expression of *DERL1, PDIA6, DNAJC3, DNAJB11,* and *DNAJB9.* Conversely, the mRNA expression analysis demonstrated that activation of the IRE1-XBP1 pathway in target-stimulated NK cells did not significantly up-regulate the expression of these genes (Figure 5, 6 and, 7). These observations were consistent across different NK cell lines.

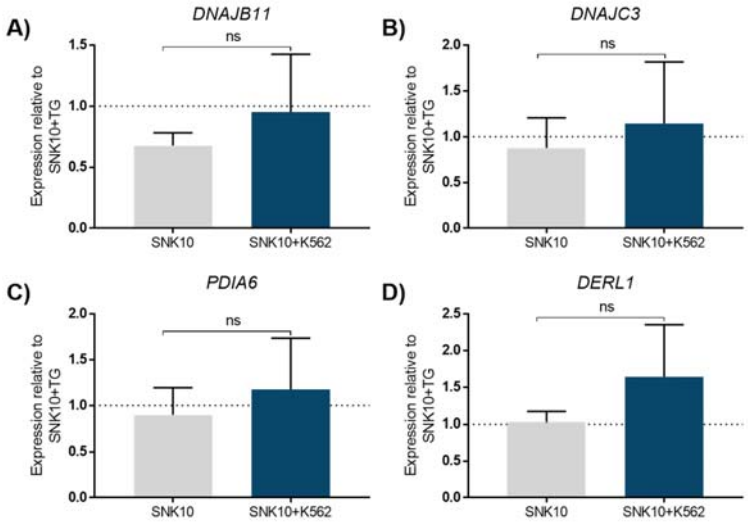

Figure 3.5: The UPR is not activated during SNK10 cell-mediated cytotoxicity. Real-time PCR analysis was utilised to assess the expression **of** well-described targets of XBP1s including DNAJB9, DNAJB11, DNAJC3 and PDIA6. No changes were observed in SNK10 cells alone (unstimulated) or co-cultured with K562 target cells (direct cytotoxicity). Real time expression data is normalised to the housekeeping gene *B2M* and presented relative to expression by SNK10 cells treated with TG (dotted line). Analysis: paired two-tailed Student's t-test (n=3), ns - not significant.

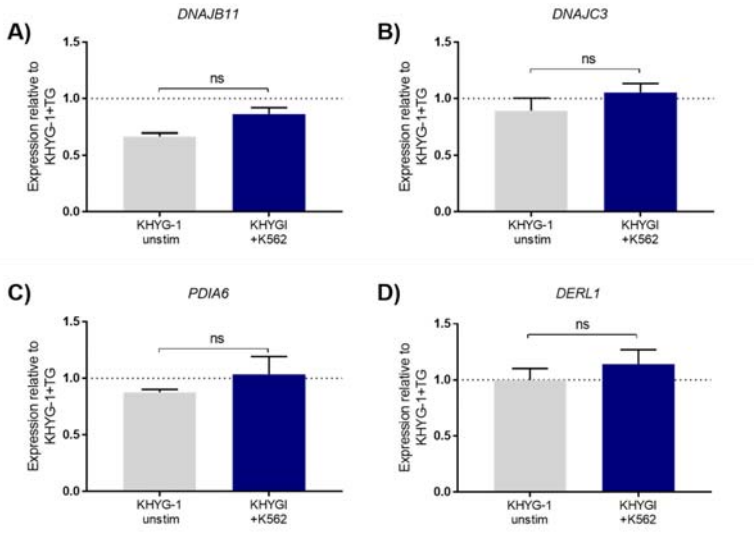

Figure 3.6: The UPR is not activated during KHYG-1 cell-mediated cytotoxicity. Real-time PCR analysis was utilised to assess the expression of well-described targets of XBP1s including *DNAJB9, DNAJB11, DNAJC3* and *PDIA6*. No changes were observed in KHYG-1 cells alone (unstimulated) or co-cultured with K562 target cells (direct cytotoxicity). Real time expression data is normalised to the housekeeping gene *B2M* and presented relative to expression by KHYG-1 cells treated with TG (dotted line). Analysis: paired two-tailed Student's t-test (n=3), ns - not significant.

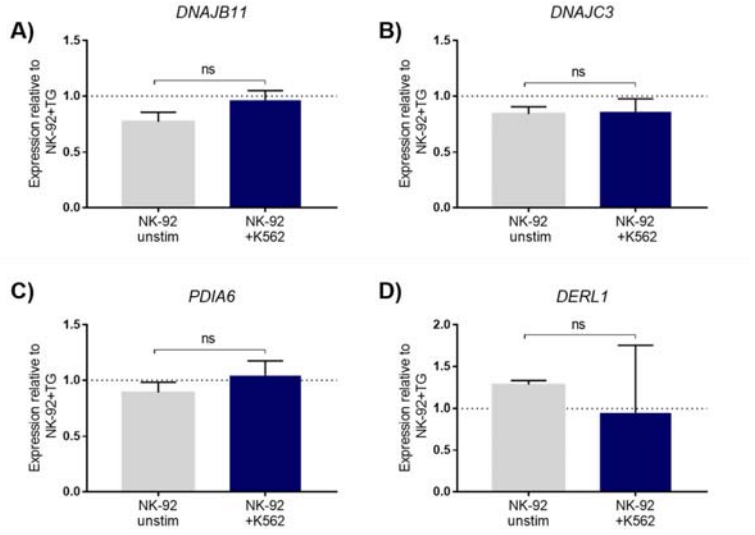

Figure 3.7: The UPR is not activated during NK-92 cell-mediated cytotoxicity. Real-time PCR analysis was utilised to assess the expression of well-described targets of XBP1s including *DNAJB9, DNAJB11, DNAJC3* and *PDIA6*. No changes were observed in NK-92 cells alone (unstimulated) or co-cultured with K562 target cells (direct cytotoxicity). Real time expression data is normalised to the housekeeping gene *B2M* and presented relative to expression by NK-92 cells treated with TG (dotted line). Analysis: paired two-tailed Student's t-test (n=3), ns - not significant.

3.3.4 XBP1 splicing is effectively blocked in the presence of IRE1 inhibitor

The small molecule inhibitor, 4-methyl umbelliferone 8-carbaldehyde (4μ8c), has been demonstrated to specifically block substrate access to the active site of IRE1, thereby preventing *XBP1* splicing as well as IRE1-mediated mRNA degradation (RIDD) [150]. Further, the application of 4μ8c in MEF cells treated with ER-stress inducer (tunicamycin) inhibited cleavage of *XBP1* in a dose-dependent manner, with a dose of 64μM showing the optimal efficacy [150]. I wanted to investigate whether this small molecule could also inhibit IRE1-mediated splicing of *XBP1* in NK cells. For this, a range of NK cell lines was stimulated with K562 target cells in the presence of 60μM of 4μ8c for 2 hours prior the mRNA or protein expression analysis. As expected, the expression of the *XBP1s* mRNA was significantly inhibited upon the IRE1 blockade (Figure 3.8). Importantly, these changes were also reflected on the protein level (Figure 3.9).

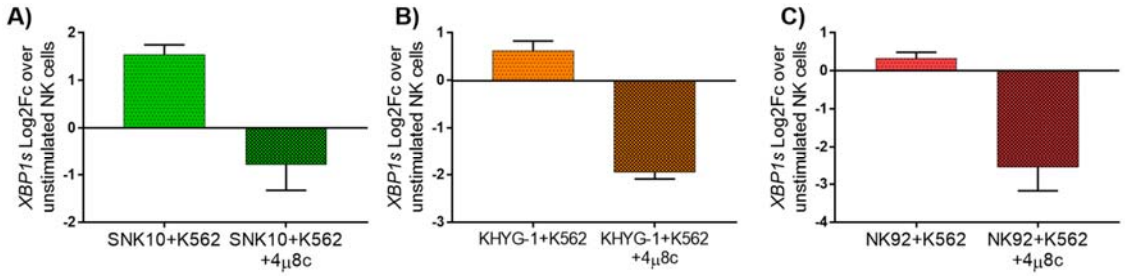

Figure 3.8: Production of XBP1s RNA is inhibited by 4μ8c. XBP1 splicing was assessed by the RT qPCR. The efficacy of IRE1 inhibitor in preventing XBP1 splicing was tested in a range of NK lines: SNK10 cells (A), KHYG-1 (B), and NK-92 (C) stimulated with targets (K562) in the presence or absence of IRE1 blockade for 2 hours. The expression was normalised to the housekeeping gene *B2M*. Log2 fold-change expression in stimulated NK cells over unstimulated NK cells or Log2FC expression in stimulated NK cells in the presence of IRE1 inhibitor over stimulated NK cells is presented; unstimulated NK cells (Log2FC=0).

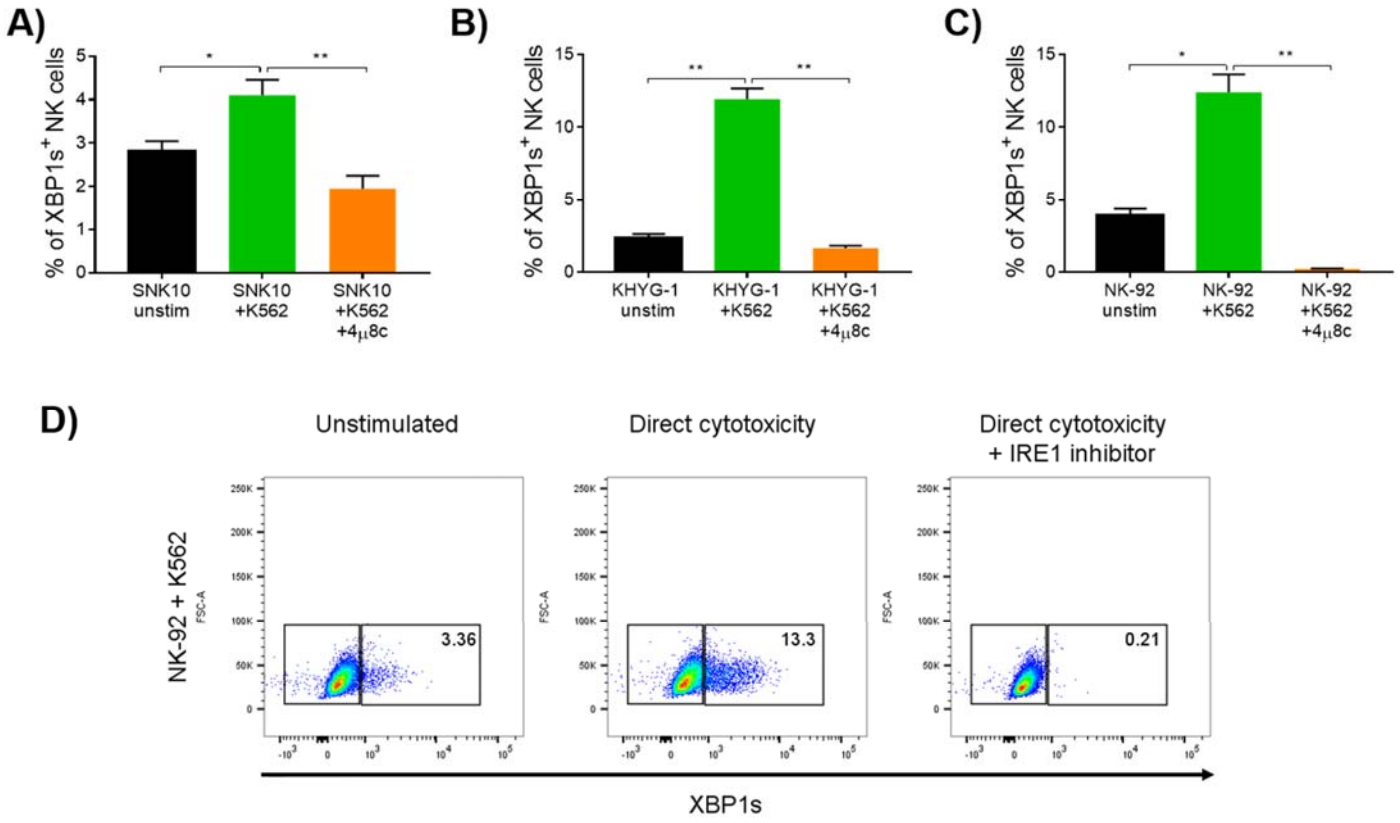

Figure 3.9: Production of XBP1s protein is inhibited in the presence of IRE1 inhibitor 4μ8c. Flow cytometry was utilised to assess XBP1s expression in SNK10 (A), KHYG-1 (B), and NK-92 cells (C) in the presence or absence of 60μM of 4μ8c for 2 hours. A representative FACS plot demonstrates changes in XBP1s expression in unstimulated NK-92 cells and those stimulated with K562 target cells in the presence or absence or IRE1 inhibitor (D). Analysis: paired two-tailed Student's t-test (n=3), **P<0.05, **P<0.01*.

3.3.5 IRE1 inhibitor does not affect cell viability

Multiple studies have utilised 4μ8c to study the role of the IRE1-XBP1 pathway in various cell and disease models. The available literature indicates that 4μ8c is a potent and safe small molecule inhibitor that does not affect cell viability [172] [150] [173]. I also determined whether treatment of NK cells with this inhibitor impacts the cell survival. Typically, NK cells were incubated with 60μM of the IRE1 inhibitor for no longer than 8 hours. Thereby, I examined the influence of 60uM of 4μ8c on cell viability by utilising the live/dead staining of the NK cells stimulated with target cells in the presence or absence of IRE1 inhibitor for up to 8 hours. In addition, I also interrogated the target cell compartment to examine if the inhibitor affects the viability of these cells.

I did not find significant changes in NK cell viability following incubation of NK cells in the presence of the inhibitor over the course of time (Figure 10). Although a decreasing trend in the number of viable cells was observed this did not reach a statistical significance (Figure 10.B).

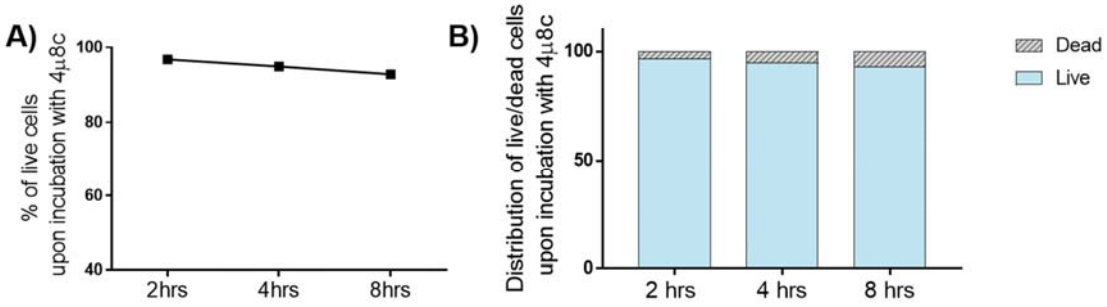

Figure 3.10: IRE1 inhibitor, 4μ8c, does not significantly impair NK cell viability. SNK10 cells were treated with 60μM of IRE1 inhibitor for 2, 4, and 8 hours prior assessment of the viability with Zombie NIR staining. Graphs present percentage of viable cells (A) upon treatment with 4μ8c, as well as distribution of live and dead populations in the presence of 4μ8c (C). Analysis: one-way ANOVA test; no significant differences were found.

Analysis of the target cell compartment revealed that the IRE1 inhibitor also did not significantly affect the viability of KM-H2 or HDLM-2 cells (Figure 11). The distribution analysis of live and dead cells shows that dead cells were accounting for less than 15% of cells at the end of 8 hour-incubation.

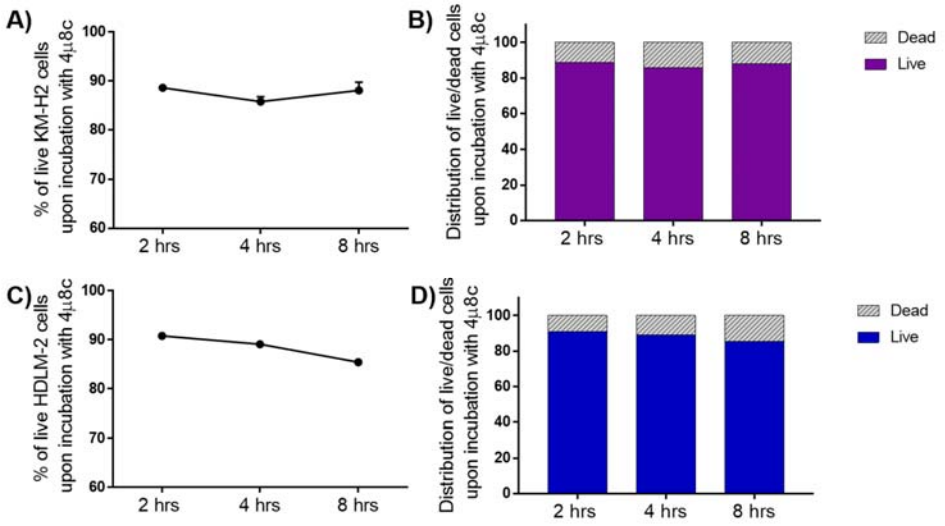

Figure 3.11: IRE1 inhibitor, 4μ8c, does not significantly impair target cells viability. KM-H2 or HDLM-2 cells were treated with 60μM of IRE1 inhibitor for 2, 4, and 8 hours prior assessment of the viability with Zombie NIR staining. Graphs present percentage of viable KM-H2 (A) or HDLM-2 (C) cells upon treatment with 4μ8c, as well as distribution of live and dead KM-H2 (B) or HDLM-2 (D) cells in the presence of 4μ8c. Analysis: one-way ANOVA test; no significant differences were found.

3.3.6 Concomitant with *XBP1* splicing, expression of selected NK cell effector RNA molecules is increased

Activation of the IRE1-XBP1 pathway has been linked with enhanced cytokine secretion in macrophages and T cells [122] [125]. Despite target cell lysis, NK cells have also a capacity to release immunoregulatory cytokines to recruit other immune cells, thereby shaping host's immunity. In addition, NK cell-mediated function is restricted by the balance of activating and inhibitory signals received by receptors. To investigate the potential role of XBP1s in NK cell effector function I examined the gene expression of a set of established molecules known to be important for NK cell function. These molecules can be categorized into three groups pertaining to: cytokine production (*IFNγ, TNFα*), receptor expression (*NKG2D, CD16*), and target cell lysis (*GZMB, FASL*). To ensure that any potential changes in the expression of these genes are observable across different NK cell lines, three NK cell lines were tested: SNK10, KHYG-1, and NK-92. For this I utilised RT qPCR, and the gene expression was interrogated in the NK lines stimulated with K562 target cells for two hours in the presence or absence of IRE1 inhibitor. To ensure that the gene expression analysis encompasses only NK cells, but not target cells, at the end of NK cell stimulation target cells were removed by magnetic beads

labelling and on-column separation. Additionally, the purity of isolated NK cells was tested after each sort (refer to Chapter 2, section 2.8.1).

Initially, to determine the contribution of the IRE1-XBP1 pathway in cytokine production, transcript expression of both *IFNγ* and *TNFα* was examined in stimulated NK cells in the presence or absence of IRE1 inhibitor. A significant reduction in the expression of both *IFNγ* and *TNFα* in stimulated NK cells following IRE1 inhibition was observed. This reduction was found to be significant for each tested cell line (Figure 3.12 Figure 3.13). The cytokine production in both unstimulated NK cells treated with the canonical IRE1- XBP1 ER stress inducer (TG) and with (non-canonical) target-stimulated NK cells was significantly up-regulated, indicating that distinct mechanisms of upregulation are operational.

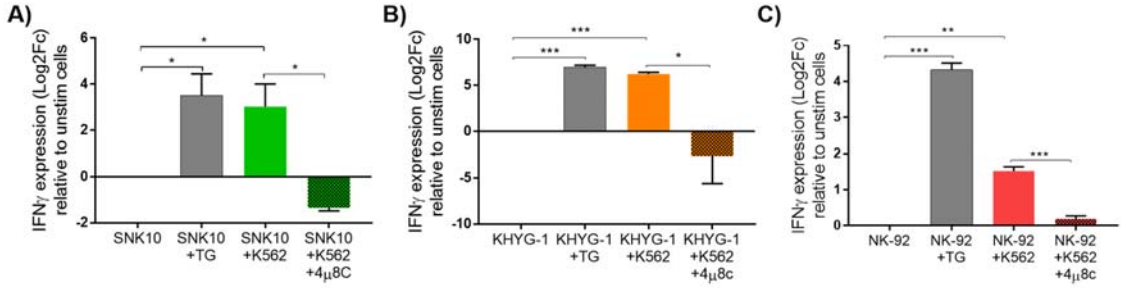

Figure 3.12: Inhibition of IRE1 reduces *IFNγ* expression. NK cell lines treated with DMSO, 100nM TG or 60μM of IRE1 inhibitor were stimulated with K562 targets for 2 hours. RT qPCR was used to assess expression of genes encoding interferon γ (*IFNγ*) in SNK10 cells (A), KHYG-1 cells (B), or NK-92 cells (C). The gene expression was normalized to a house-keeping gene *B2M* and expression of *IFNγ* relative to unstimulated (unstim) NK cells is presented. Analysis: paired two-tailed Student's t-test (n=3), **P<0.05, **P<0.01, ***P<0.001*.

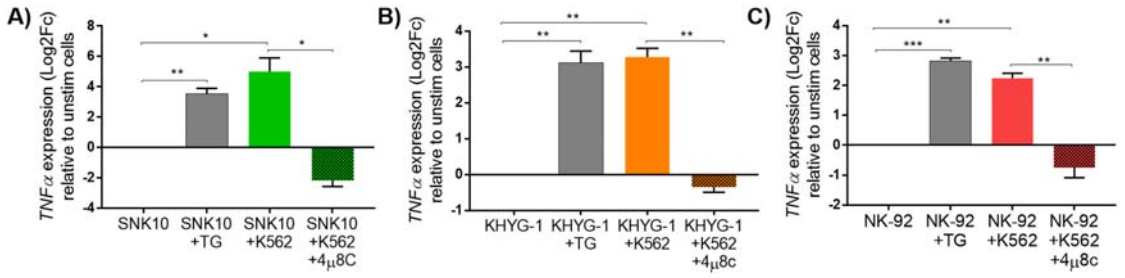

Figure 3.13: Inhibition of IRE1 reduces *TNFα* expression. NK cell lines treated with DMSO, 100nM TG or 60μM of IRE1 inhibitor were stimulated with K562 targets for 2 hours. RT qPCR was used to assess expression of genes encoding *TNFα* in SNK10 cells (A), KHYG-1 cells (B), or NK-92 cells (C). The gene expression was normalized to a house-keeping gene *B2M* and expression relative to unstimulated (unstim) NK cells is presented. Analysis: paired two-tailed Student's t-test (n=3), **P<0.05, **P<0.01, ***P<0.001*.

Then, to address the involvement of the IRE1-XBP1 axis in the production of molecules relevant for target cell lysis, I analysed the transcriptional expression of *FASL* and *GZMB*. Granzyme B (*GZMB*) is a protease that is a part of the lytic granule content that is released onto a target cell during NK cell-mediated cytotoxicity [79]. FASL is also a part of the lytic granule content, that induces apoptotic cell death via binding FAS (CD95) present on the surface of the target cells [174]. I found that upon the IRE1 blockade in stimulated NK cells the transcriptional expression of both molecules was significantly down-regulated, although to a different extent (Figure 3.14 and Figure 3.15). Again, pharmacological induction of the ER stress also induced the increased expression of *FASL* and *GZMB,* but to a different extent than stimulation with target cells. In case of the SNK10 cells, the induction of *GZMB* expression upon TG treatment did not lead to a significant increase in its expression. This might result from a high level of variation observed between analysed replicates, and there was a non-significant trend.

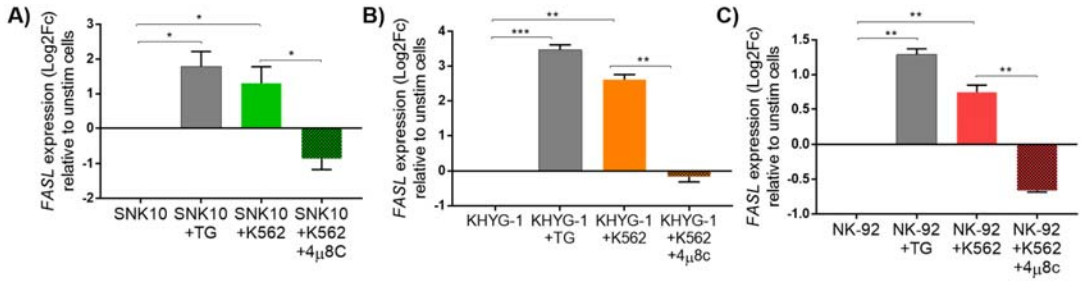

Figure 3.14: Inhibition of IRE1 reduces *FASL* expression. NK cell lines treated with DMSO, 100 nM of TG or 60μM of IRE1 inhibitor for 2 hours. RT qPCR was used to assess expression of genes encoding *FASL* in SNK10 cells (A), KHYG-1 cells (B), or NK-92 cells (C). The gene expression was normalized to a house-keeping gene B2M and expression of FASL relative to unstimulated (unstim) NK cells is presented. Analysis: paired two-tailed Student's t-test (n=3), **P<0.05, **P<0.01, ***P<0.001*.

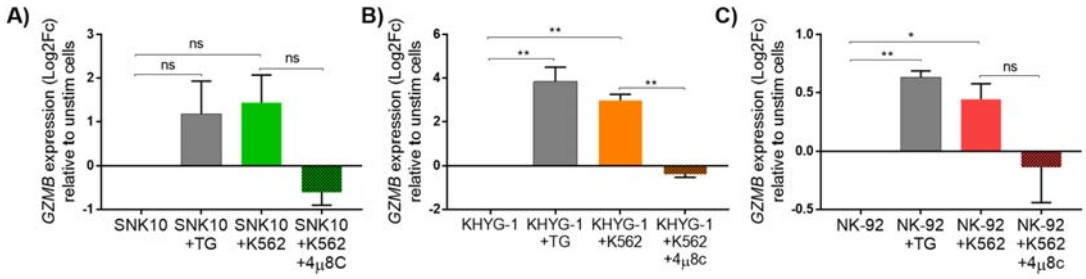

Figure 3.15: Inhibition of IRE1 reduces *GZMB* expression. NK cell lines treated with DMSO, 100 nM of TG or 60μM of IRE1 inhibitor for 2 hours. RT qPCR was used to assess expression of genes encoding GZMB in SNK10 cells (A), KHYG-1 cells (B), or NK-92 cells (C). The gene expression was normalized to a house-keeping

gene *B2M* and expression relative to unstimulated (unstim) NK cells is presented. Analysis: paired two-tailed Student's t-test (n=3): ns - not significant, *$P<0.05$, **$P<0.01$.

Lastly, I also assessed the contribution of the IRE1-XBP1 pathway to the expression of the activating receptor *NKG2D*. This revealed that both *NKG2D* expression is significantly down-regulated upon inhibition of IRE1 in the majority of NK cell lines tested (Figure 3.16).

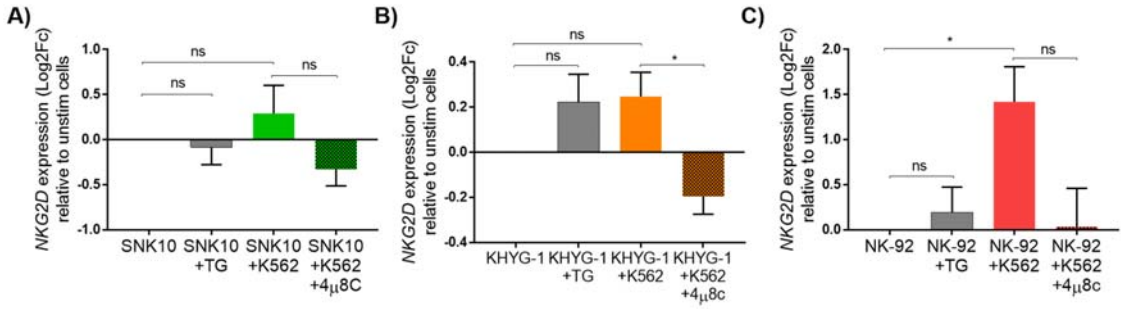

Figure 3.16: Inhibition of IRE1 reduces *NKG2D* expression. NK cell lines treated with DMSO, 100 nM of TG or 60μM of IRE1 inhibitor for 2 hours. RT qPCR was used to assess expression of genes encoding *NKG2D* in SNK10 cells (A), KHYG-1 cells (B), or NK-92 cells (C). The gene expression was normalized to a house-keeping gene *B2M* and expression relative to unstimulated (unstim) NK cells is presented. Analysis: paired two-tailed Student's t-test (n=3): ns - not significant, *$P<0.05$.

A collective analysis of all tested genes revealed that inhibition of IRE1 with 4μ8c significantly impairs expression of *IFNγ, TNFα, GZMB*, *FASL, and NKG2D*. Importantly, this observation was universal across the majority of tested NK cell lines (Figure 3.17). To establish whether inhibition of IRE1 affects NK cell function I decided to investigate the protein expression of the same set of molecules.

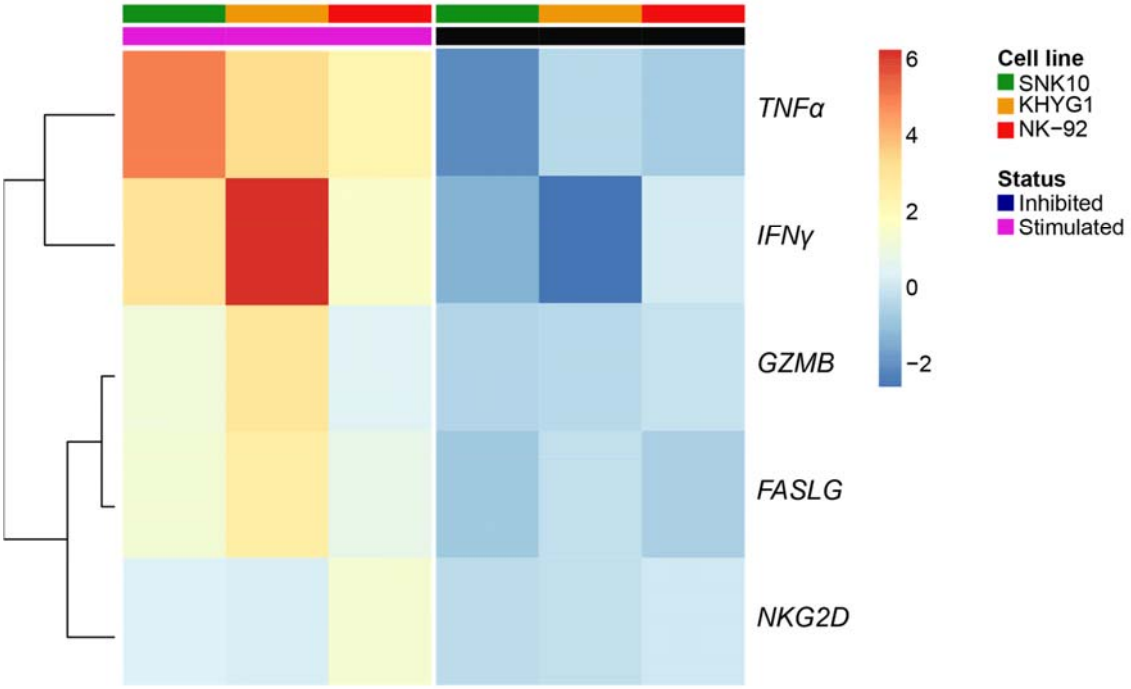

Figure 3.17: The expression of selected genes is affected upon inhibition of IRE1. Gene expression of selected genes, relevant for NK cell function, was measured by the RT qPCR. Gene profiling was performed in a range of NK cell lines: SNK10 (green tab), KHYG-1 (orange tab), and NK-92 (red tab). Heatmap presents fold changes of mRNA expression of these genes in NK cells stimulated with K562 target cells over unstimulated NK cells (stimulated - pink) and fold changes of mRNA expression in NK cells stimulated with K562 target cells in the presence of the IRE1 blockade over NK cells stimulated with K562 target cells (inhibited - black). The gene expression was normalized to a house-keeping gene *B2M*. Unsupervised clustering was performed, and fold changes are presented as z-scores.

3.3.7 Inhibition of IRE1 impairs cytokine protein secretion

Based on the gene expression data I decided to examine the protein expression of the same set of molecules, i.e. IFNγ, TNFα, FASL, GZMB, and NKG2D, to establish the contribution of the IRE1-XBP1 axis in NK cell effector functions. For this, either unstimulated NK cells or NK cells stimulated with target cells (K562) in the presence or absence of IRE1 inhibitor were examined. Typically, NK cells (SNK10/KHYG-1/NK-92) were stimulated for 2 hours with target cells, except for the analysis of intracellular proteins such as IFNγ, TNFα, and GZMB, where the cells were incubated for 4 hours to allow for accumulation and subsequent detection of tested proteins. The fold change of protein expression in stimulated NK cells over unstimulated and in stimulated NK cells in the presence of the IRE1 inhibitor over stimulated NK cells was interrogated to enable direct comparison with the transcriptome expression. The

protein expression analysis encompasses the percentages of the cells expressing certain protein as well as the mean fluorescence intensity (MFI) data to enable a comprehensive analysis. The percentages of a protein expression provide the information on the distribution of the protein expression within a cell population, while the MFI provides the information on the level of the expression in the proportion of cells that do express the protein. Altogether, I observed that inhibition of the IRE1 altered the expression of all tested molecules, depending on a tested molecule it either caused an up- or down-regulation of the protein expression.

The most prominent down-regulation following the IRE1 inhibition in SNK10 cells was observed in the expression of both IFNγ and TNFα, notably this observation was consistent between the percentages and MFI (Figure 3.18). A similar trend was observed for GZMB. While the fold change of the FASL-expressing cells did not change significantly upon the IRE1 blockade, the amount of the protein expression within a positive population significantly increased. A consistent increasing trend following the IRE1 inhibition was observed in the NKG2D expression (Figure 19).

The analysis of the protein expression data in the KHYG-1 cells revealed that IFNγ and TNFα were also the molecules which expression was significantly impaired upon the IRE1 inhibition. Similarly, the expression of NKG2D was also impaired in KHYG-1 cells treated with the IRE1 inhibitor, and this observation refers to both the percentages and MFI analysis. Even though, the inhibition of the IRE1 did not induce significant changes in FASL and GZMB, expression as demonstrated in the analysis of percentages, a decreasing trend in the level of their expression was observed in the MFI analysis (Figure 3.19).

Finally, the analysis of the protein expression in NK-92 cells following the IRE1 inhibition indicates that the cytokine secretion demonstrated a decreasing trend, but a great level of variation observed in the TNFα expression contributed to the lack of statistical significance (Figure 3.20). The analysis of the FASL, GZMB and NKG2D molecules expression indicates that following the IRE1 inhibition their expression decreases, and this observation applies to both frequencies and MFI expression. Unexpectedly, the analysis of GZMB expression shows an inconsistent trend between the fold change of the percentages and the MFI, with the latter one exerting an increasing trend.

In summary, a consistent decreasing trend following the IRE1 inhibition was observed across all tested cell lines in the expression of IFNγ and TNFα. Although NKG2D expression was also significantly impaired following the IRE1 blockade, this observation was restricted to the

KHYG-1 and NK-92 cells, but not SNK10. Whereas the remaining molecules exerted a lot of variation trend-wise (increasing vs decreasing) and cell line-wise. Collectively, the gene and protein expression data suggest that the cytokine secretion is significantly affected in various NK cell lines following the IRE1 inhibition and these changes are consistently detectable at both mRNA and protein level.

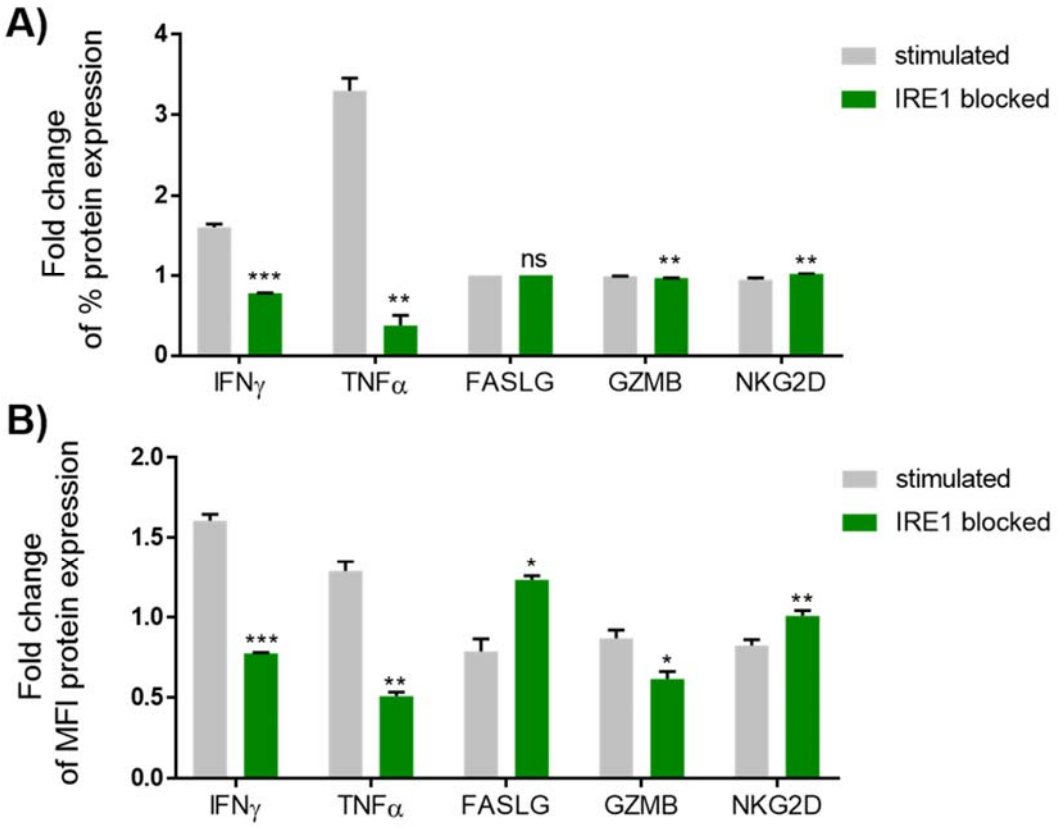

Figure 3.18: Inhibition of IRE1 impairs expression of selected effector molecules in SNK10 cells. Flow cytometry was utilised to assess the protein expression in SNK10 cells. Protein expression was assessed in unstimulated SNK10 cells and SNK10 cells treated with DMSO or 60μM of IRE1 inhibitor and stimulated with K562 targets (direct cytotoxicity). The graphs present fold change in protein expression in stimulated SNK10 cells over unstimulated cells and in IRE1 treated stimulated cells over stimulated cells based on the percentage (A) or the MFI (B) expression**.** Analysis: paired two-tailed Student's t-test (n=3), ns - not significant, **P<0.05, **P<0.01, ***P<0.001*.

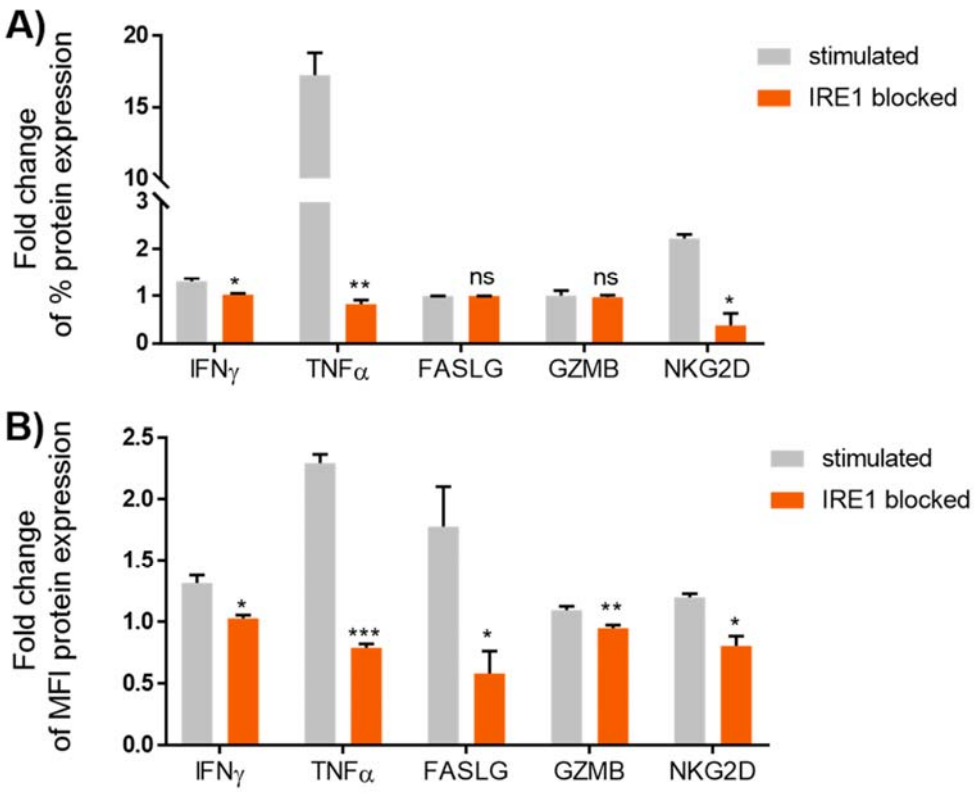

Figure 3.19: Inhibition of IRE1 impairs expression of selected effector molecules in KHYG-1 cells. Flow cytometry was utilised to assess the protein expression in KHYG-1 cells. Protein expression was assessed in unstimulated KHYG-1 cells and KHYG-1 cells treated with DMSO or 60μM of IRE1 inhibitor and stimulated with K562 targets (direct cytotoxicity). The graphs present fold change in protein expression in stimulated KHYG-1 cells over unstimulated cells and in IRE1 treated stimulated cells over stimulated cells based on the percentage (A) or the MFI (B) expression. Analysis: paired two-tailed Student's t-test (n=3), ns - not significant, **P<0.05, **P<0.01, ***P<0.001*.

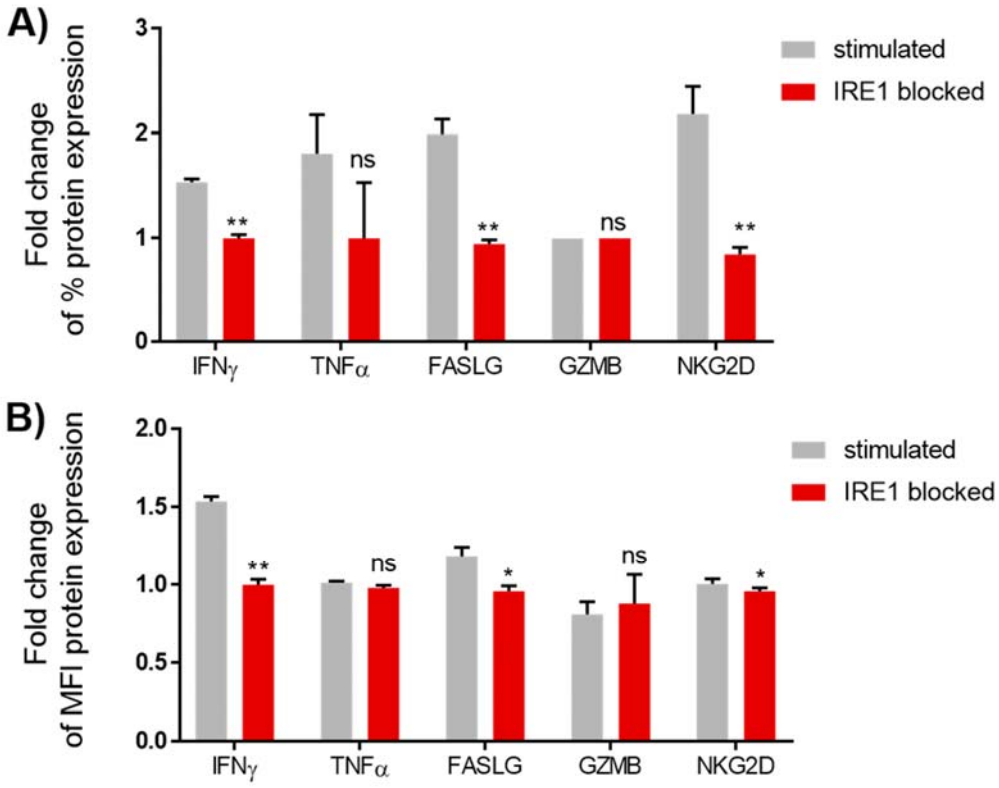

Figure 3.20: Inhibition of IRE1 impairs expression of selected effector molecules in NK-92 cells. Flow cytometry was utilised to assess the protein expression in NK-92 cells. Protein expression was assessed in unstimulated NK-92 cells and NK-92 cells treated with DMSO or 60μM of IRE1 inhibitor and stimulated with K562 targets (direct cytotoxicity). The graphs present fold change in protein expression in stimulated NK-92 cells over unstimulated cells and in IRE1 treated stimulated cells over stimulated cells based on the percentage (A) or the MFI (B) expression**.** Analysis: paired two-tailed Student's t-test (n=3), ns - not significant, *$P<0.05$, **$P<0.01$.

3.3.8 Activation of the IRE1-XBP1 pathway is associated with increased expression of cytokine proteins

NK cell function involves target cell lysis and cytokine secretion to recruit other immune cells to the immune response. Based on the compiled analysis of the gene and protein expression data in stimulated NK cell lines, I selected molecules that were down-regulated following IRE1 blockade at both the mRNA and protein level, to be further examined. The molecules selected for this analysis include the cytokines i.e. IFNγ and TNFα. I sought to determine whether

stimulation of NK cells with various target cells induces similar responses. To do so, I utilized SNK10 cell line as NK cell model and three types of target cells such as K562, KM-H2, and HDLM-2. Notably, KM-H2 cell line expresses MHC-I molecules, while the other two cell lines, HDLM-2 and K562, do not express such molecules. For this, NK cells were stimulated with appropriate target cell type in a 1:1 ratio for a total of 6 hours in the presence or absence of IRE1 inhibitor.

I noticed that IFNγ expression is significantly reduced upon IRE1 blockade, with the most prominent reduction of its expression in response to HDLM-2 cells. Similar rate of IFNγ secretion impairment was observed in response to K562 cells, and the lowest decrease in response to KM-H2 cells (Figure 3.21). In line with these observations, HDLM-2 cells induced the strongest secretion of IFNγ, K562 cells moderate, while KM-H2 cell the weakest. These differences may stem from the phenotypic differences across target cell types, including presence of MHC-I on KM-H2 cells. Nevertheless, the inhibition of IFNγ secretion occurs in response to all three target cell types but to a different extent.

Interestingly, I observed similar response trends with regards to TNFα secretion. Particularly, the strongest response was induced by HDLM-2 cells, then by K562 cells, and the weakest by KM-H2 cells (Figure 3.22). Whereas following the inhibition of the IRE1 the secretion of TNFα was significantly reduced in stimulated NK cells with each of tested target cells. Altogether, the experiments presented in this section suggest that activation of the IRE1-XBP1 signalling pathway by the innate immune system in NK cells is required for the optimal secretion of cytokines such as IFNγ and TNFα.

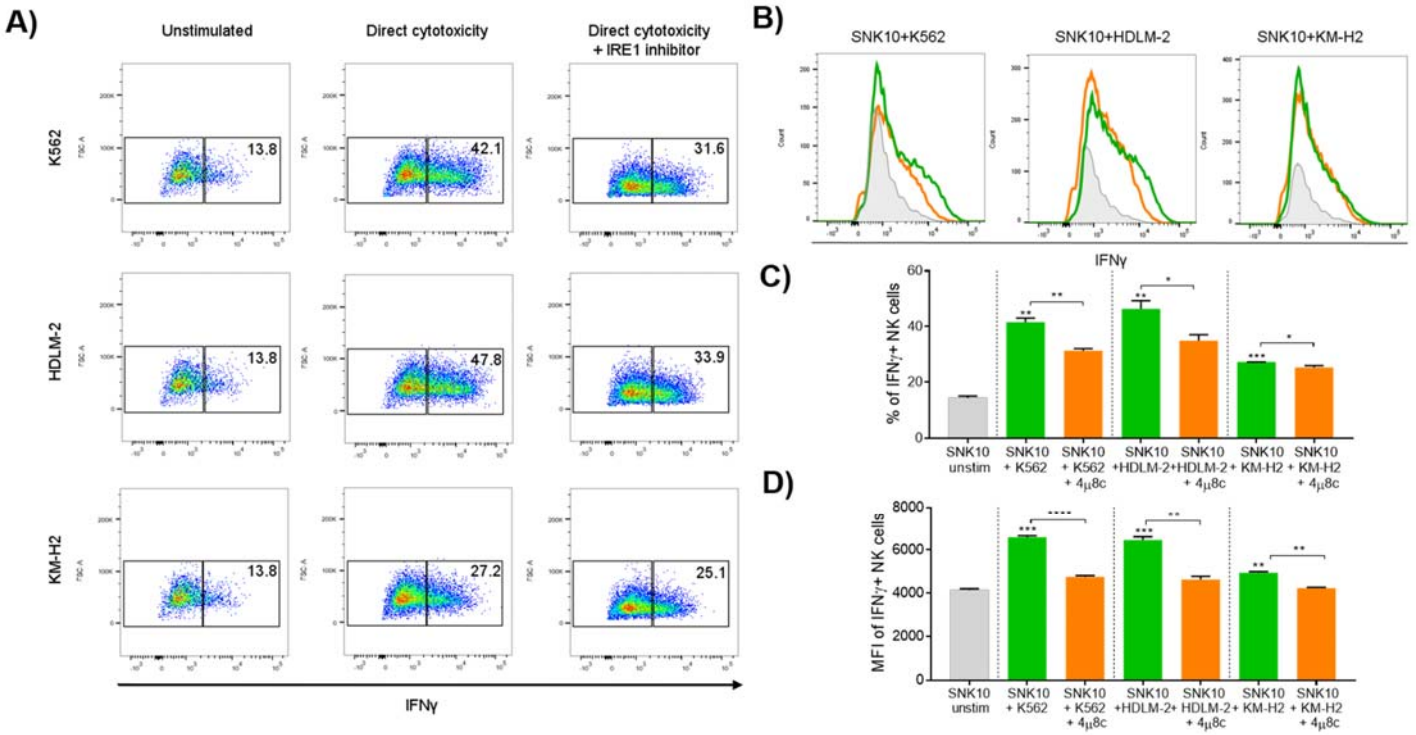

Figure 3.21: Inhibition of the IRE1 impairs IFNγ secretion by NK cells stimulated with different target cells. Flow cytometry was utilised to assess the protein expression in SNK10 cells in response to K562, HDLM-2 or KM-H2 cells. Protein expression was assessed in unstimulated SNK10 cells and SNK10 cells treated with DMSO or 60μM of IRE1 inhibitor and stimulated with K562 targets (direct cytotoxicity). The graphs present a representative plot showing IFNγ protein expression in SNK10 cells (A). Representative histograms are shown (B). Green line: SNK10 cells following stimulation, orange line: SNK10 cells following stimulation in the presence of 60μM IRE1 inhibitor, grey line: unstimulated SNK10 cells. Changes in the percent of IFNγ producing cells (C) and the relative amounts of IFNγ being produced (D) was analysed. Analysis: paired two-tailed Student's t-test (n=3), **P<0.05, **P<0.01, ***P<0.001*.

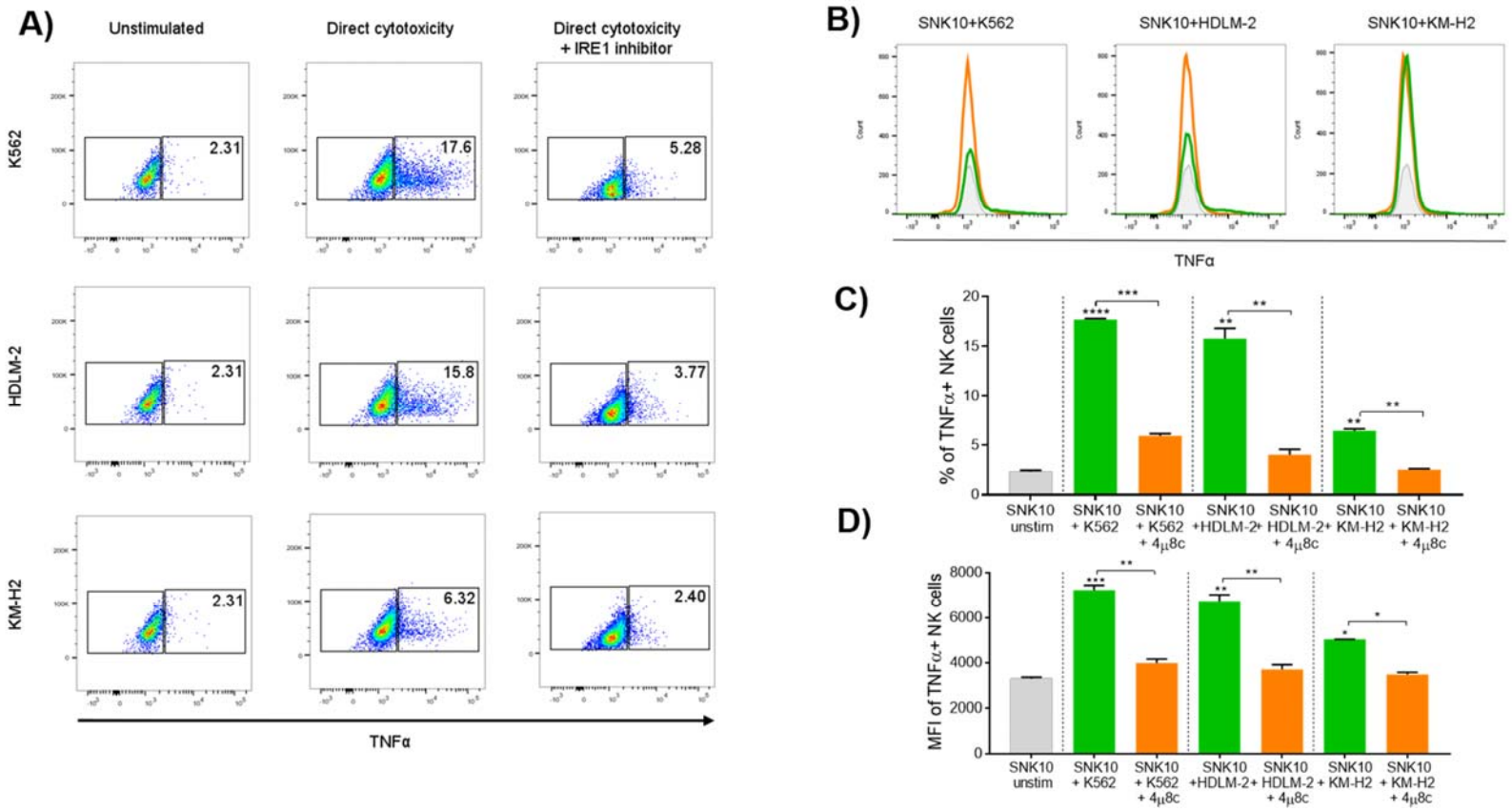

Figure 3.22: Inhibition of the IRE1 impairs TNFα secretion by NK cells stimulated with different target cells. Flow cytometry was utilised to assess the protein expression in SNK10 cells in response to K562, HDLM-2 or KM-H2 cells. Protein expression was assessed in unstimulated SNK10 cells and SNK10 cells treated with DMSO or 60μM of IRE1 inhibitor and stimulated with K562 targets (direct cytotoxicity). The graphs present a representative plot showing TNFα protein expression in SNK10 cells (A). Representative histograms are shown (B). Green line: SNK10 cells following stimulation, orange line: SNK10 cells following stimulation in the presence of 60μM IRE1 inhibitor, grey line: unstimulated SNK10 cells. Changes in the percent of IFNγ producing cells (C) and the relative amounts of TNFα being produced (D) was analysed. Analysis: paired two-tailed Student's t-test (n=3), **P<0.05, **P<0.01, ***P<0.001*.

3.3.9 Inhibition of *XBP1* splicing does not affect NK cell-target cell conjugate formation

One of the earliest events in the immunological synapse formation process is the conjugation of the NK cell with a target cell. The adhesion of these two cells, which is a part of the pre-effector stage of the immune synapse formation, initiates a signalling cascade that triggers downstream conformational changes in NK cell leading to the NK cell-mediated anti-tumour responses [158]. I sought to determine whether the IRE1-XBP1 pathway is required for the NK cell-mediated conjugate formation. A model NK cell line KHYG-1 was employed to assess the ability of NK cells to form conjugates with HDLM-2 target cells. For this NK cells were mixed with target cells and incubated for up to 30 minutes in the presence or absence of IRE1 blockade to allow for the conjugate formation. At the end cells were fixed and analysed by flow cytometry to determine the percentage of conjugated NK cells in the presence or absence of IRE1 blockade (Figure 3.23). Unexpectedly, NK cells did not display a significant reduction in conjugate formation with HDLM-2 cells in the presence of IRE1 blockade (Figure 3.24). Therefore, the IRE1-XBP1 pathway does not appear to be required for the NK cell-mediated conjugation of target cells.

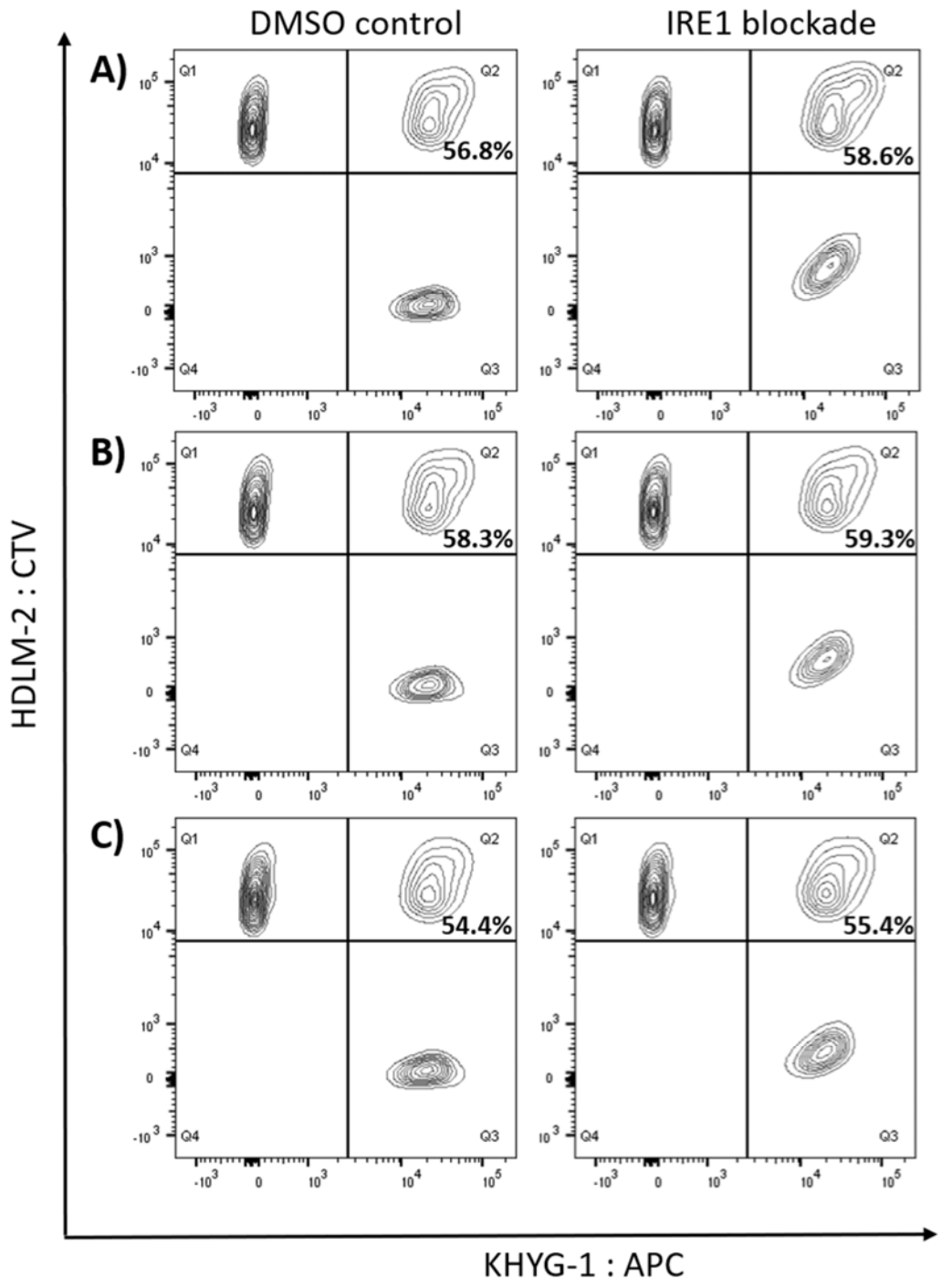

Figure 3.23: The number of NK cells-HRS cells conjugates is not affected by IRE1 blockade. Contour plots show the percentage of collected events within the double-positive gate (Q2) denoting conjugates between Cell Tracker Violet (CTV)-labelled HDLM2 cells and Cell Tracker Red (APC)-labelled KHYG-1 cells formed after 5 (A), 15 (B), and 30 (C) minutes of incubation in the presence or absence of IRE1 blockade.

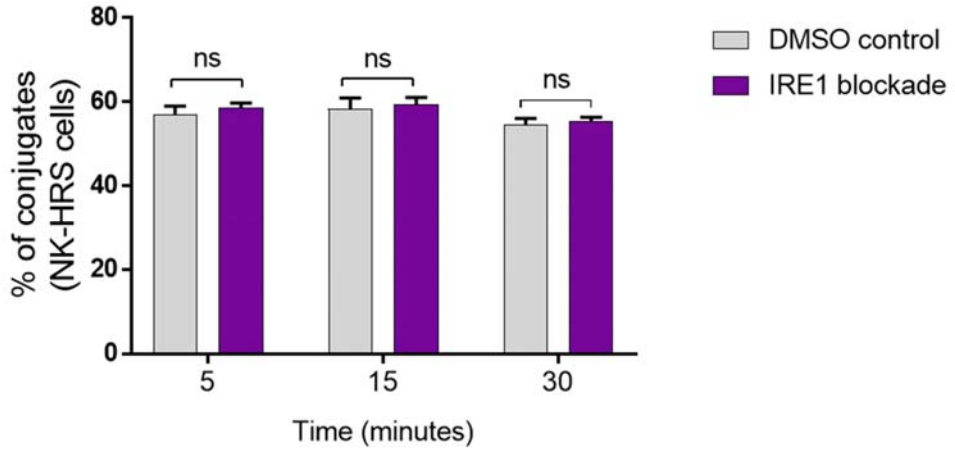

Figure 3.24: Inhibition of IRE1 does not affect the adhesion of NK cells to target cells is not affected. Flow cytometry was utilised to determine the number of conjugates formed between NK cells and HRS cells that were co-cultured for 5, 15, and 30 minutes and fixed prior to acquisition on the FACS. The graph shows percentages of conjugates formed between NK cells (KHYG-1) and HRS cells (HDLM-2) over time. Analysis: paired two-tailed Student's t-test (n=3), ns - not significant.

3.3.10 Inhibition of *XBP1* splicing impairs actin polarization at the NK cell immune synapse interface

To execute cytolytic function NK cells need to engage with a target cell to establish an immunological synapse (IS). Upon recognition of a target cell, a cytoskeleton rearrangement involving F-actin polymerization is an event that is a prerequisite step in the formation of the IS. I examined the IS formed between the KHYG-1 NK cell line and the HRS cell line (HDLM-2) in the presence and absence of the IRE1 inhibitor. To test this, conjugates formed (within 30 mins) between NK cells and HRS cells, were examined for the distribution of F-actin after staining with phalloidin. The extent of actin polymerization in NK cell conjugates was compared between untreated and treated with 4μ8c cells by quantitative analysis of fixed conjugates images taken by confocal microscopy. As expected, quantification of F-actin polymerization at the NK cell–HRS cell contact site showed that most conjugates, where NK cells were treated with 4μ8c, exhibited a weak band of F-actin at the immune synapse in comparison to the untreated cells (Figure 3.25). These data demonstrate that inhibition of the IRE1-XBP1 pathway in NK cells results in impaired actin polarization at the IS interface, indicating formation of a greater number of less stable conjugates.

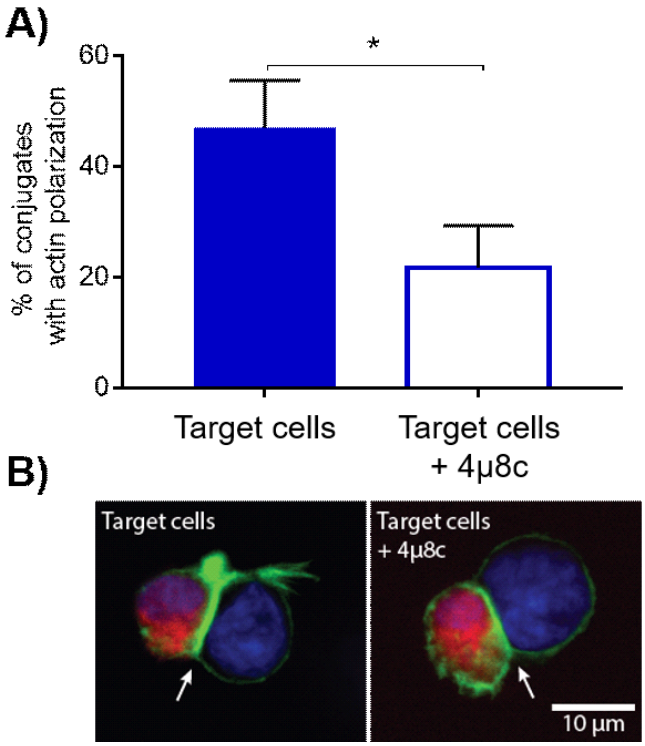

Figure 3.25: IRE1 blockade impairs NK cell immune synapse formation with HRS cells. NK cells were allowed to conjugate with an HRS cell line HDLM-2 for 30 min in the presence or absence of IRE1 inhibitor. Conjugates were then fixed, stained, and scored for F-actin (phalloidin, green) polarization at the NK cell immune synapse. Data are the mean ± SD from 3 independent experiments with 30 conjugates analysed per experiment. Representative images of NK cell synapse formation between KHYG-1 (DAPI, blue) and HRS cells (APC, red) are shown (B). Arrows indicate actin accumulation at the NK cell–HRS synapse site imaged with the Nikon spinning disc confocal microscope. Original magnification ×63. Statistical differences between experimental groups were evaluated by unpaired Student's t-test (n=3), *P<0.05.

3.3.11 Inhibition of IRE1 impairs NK cell migration

A prerequisite for NK cell-mediated surveillance is their cytoskeleton integrity and ability to migrate to remove malignant cells from the microenvironment. This aspect of NK cell function is controlled not only by the composition of chemokines present in the NK cell microenvironment, but also intracellular modulation of cytoskeleton required for NK cell to migration toward target cells. To determine whether IRE1 blockade affects NK cell migration, the NK cell line (KHYG-1) was seeded onto the migration chamber and incubated for 5hrs in the presence or absence of the IRE1 blockade. Addition of the IRE1 inhibitor impaired the migration of KHYG-1 cells which is demonstrated by a significant reduction in the number of cells which migrated through the transwell after 5 hours of incubation (Figure 3.26).

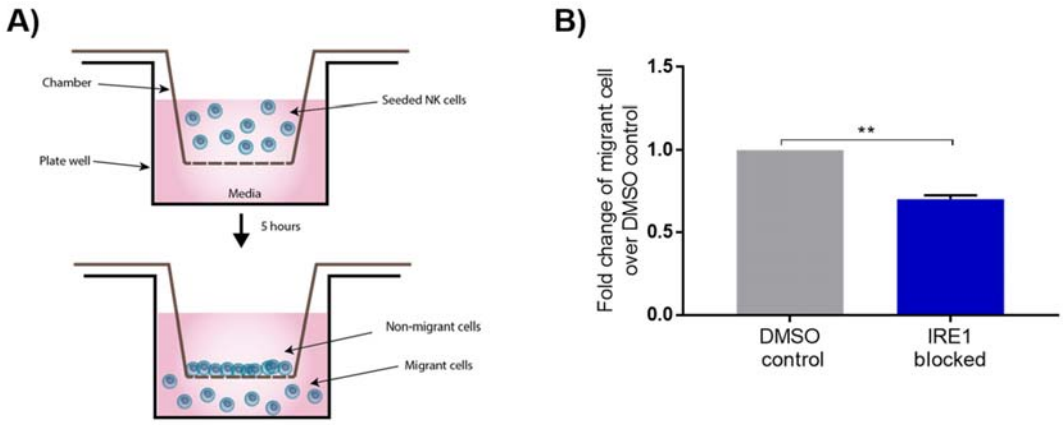

Figure 3.26: IRE1 blockade impairs migration of NK cells. NK cell line, KHYG-1, in the presence of IRE1 blockade or DMSO control, was seeded onto a transwell chamber with 5μM pore-size and incubated for 5 hours to allow cell migration to the bottom well containing medium (migration) (A). Migrant cells were collected from the well, stained, and analysed by the flow cytometry. The fold change of migrant cells treated with IRE1 inhibitor over untreated cells (DMSO control) are presented (B). Statistical differences between experimental groups were evaluated by paired Student's t-test (n=3), **P<0.01.

3.3.12 Summary of results

The main aim of this chapter was to determine whether stimulation of NK cells with various target cells induces *XBP1* splicing that is a marker of the IRE1-XBP1 pathway activation. Consistent with the previous results generated in my supervisor's laboratory, it was demonstrated that stimulation of the SNK10 NK cell line with K562 leads to *XBP1* splicing. In addition, it was found that the *XBP1* splicing occurs in two other NK cell lines, KHYG-1 and NK-92, upon the simulation with the same target cells. Interestingly, *XBP1* splicing was also demonstrated to occur, in response to activation by HL target cell lines suggesting that it may be a general response of NK cells to stimulation with malignant target cells. Further, I have demonstrated that, although *XBP1* is spliced in NK cells following addition of target cells, this appears to be independent of the canonical UPR system. Next, I have demonstrated that the IRE1-mediated splicing of *XBP1* can be successfully inhibited using a small molecule inhibitor in stimulated NK cells. Subsequently, activation of the IRE1-XBP1 pathway, through stimulation with various target cells, was associated with the increased transcriptome and protein expression of cytokines such as IFNγ and TNFα. Notably, their expression was significantly down-regulated upon the IRE1 blockade indicating that the IRE1-XBP1 pathway is required for optimal secretion of these cytokines. In addition, I demonstrated that inhibition of *XBP1* splicing significantly impairs NK cell migration. While application of this inhibitor did not affect NK cell adhesion to target cells, it impaired polarization of actin at the interphase of the IS indicating that XBP1s is critical for the IS formation.

3.4 DISCUSSION

3.4.1 *XBP1* splicing occurs following NK cell activation

Here I demonstrate that activation of the IRE1-XBP1 pathway via the contact-dependent interaction between NK cell and target cell leads to the optimal NK cell function involving migration, target cell recognition, and cytokine secretion. My findings suggest that NK cells utilize the IRE1-XBP1 pathway, the most conserved branch of the UPR system, to ensure optimal recognition and response to target cells. Indeed, XBP1s is one of the most promising targets of the UPR pathway in cancer therapy e.g. in MM, where XBP1s promotes growth and survival of malignant cells[175], its high expression is a favourable prognosticator in patients treated with bortezomib [176] [177]. I show that activation of this pathway is involved in NK cell effector function, suggesting that targeting the pathway via proteasome inhibitors such as bortezomib (an agent typically used in MM) may potentially have adverse off target effects on innate immunity.

The IRE1-XBP1 pathway has been extensively studied in a range of immune cells and diseases. Activation of this pathway i.e. detection of the *XBP1* splicing and its importance for the immune cell functions was first demonstrated in plasma cells. It was shown that XBP1s is required for differentiation of B cells into plasma cells [121]. This discovery was followed by a series of studies investigating the IRE1-XBP1 pathway in other immune cells including T cells, macrophages, dendritic cells and eosinophils in a diverse array of diseases [123] [178] [122] [125] [162] [124]. A large body of evidence demonstrates that activation of the IRE1-XBP1 pathway is initiated via different mechanisms and is highly context-specific. I found that *XBP1* splicing occurs also in a range of NK cell lines stimulated with leukemia or lymphoma target cells.

In macrophages, TLR signalling induces the IRE1-mediated *XBP1* splicing without triggering the canonical UPR [122]. In line with this finding, the induction of *XBP1* splicing in stimulated NK cells, was not associated with increased expression of well-described target genes of XBP1s. This observation suggests that the IRE1-XBP1 pathway operates in NK cells outside of the canonical UPR. Conversely, in a study conducted in NK cells from patients with a type 2 diabetes (T2D), in whom high level of glucose triggers the ER stress, it was found that a range of ER stress related molecules including XBP1s is upregulated. This observation was associated with alterations in NK cell phenotype i.e. reduced expression of *NKG2D* [179].

Multiple studies have shown that a small molecule inhibitor known as 4μ8c, which specifically targets the RNase activity of IRE1, efficiently inhibits IRE1-mediated splicing of *XBP1* in different cell types [150] [176] [180]. To interrogate the role of IRE1-XBP1 pathway in NK cells, I also employed this

small molecule inhibitor. Consistent with previous findings, application of 4μ8c in stimulated NK cells successfully inhibited *XBP1* splicing, as demonstrated by reduced expression of XBP1s, both mRNA and protein.

3.4.2 XBP1s is required for NK cell effector function

As mentioned previously, Martinon *et al.* have demonstrated in an elegant study that the IRE1-XBP1 pathway is activated in macrophages in an uncanonical manner. Further, XBP1s was shown to directly regulate expression of selected cytokines, amongst them TNFα, through binding to their promoter regions, thereby contributing to their optimal secretion [122]. Similarly, I also observed that activation of the IRE1-XBP1 pathway is associated with optimal production of TNFα and IFNγ by NK cells in response to various target cells. Notably, following the IRE1 inhibition the expression of these cytokines was consistently affected, both on mRNA and protein level. Conversely, in the study of the ovarian cancer it was demonstrated that activation of the IRE1-XBP1 pathway was associated with impaired secretion of IFNγ by T cells [126]. Whereas, in a study involving T helper cells, it was found that inhibition of the IRE1 with a small molecule inhibitor did not affect IFNγ secretion but it significantly reduced IL-4 production [181].

A recent study reported that suppression of *XBP1* splicing is associated with impaired migration of endothelial cells (EC). Damaging the endothelium led to increased expression of XBP1s that interacted with endothelial nitric oxide synthase (eNOS) to contribute to enhance migration of EC [182]. Interestingly, I also found that inhibition of IRE1, i.e. suppression of *XBP1* splicing, significantly impairs migration of NK cell line KHYG-1.

Dejeans *et al.* in their study demonstrated that impairment in IRE1 activity is associated with improved adhesion and migration of glioma cells. It was shown that IRE1 directly regulates expression of SPARC via regulated IRE1-dependent decay of mRNA (RIDD) mechanisms. In the event of the IRE1 inactivity the expression of extracellular matrix protein SPARC increases and contributes to changes in glioma cell adhesion and migration [183]. I did not observe any changes in NK cell-mediated adhesion to target cells, but I noticed that in the presence of the IRE1 inhibitor the accumulation of actin at the IS interphase is significantly impaired, which suggests that formed conjugates are less stable. However, the exact mechanism of action is yet to be established.

3.4.3 Conclusion

In this study I present data showing that *XBP1* splicing occurs following NK cell stimulation with leukaemia and HL MHC-I intact and deficient target cells, and it appears that XBP1s is acting outside

of a canonical UPR system. Next, I successfully inhibited *XBP1* splicing in stimulated NK cells to enable interrogation of the IRE1-XBP1 pathway and its relationship with NK cell effector function. Specifically, the inhibition of the IRE1-mediated splicing of *XBP1* affected the expression of cytokines known to be secreted by NK cells, including cytokines that have not previously been linked to the IRE1-XBP1 pathway. In concordance with the gene expression profile the analysis of protein levels of these cytokines indicated that upon IRE1 inhibition the expression decreases. These results suggest that XBP1s may have a key role in cytokine production by NK cells and subsequent recruitment of immune cells to potentiate anti-tumour responses. Further, I also show that NK cell migration and immune synapse formation with blood cancer target cells is significantly impaired in the presence of an IRE1 inhibitor.

Collectively, I demonstrate a novel role of XBP1s during NK cell-mediated cytotoxicity in migration, formation of the immune synapse, and cytokine secretion by NK cells. To place these findings within a translational context, my next step was to determine if this pathway is dysfunctional in NK cells from patients with HL.

CHAPTER 4:

The IRE1-XBP1 pathway is dysregulated in NK cells from Hodgkin lymphoma

4.1 INTRODUCTION

4.1.1 The IRE1-XBP1 pathway in blood cancers

XBP1s is an important transcription factor involved in the UPR signalling pathway. Under conditions of ER stress, XBP1 is activated through unconventional splicing by IRE1, excising a 26-nucleotide intron from its mRNA [118] [117] [109]. Removal of this intron causes a frame shift in the open reading frame, resulting in a 376-amino acid long protein with an alternate carboxy-terminus containing a transactivation domain (XBP1s). XBP1s then translocates to the nucleus where it binds the ER stress responsive element to cause an increase in transcription of chaperones and to the UPR element resulting in increased transcription of genes involved in protein degradation [170] [169]. A requirement for XBP1s during a healthy immune response was first recognized when XBP1s was identified as an essential transcription factor for plasma cell differentiation [121]. Since then, XBP1s has been demonstrated to be involved in both innate and adaptive immune responses [121] [184] [120] [123] [125] [122].

The research on the IRE1-XBP1 pathway in the context of HL is sparse. In a study by Maestro *et al*., an immunohistochemistry assay was implemented to assess expression pattern of XBP1s in various lymphomas. While high expression of XBP1s was detected in plasmablastic DLBCL (64% of positive cases) and myeloma (100% positive cases), none of the tested HL cases expressed XBP1s [185].

Furthermore, it was established that GCB DLBCL are characterised by a defective IRE1-XBP1 pathway with reduced expression of IRE1 that prevents activation of XBP1. Importantly, it was demonstrated that reconstitution of the pathway in GCB DLBCL reduced tumour growth in a mouse xenograft model. In contrast, in the setting of multiple myeloma the IRE1-XBP1 pathway is implicated in a tumour-promoting role [186] [175]. These data emphasise a critical role of the IRE1-XBP1 pathway in malignancies and indicate that it can either contribute to tumour promotion or tumour suppression.

Although XBP1s is required for the function of specific immune cell subsets (e.g. plasma cells and macrophages), and for the differentiation and/or maturation of others (e.g. plasma cells, DCs and T cells), its role in NK cells has not been explored. In the previous chapters, I demonstrated a requirement for XBP1s during healthy NK cell effector function to ensure an optimal response against target cells. The malignant cells in HL are known to significantly affect the function of immune cells infiltrate in the TME. I sought to determine whether the IRE1-XBP1 pathway is dysregulated in circulating NK cells of patients with HL.

In the setting of HL, the lack of MHC-I expression on HRS cells prevents T cells from mounting effective anti-tumour responses. Nevertheless, HRS cells are amenable to NK cell-mediated cytotoxicity as their function is not restricted by MHC-I are able to instigate such responses. To investigate the function of NK cells in patients with HL I sought to investigate whether the IRE1-XBP1 pathway is operative to ensure NK cells anti-tumour capacity is optimal.

4.1.2 NK cells in Hodgkin lymphoma

NK cells represent an attractive component of host immunity to eliminate cancer cells as they are able to respond to tumour cells without previous sensitization [10]. Indeed, a longitudinal study of healthy participants, examining NK cell cytotoxic activity and cancer incidence, found an inverse association between NK cell cytolytic activity and the subsequent development of cancer [86].

To execute their function, NK cells form an immunological synapse with a target cell to either mediate target cell death or secrete immunoregulatory cytokines. The outcome of this interaction is dictated by the balance of activating and inhibitory signals received by the array of receptors expressed at the surface of the NK cell [3]. One of the most critical molecules for NK cell function is MHC-I. According to the "missing-self" hypothesis, introduced by Ljunggren and Karre, NK cells preferentially lyse cells with reduced expression of MHC-I molecules while sparing cells with intact MHC-I expression [36].

Notably, a multitude of cancer types, to escape T cell-mediated anti-tumour responses, exert decreased or lost expression of MHC-I molecules. The lack of MHC-I molecules renders malignant cells as potential targets for NK cell-mediated cytotoxicity [99]. The HRS cells (the malignant cells in HL), not only frequently exert a loss of MHC-I molecule on their surface, which prevents mounting T cell-mediated responses, but also have high expression of PD-L1 and PD-L2 ligands, which by engaging with the PD-1 molecule on effector cells (T cells, NK cells) dampen their function [140] [187]. Hence, a seemingly T cell rich TME in HL may instigate only modest anti-tumour responses [188].

To overcome this issue, current treatment regimens include immunotherapeutic antibodies targeting immune cells to potentiate their anti-tumour function. In HL, PD-1 blockade has proven clinical efficacy, but to date, the emphasis has been on the role of T cells, with data on NK cells relatively sparse. Nevertheless, given existing T cell evasion mechanisms in the setting of HL, it is important to delineate the role of NK cells in the clearance of malignant cells upon PD-1 blockade. It is particularly important in the light of a recent study by Vari *et al*., which demonstrated expansion of

the $CD3^{-}CD56^{bright}CD16^{lo}PD\text{-}1^{+}$ subset of NK cells in HL that is likely triggering the unique sensitivity of this disease to PD-1 blockade [93].

4.1.3 PD-1 blockade in HL

PD-1 and its cognate ligands, PD-L1 and PD-L2, are known to play a critical role in the regulation of T cell function. In health, the interaction between these molecules promotes self-tolerance and regulates autoimmunity. Specifically, the signalling via PD-1/PD-L1/PD-L2 axis inhibits T cell activation, proliferation, and cytokine production [189]. This checkpoint inhibitor is expressed not only by 'exhausted' T cells but also NK cells, whereas its counter molecules, PD-L1 and PD-L2, are expressed on APCs or malignant cells. The latter often exploit this pathway, by expressing checkpoint ligands on their surface, to evade anti-tumour responses and thrive in the tumour microenvironment [187]. Hence, targeting PD-1 axis with monoclonal antibodies to reverse exhaustion of the immune cells and unleash their anti-tumour potential is an attractive therapeutic target [190].

First clinical trials, in patients with relapsed/refractory HL, were to investigate the clinical efficacy of PD-1 blockade using two humanized monoclonal antibodies, known as nivolumab and pembrolizumab. The Phase I trial of nivolumab (CHECKMATE 039) resulted in the overall response rate (ORR) 87% and a complete response (CR) 17%. Evaluation of pembrolizumab in the Phase I trial KEYNOTE 013 resulted in similar outcomes: ORR 65% and CR 16%. These promising results led to subsequent Phase II trials to further investigate the clinical effect of PD-1 inhibitors, nivolumab in CHECKMATE 205 and pembrolizumab in KEYNOTE 087. The clinical efficacy of these agents was tested in two independent patient cohorts and resulted in the ORR 69% and CR 16% for nivolumab and ORR 69% and CR 22% for pembrolizumab [134] [187] [191] [192].

After the success of these clinical trials both antibodies targeting PD-1 were approved in patients with relapsed/refractory HL. Nivolumab, was approved in May 2016 by the Food and Drug Administration (FDA) and in November 2016 by the European Medicines Agency (EMA), while pembrolizumab was approved almost a year later in March and May 2017 by FDA and EMA, respectively. Overall, the PD-1 blockade is associated with high response rates and durable effects with acceptable safety profiles in patients with relapsed/refractory HL [191] [192].

Notably, the advent of PD-1 inhibitors has improved treatment outcomes in patients with relapsed/refractory HL. The unique sensitivity of HL to PD-1 blockade therapies might be due to the malignant cells of HL that overexpress PD-L1 and PD-L2 ligands which by engaging with PD-1 molecules on T-cells drive their exhaustion [134] [187]. However, HRS cells often have a variable loss of MHC-I/II expression, therefore a high response rate to PD-1 blockade is likely not solely

mediated by CD8 and CD4 T cells. Conversely, the loss of MHC-I may render HRS cells sensitive to NK cell-mediated cytotoxicity. However, the knowledge about the exact mechanism of PD-1 blockade on unleashing NK cell function is limited and further investigations are necessary [189]. Overall, PD-1 blockade is an attractive way to reinstate host's immune function in HL, but its effect on various immune cells needs to be further elucidated to ensure optimal benefits.

4.2 AIMS

Based on studies in NK cell lines it was determined that following recognition of a target cell, IRE1-XBP1 pathway is activated to ensure appropriate NK cell effector function. I hypothesise that IRE1-XBP1 pathway is dysregulated in HL and that this can be reversed by PD-1 blockade. The main aim of this chapter was to determine if the IRE1-XBP1 pathway is dysregulated in NK cells from Hodgkin lymphoma patients during NK cell-mediated effector function and to establish if this dysregulation affects NK cell functions. Next, the ability of PD-1 blockade to reverse IRE1-XBP1 pathway-mediated NK cell effector dysfunction was tested. The specific aims of this chapter are:

1. To determine if the IRE1-XBP1 pathway is dysregulated in pNK from the peripheral blood of pre-therapy HL patients.

2. To characterise in detail, the nature of NK cell dysfunction and its relationship with the IRE1-XBP1 pathway in HL.

3. To test the ability of PD-1 blockade to reverse IRE1-XBP1 pathway associated pNK cell dysfunction.

4.3 RESULTS

4.3.1 The IRE1-XBP1 pathway is not activated in the CD56^{bright}CD16^{-} subset of NK cells from HL patients

In the previous chapter (refer to Chapter 3), the relevance of the IRE1-XBP1 pathway activation for appropriate NK cell function was demonstrated. Hence, I sought to determine whether the IRE1-XBP1 pathway operates in the circulating NK cells of HL patients; the expression of XBP1s, an active form of XBP1, was assessed in unstimulated and HRS-stimulated NK cells from HL patients and age-matched healthy controls. NK cell subset characterization was performed on peripheral blood CD3^{-}CD14^{-}CD19^{-}CD56^{+} mononuclear cells (Figure 4.2). NK cells were defined based on CD56 and CD16 expression, and two subsets were further identified as follows: CD56^{bright}CD16^{-}, CD56^{dim}CD16^{+}. First, to establish the optimal time of pNK cells stimulation with HRS cells, a time-course experiment involving healthy individual cells was performed. Based on the results of this analysis a 4-hour time-point was selected for further analysis (Figure 4.1). It was found that following HRS-stimulation, XBP1s expression in NK cells from HL was significantly lower than in age-matched healthy controls (Figure 4.3 A). This observation was restricted to the CD56^{bright}CD16^{-} subset of NK cells.

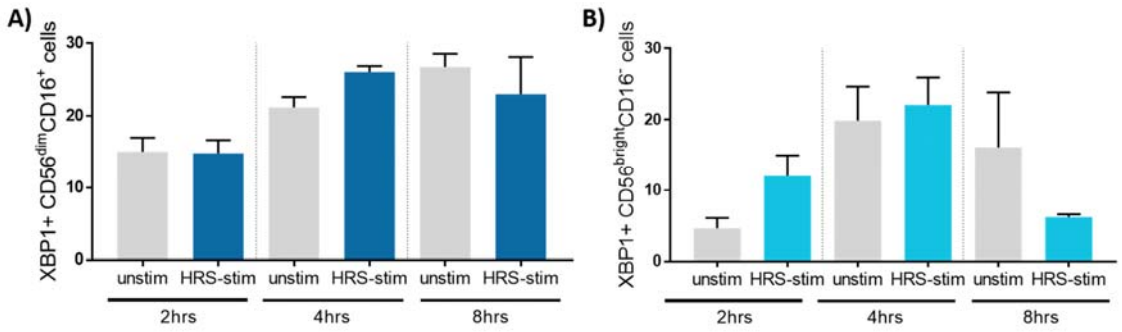

Figure 4.1: A time-course of XBP1s expression in different subsets of pNK cells from healthy individuals in response to HRS cells-stimulation. The expression of XBP1s in NK cells from healthy individuals was tested by flow cytometry. Cells were stimulated with HRS cells (KM-H2 cell line) over the course of time to select a time-point with optimal activation of the IRE1-XBP1 pathway. Both subsets CD56^{dim}CD16^{+} and CD56^{bright}CD16^{-} of healthy pNK cells display similar kinetics of the IRE1-XBP1 pathway activation, with the peak at 4-hour time-point, which was selected for further analysis.

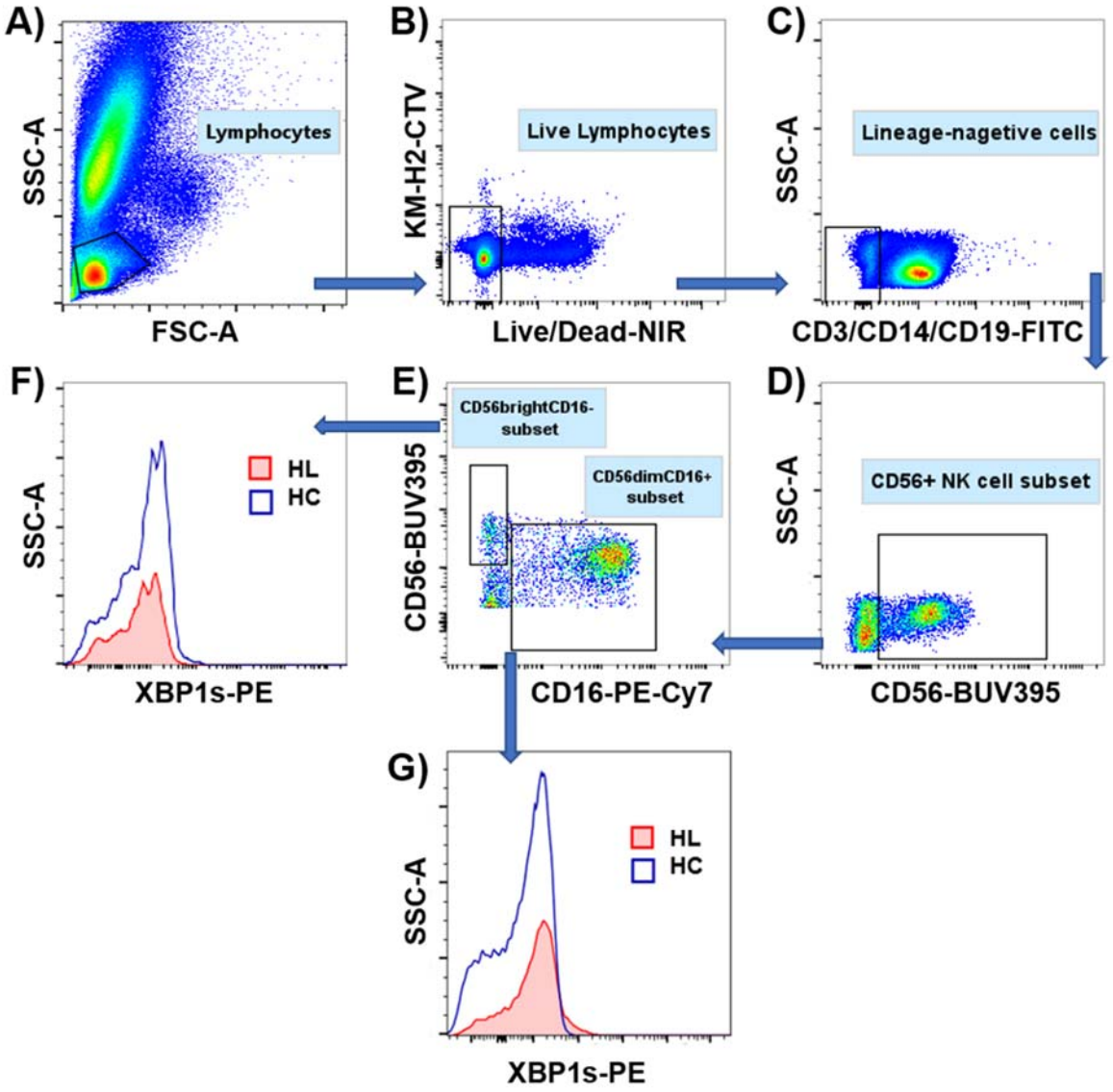

Figure 4.2 : Gating strategy of different pNK cell subsets and XBP1s. NK cells were identified from total lymphocytes as shown (A). Then, both dead cells and targets cells were removed from analysis by gating on KM-H2-CTV/Live/dead^{-} events (B). Successive gates were applied to exclude monocytes, T and B cells from analysis (C). To proceed with NK cell analysis CD56+ cells were gated on (D), which allowed to stratify them into two different subsets based on CD56 and CD16 expression (E). Representative plots showing the expression of XBP1s in stimulated CD56^{bright}CD16^{-} (F) and CD56^{dim}CD16^{+} (G) cells from a healthy control (HC, blue line) and a HL patient (HL, red line with shading) are presented.

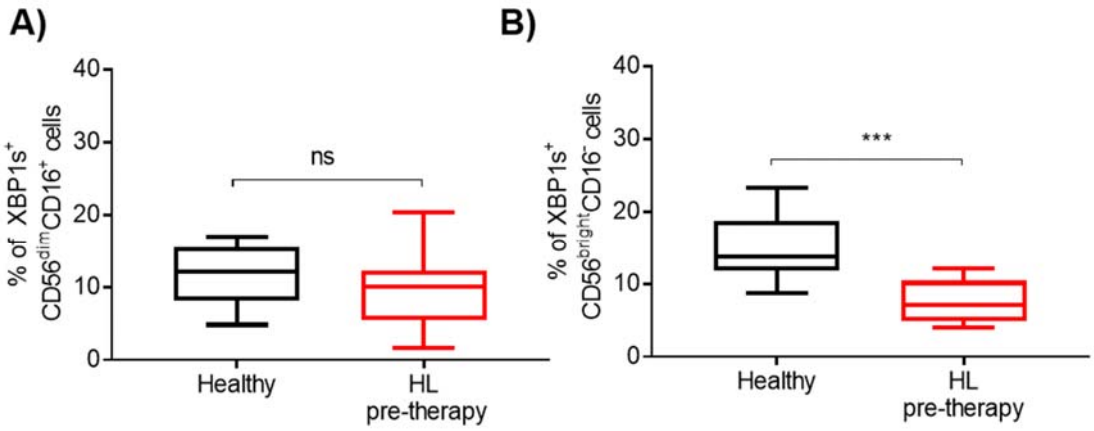

Figure 4.3: XBP1s is not activated in primary NK cells from HL patients. The effect of HRS cells on XBP1s activation was tested in pNK cells of HL patients and age-matched healthy controls. PBMCs were incubated for 4 hours in the presence of HRS-cells (KM-H2) admixed in 1:1 ratio. XBP1s expression was measured by flow cytometry. XBP1s is suppressed in the $CD56^{bright}CD16^{-}$ cells from HL patients following the stimulation with HRS-cells (A) but not in the $CD56^{dim}CD16^{+}$ cells (B). Analysis Mann-Whitney test (n=10), ***P<0.001.

4.3.2 The absolute NK cell count is reduced in patients with Hodgkin lymphoma

To determine whether the size of NK cell compartment in the circulation of HL patients is altered, NK cell absolute counts in PBMCs from HL pre-therapy patients and age-matched healthy controls were calculated and compared. It was noted that the number of CD3-CD56+ NK cells in the peripheral blood of HL patients was significantly reduced in comparison to healthy controls (Figure 4.4.A). The analysis of the two conventional NK cell subsets, the $CD56^{bright}$ $CD16^{-}$ (Figure 4.4 B) and the $CD56^{dim}$ $CD16^{+}$ (Figure 4.4 C), demonstrated the numbers of NK cells are decreased in both subsets in comparison to the healthy controls. In healthy participants, NK cells account for ˜10% of all lymphocytes. However, the number of NK cells in HL appeared significantly lower than in the healthy participants, in line with the recent finding demonstrated by Vari *et al.* [93].

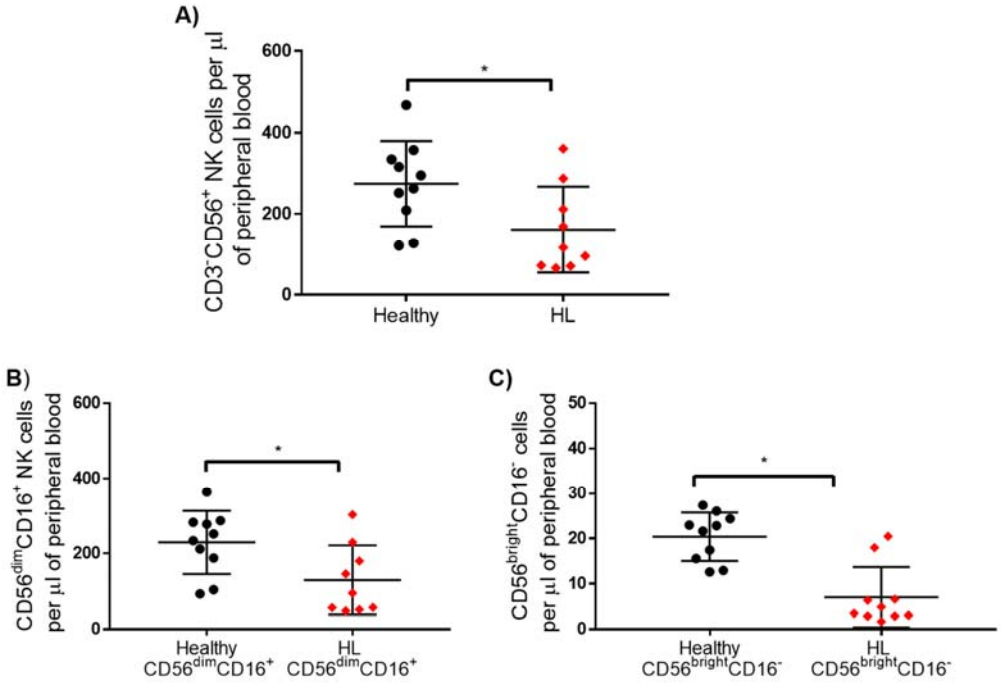

Figure 4.4: NK cell compartment in Hodgkin lymphoma is contracted. The absolute numbers of NK cells in the peripheral blood of HL pre-therapy patients and age-matched healthy controls were calculated. The number of NK cells in HL patients is significantly lower than in healthy controls, which is reflected in the total NK cell counts (A), and individual NK cell subsets: $CD56^{dim}CD16^{+}$ (B) and $CD56^{bright}$ $CD16^{-}$ (C). Analysis Student's t-test (n=10) *P<0.05.

4.3.3 XBP1s suppression is associated with impaired NK cell immune synapse formation

To execute cytolytic function NK cells need to engage with a target cell to establish an IS. Upon recognition of a target cell, a cytoskeleton rearrangement involving F-actin polymerization is an early event that is a prerequisite step in the formation of the IS. Previous experiments demonstrated that following inhibition of the IRE1-XBP1 pathway with 4µ8c the IS between the KHYG-1 NK cell line and the HRS cell line (HDLM-2) was impaired as demonstrated by weak F-actin accumulation at the IS site. Here, I sought to determine whether inhibition of the IRE1-XBP1 pathway in pNK cells obtained from HL patients also display a similar defect in the IS formation. To test this, conjugates formed (within 30mins) between pNK cells and HRS cells, were examined for the distribution of F-actin after staining with phalloidin. The extent of actin polymerization in NK cell conjugates from HL patients was compared between cells untreated and treated with 4µ8c by quantitative analysis of fixed conjugates by confocal microscopy. As expected, quantification of F-actin polymerization at the pNK cell–HRS cell contact site showed that most conjugates, where pNK cells were treated with 4µ8c, exhibited a weak band of F-actin at the immune synapse in comparison to the untreated cells

(Figure 4.5). These data demonstrate that inhibition of the IRE1-XBP1 pathway in pNK cells in patients with HL results in impaired actin polarization.

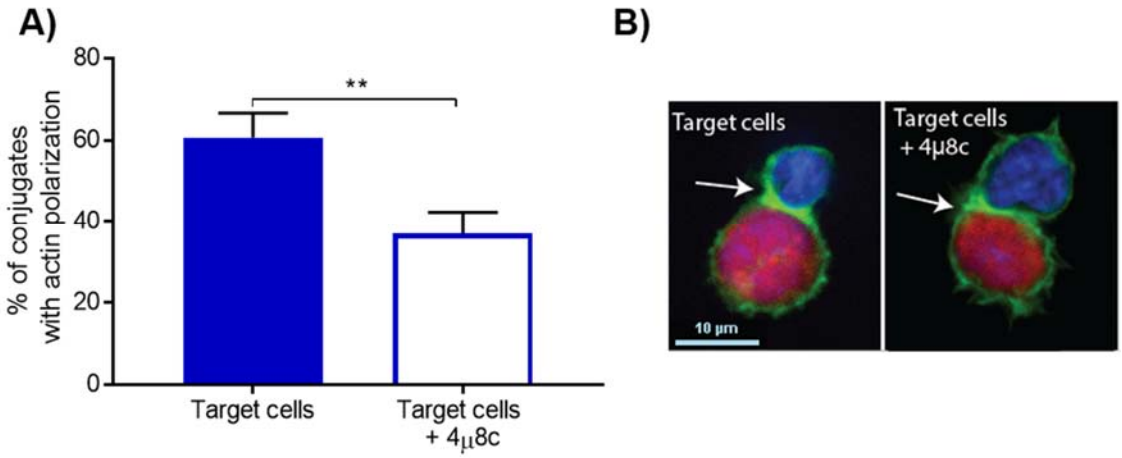

Figure 4.5: IRE1 blockade impairs NK cell immune synapse formation with HRS cells. NK cells from HL patients (A) were allowed to conjugate with an HRS cell line HDLM-2 for 30 min in the presence or absence of IRE1 inhibitor 4μ8c. Conjugates were then fixed, stained, and scored for F-actin (phalloidin, green) polarization at the NK cell immune synapse. Data are the mean ± SD from 3 independent experiments with 30 conjugates analysed per experiment. Representative images of NK cell synapse formation between $CD3^{-}CD56^{+}$ pNK cell (DAPI, blue) and HRS cells (APC, red) are shown (B). Arrows indicate actin accumulation at the NK-cell–HRS synapse site imaged with the Nikon spinning disc confocal microscope. Original magnification ×63. In the control assays, target cells and NK cells were co-incubated with IgG_4 isotype control. Statistical differences between experimental groups were evaluated by Student's t-test (n=3) **P<0.01.

4.3.4 PD-1 blockade rescues immune synapse formation

To better understand if this defect in NKIS formation resulted from the signalling via PD-1/PD-L1/PD-L2 axis (Figure 4.6), I also examined the potential improvement of actin accumulation at the IS upon a blockade of PD-1 with pembrolizumab, and whether it can reverse the impairment driven by the suppression of the IRE1-XBP1 pathway. The extent of actin polymerization in pNK cell conjugates from patients with HL was compared across cells treated with pembrolizumab or isotype control by quantitative analysis of fixed conjugates, randomly selected for analysis with confocal microscopy (Figure 4.7). As expected, quantification of F-actin polymerization at the pNK cell–HRS cell contact site showed that most conjugates formed with pNK cells treated with pembrolizumab exhibited a prominent band of F-actin at the immune synapse in comparison to the cells treated with isotype control. Interestingly, PD-1 blockade appears to be capable of enhancing F-actin polymerization at the IS, as well as partially reversing the impairment driven by suppressed XBP1s.

Collectively, these data demonstrate that PD-1 blockade enhances actin accumulation at the IS between pNK cells of HL and HRS cells contributing to formation of a stable contact.

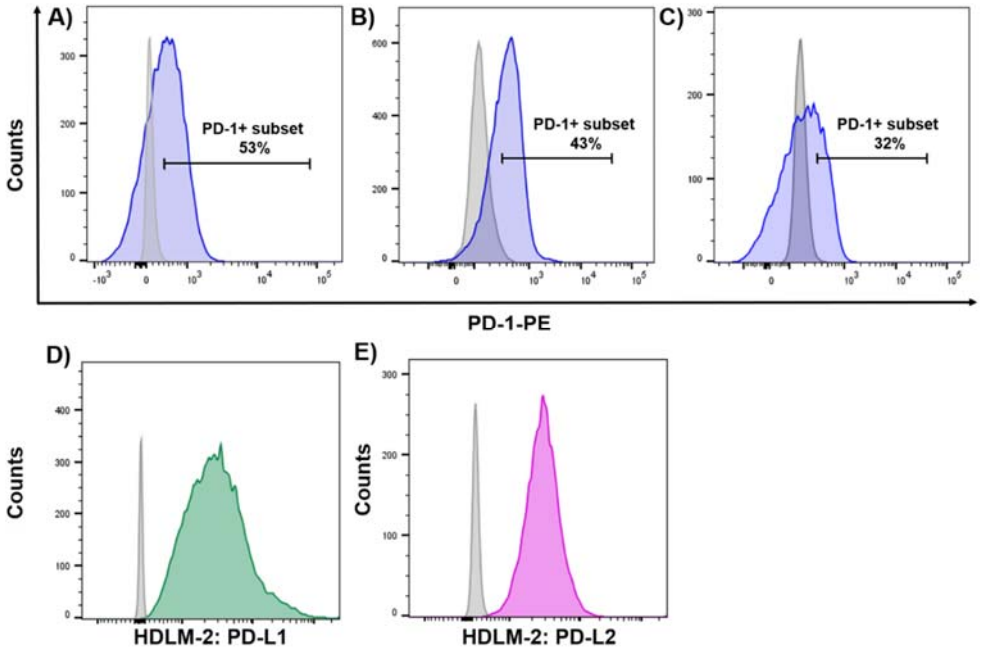

Figure 4.6: Expression of PD-1/PD-L1/PD-L2 axis molecules on pNK cells and HDLM-2 cells. Following the expansion of pNK cells the PD-1 expression was tested on $CD3^{-}CD56+$ pNK cells of each patient's sample (A, B, C). These cells were utilised for all functional experiments. In addition, expression of PD-1 ligands: PD-L1 (D) and PD-L2 (E), was assessed on HDLM-2 cell line that was also utilised in all functional experiments. FACS plots present expression of tested molecules in unstained control (grey), PD-1 expression (blue), PD-L1 (green), PD-L2 (fuchsia).

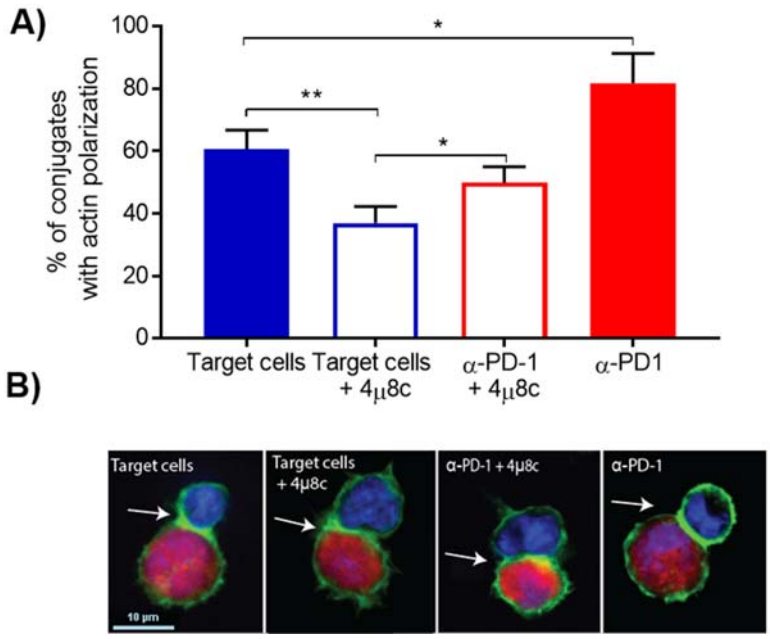

Figure 4.7: PD-1 blockade enhances pNK cell immune synapse formation with HRS cells and rescues. pNKIS formation in NK cells with a suppressed IRE1-XBP1 pathway. pNK cells from patients with HL (A) were allowed to conjugate with HRS cells HDLM-2 for 30 min in the presence or absence of PD-1 blockade and/or the IRE1 inhibitor 4μ8c. Conjugates were then fixed, stained, and scored for F-actin (phalloidin, green) polarization at the NK-cell immune synapse. Data are the mean ± SD from 3 independent experiments with 30 conjugates analysed per experiment. Representative images of NK cell synapse formation between $CD3^{-}CD56^{+}$ pNK cell (DAPI, blue) and HRS cells (APC, red) are shown (B). Arrows indicate actin accumulation at the NK-cell–HRS synapse site. Original magnification × 63. In the control assays, HRS target cells and pNK cells were co-incubated with immunoglobulin G4 isotype control. Statistical differences between experimental groups were evaluated by Student's t-test (n=3) *P<0.05, **P<0.01.

4.3.5 PD-1 blockade improves NK cell migration

Next, I tested whether PD-1 blockade could increase NK cell migration *in vitro*. For this, I used the KHYG-1 NK cell leukemia cell line characterised by high expression of PD-1 (Figure 4.8 B). Migration fold change was calculated by dividing the number of migrant NK cells with blocking antibody by the number of migrant cells treated with isotype control; statistical significance was calculated against a fold change of 1.0. Compared with culture with isotype control antibodies, KHYG-1 cultured with pembrolizumab significantly improved migration of NK cells (Figure 4.8 A). This indicates that the interruption of the PD-1/PD-L1 axis is sufficient to enhance $PD\text{-}1^{+}$ NK cells migration in an *in vitro* model.

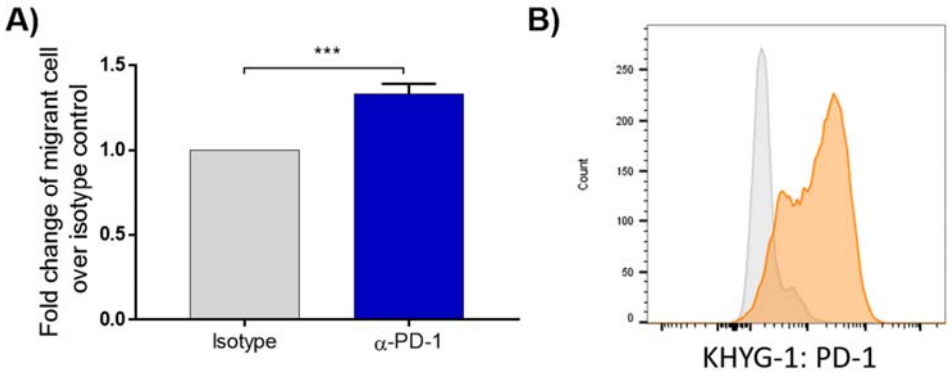

Figure 4.8: PD-1 blockade improves NK cell migration. KHYG-1 cells, in the presence of PD-1 blockade or isotype control, were seeded into a transwell chamber with 5μM pore-size and incubated for 5 hours to allow cell migration to the bottom well containing medium. Migrant cells were collected from the well, stained, and analysed by the flow cytometry. The fold change of migrant cells treated with pembrolizumab over cell treated with isotype control are presented (A). Statistical differences between experimental groups were evaluated by Student's t-test (n=3) ***P<0.001. Flow cytometry was utilised to assess expression of immune checkpoint PD-1 on KHYG-1 cell line (B). Plot presents expression of tested molecule in unstained control (grey), PD-1 expression (orange).

4.3.6 Suppression of XBP1s is associated with impaired IFNγ secretion

NK cells not only directly engage with cancer cells, but they can also recruit other cells by secretion of immunomodulatory cytokines such as IFNγ. In the previous chapter it was shown that activation of the IRE1-XBP1 pathway resulted in IFNγ secretion by pNK cells following engagement with target cells. Similarly, Iwakoshi *et al*. demonstrated that XBP1s is required for efficient production of IFNγ in DCs [123].

To determine whether downstream processes upon NKIS formation are affected by suppression of IRE1, I investigated the secretion of IFNγ by pNK cells from patients with HL with suppressed XBP1s. For this purpose, pNK cells from HL patients were expanded for 14 days in the presence of irradiated feeder LCL and supplemented with IL-2 and IL-15, as the numbers of NK cells in these patients are limited and are not sufficient to perform functional experiments. NK cells were stimulated with the HDLM-2 cell line in the presence or absence of 4μ8c, and then stained for IFNγ. To assess IFNγ expression in NK cells the gating strategy presented in Figure 4.9 was applied. A significant decrease of IFNγ production was observed in the pNK cells with suppression of the IRE1-XBP1 pathway (Target cells 50.7 ±1.5%; Target cells+4μ8c 39.8±1.3%) (Figure 4.10). This data indicates that blockade of the IRE1-XBP1 pathway results in suboptimal IFNγ production in expanded pNK cells in patients with HL.

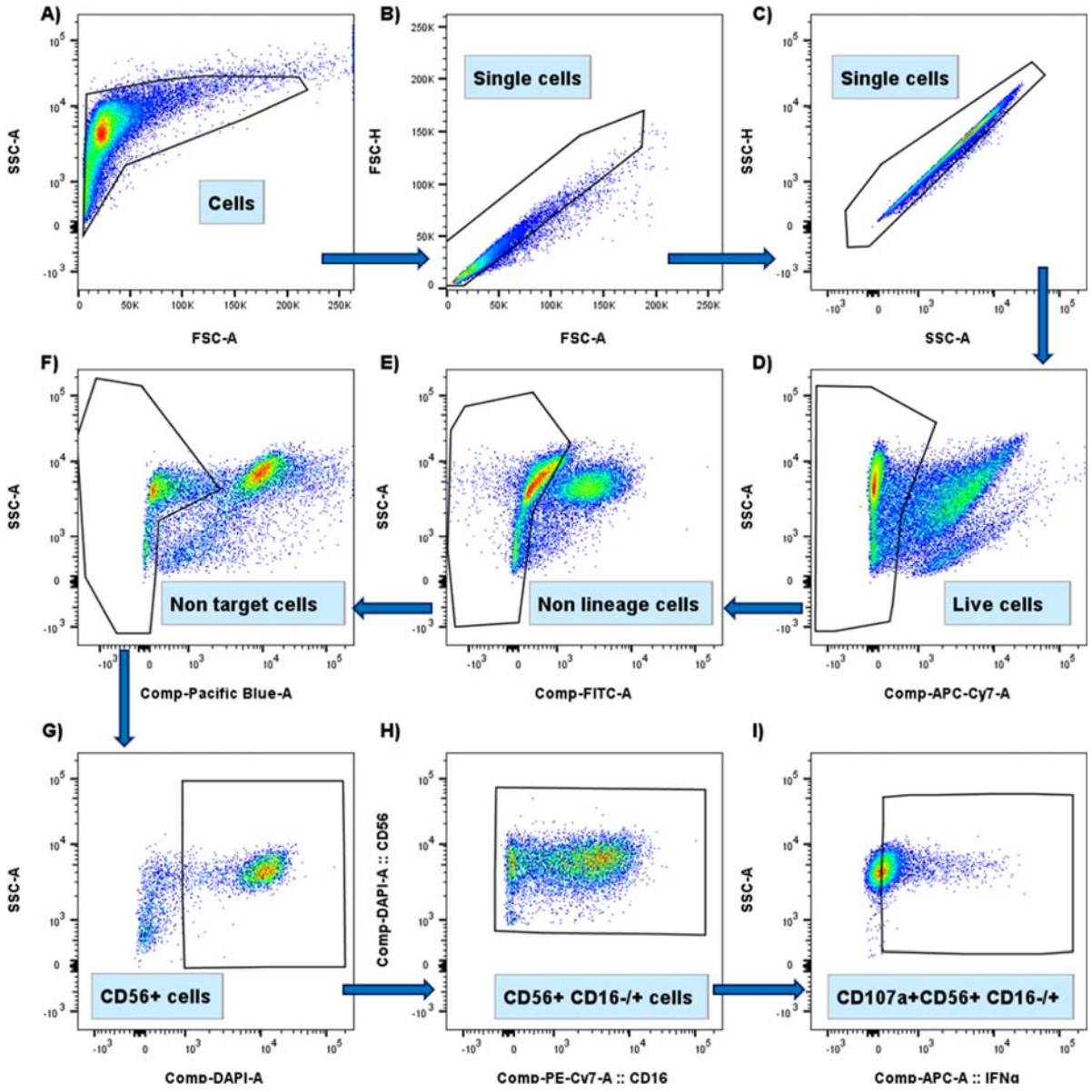

Figure 4.9: Gating strategy of IFNγ in NK cell subset. NK cells were identified from total lymphocytes as shown (A). Then, based on FSC-A/FSC-H (B) and SSC-A/SSC-H (C) scatters single cells were selected for further analysis. Dead cells were excluded from analysis by gating on APC-Cy7^{neg-} events (D). Successive gate was applied to exclude from analysis non-lineage cells (CD3-CD14-CD19-) (E) and target cells stained with CellTrackerViolet (F). To proceed with NK cell analysis, CD56+ cells were gated on (G), which allowed to subsequently gate on CD56^{+}CD16$^{-/+}$ cells (H) and assess IFNγ expression in general NK cell population (I).

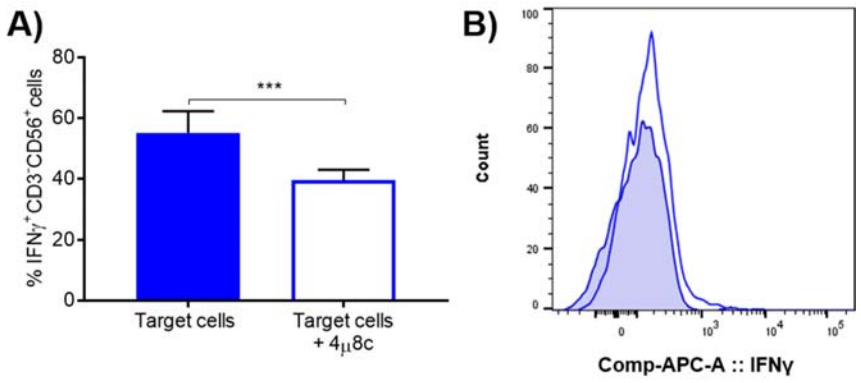

Figure 4.10: In patients with HL, expanded pNK cells with IRE1-XBP1 pathway blockade have impaired secretion of IFNγ. The expanded pNK cells from HL patients were stimulated with HRS cells for 6 hours and then stained intracellularly for IFNγ. The percent of $CD3^{-}CD56^{+}$ pNK cells untreated and treated with 60μM of 4μ8c is presented (n=3). Analysis Student's t-test (n=3) ***P<0.001. Representative FACS histogram shows changes in IFNγ in untreated (blue line) and 4μ8c treated cells (blue shade) (B).

Classically, NK cells can be subdivided into two subsets: $CD56^{dim}CD16^{+}$ and $CD56^{bright}CD16^{-}$ that display distinct functions *in vivo*. Specifically, $CD56^{dim}CD16^{+}$ cells are involved in NK cell-mediated target cell lysis, while $CD56^{bright}CD16^{-}$ cells are predominantly involved in cytokine secretion. Hence, expression of IFNγ was also interrogated in individual subsets to gain an in-depth overview of the IRE1 blockade impact on NK cell function. Following the IRE1 blockade a significant decrease of IFNγ secretion was observed in both NK cell subsets, but it was more significant in the $CD56^{bright}CD16^{-}$ subset of NK cells (Figure 4.12). This data further supports the notion that NK cells with suppressed IRE1-XBP1 pathway demonstrate a suboptimal IFNγ production in both subsets of expanded pNK cells from patients with HL.

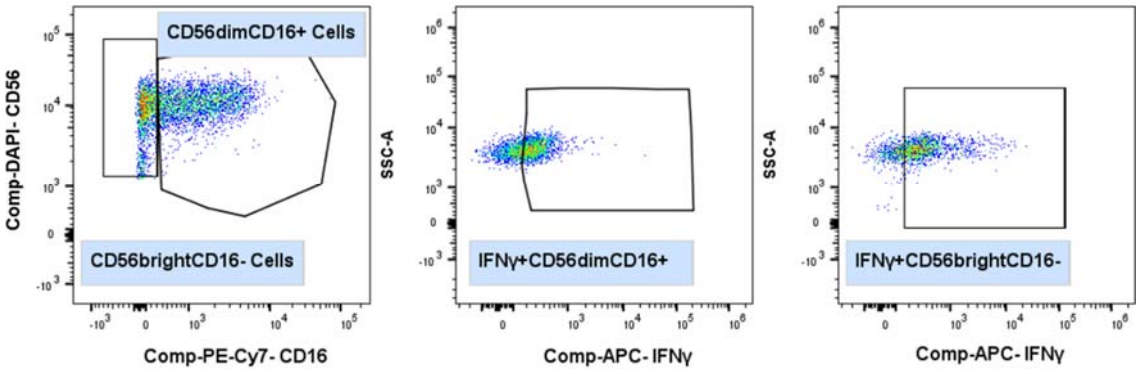

Figure 4.11: Gating strategy of IFNγ in distinct NK cell subsets. NK cells were identified from total lymphocytes as shown in Figure 4.9. Then, based on CD56 and CD16 expression NK cells were stratified into two subsets: $CD56^{dim}CD16^{+}$ and $CD56^{bright}CD16^{-}$ (A). Successive gate was applied on IFNγ+$CD56^{bright}CD16^{-}$ (B) and IFNγ+$CD56^{dim}CD16^{+}$ cells (C) to facilitate analysis of IFNγ in different NK cell subsets.

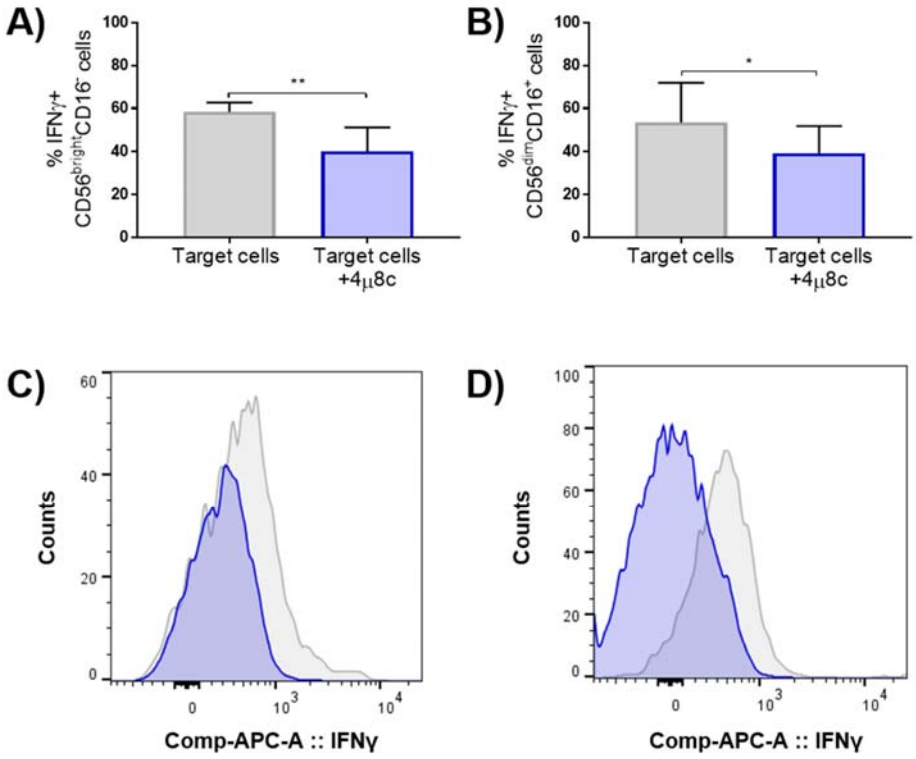

Figure 4.12: In patients with HL, distinct subsets of expanded pNK cells have impaired secretion of IFNγ upon the IRE1 blockade. Expanded pNK cells from HL patients were stimulated with HRS cells for 6 hours and then stained intracellularly for IFNγ. The percent of $CD56^{bright}CD16^{-}$ (A) and $CD56^{dim}CD16^{+}$ (B) pNK cells untreated and treated with 60μM of 4μ8c is presented (n=3). Analysis Student's t-test (n=3) *P<0.01, **P<0.01. Representative FACS histogram shows changes in IFNγ in untreated (grey shade) and 4μ8c treated (blue shade) $CD56^{bright}CD16^{-}$ (C) or $CD56^{dim}CD16^{+}$ cells (D).

4.3.7 PD-1 blockade partially reverses IFNγ secretion

PD-1 blockade has proven a clinical efficacy in the setting of relapsed/refractory HL. Nevertheless, up until now the efficacy of PD-1 blockade was attributable to reversal of T cell exhaustion. I sought to determine whether PD-1 blockade overcomes pNK cell exhaustion driven by the HL microenvironment and/or dysfunction associated with suppressed IRE1-XBP1 pathway. To determine if PD-1 blockade could affect IFNγ secretion, expanded pNK cells of HL patients were pre-incubated for 72hrs in the presence of anti-PD-1 antibody (pembrolizumab) or isotype control. Then expanded pNK cells were stimulated with HDLM2 cell line (of HL phenotype) for 6 hours in the presence or absence of 4μ8c and stained for IFNγ. I found that PD-1 blockade not only enhanced IFNγ secretion in pNK cells of patients with HL (*Target cells* 50.7±1.5; *α-PD-1* 66.3±3.1), but also partially reversed the impairment of IFNγ secretion due to IRE1-XBP1 pathway suppression (*Target cells+4μ8c* 39.8±1.3; *α-PD-1+4μ8c* 48.9±4) (Figure 4.13).

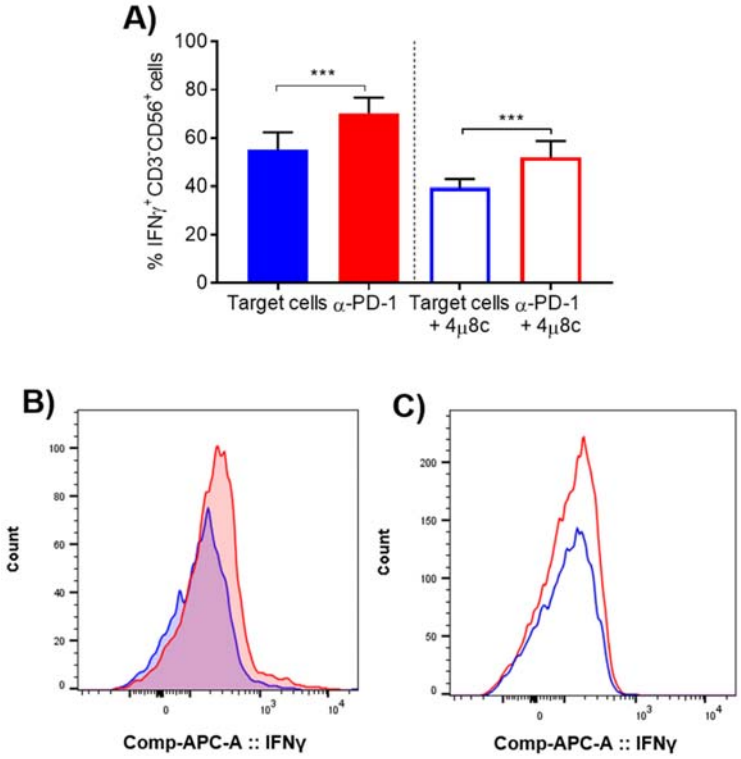

Figure 4.13: PD-1 blockade partially reverses IFNγ secretion by pNK cells from HL patients. Expanded NK cells from patients with HL were stimulated with HRS cells (HDLM-2 cell line) for 6 hours in the presence or absence of PD-1 blockade and/or IRE1 inhibitor 4μ8c. Cells were then stained, fixed, and analysed by flow cytometry to assess IFNγ secretion. In the control assays, target cells and primary NK cells were co-incubated with IgG_4 isotype control. Statistical differences between experimental groups were evaluated by Student's t-test (n=3) ***P<0.001. Representative FACS histograms present changes in IFNγ secretion in pNK cells treated with α-PD-1 (red shade) or isotype control (blue shade) (B), and 4μ8c alone (blue line) or combination of α-PD-1 and 4μ8c (red line) (C).

Changes in IFNγ secretion upon PD-1 blockade were also examined in different pNK cell subsets. Analysis indicates that application of PD-1 blockade enhanced IFNγ secretion in both pNK cell subsets (Figure 4.14). In addition, application of PD-1 blockade in pNK cells with suppressed IRE1-XBP1 pathway partially reversed IFNγ secretion but this observation was restricted to the $CD56^{bright}CD16^{-}$ subset of NK cells (Figure 4.14 A).

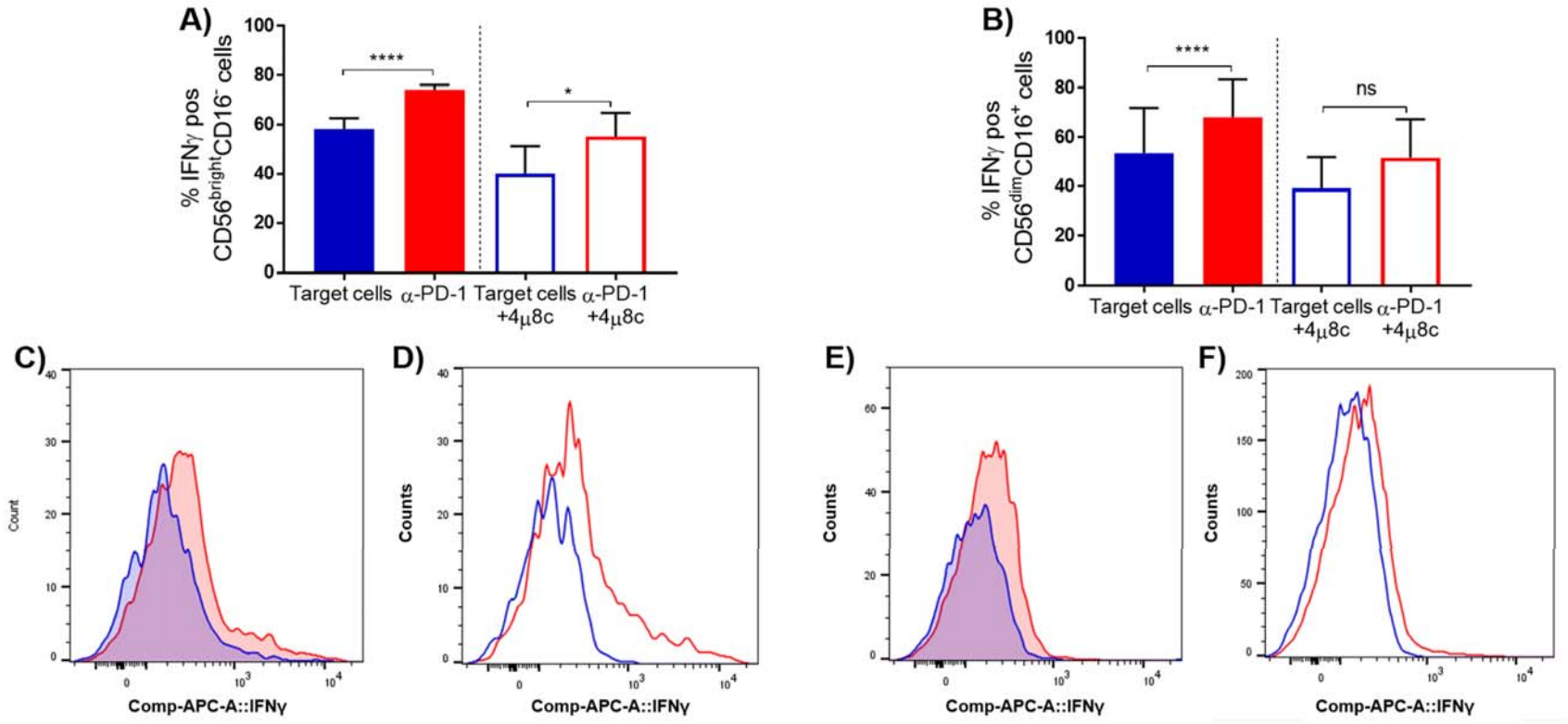

Figure 4.14: PD-1 blockade partially reverses IFNγ secretion by CD56^{bright}CD16^{-} cells from HL patients. Expanded NK cells from patients with HL were stimulated with HRS cells (HDLM-2 cell line) for 6 hours in the presence or absence of PD-1 blockade and/or IRE1 inhibitor 4μ8c. Cells were then stained, fixed, and analysed by flow cytometry to assess IFNγ secretion. In the control assays, target cells and pNK cells were co-incubated with IgG_4 isotype control. Statistical differences between experimental groups were evaluated by Student's t-test (n=3), ****P<0.001, *P<0.05, ns – not significant (p= 0.0874). Representative FACS histograms present changes in IFNγ secretion in CD56^{bright}CD16^{-} (C, D) or CD56^{dim}CD16^{+} (E, F) cells treated with α-PD-1 (red shade) or isotype control (blue shade) (C, E), and 4μ8c alone (blue line) or combination of α-PD-1 and 4μ8c (red line) (D, F).

4.3.8 The impact of IRE1 inhibition on TNFα secretion by pNK cells

Another important cytokine produced by NK cells is TNFα. Therefore, I decided to investigate whether its secretion changes upon blockade of PD-1 or IRE1 in pNK cells from patients with HL. For this purpose, expanded pNK cells from patients with HL, preincubated with pembrolizumab or isotype control, were stimulated with the HDLM2 cell line in the presence or absence of 4μ8c and then stained for TNFα. Expression of TNFα was assessed in $CD3^{-}CD56^{+}CD16^{+/-}$ cells as presented in Figure 4.15.

IRE1 inhibition caused a modest, but statistically significant, decrease in TNFα protein level (Figure 4.16). These changes were demonstrated in the frequencies of $TNF\alpha^{+}$ pNK cells (*Target cells* 13.5±3.4%; *Target cells+4μ8c* 10.3±4.5%).

In line with this finding, the analysis of individual NK cell subsets, $CD56^{dim}CD16^{+}$ and $CD56^{bright}CD16^{-}$ (Figure 4.17), demonstrated that following the IRE1 blockade secretion of TNFα is impaired in both subsets, with the $CD56^{bright}CD16^{-}$ displaying a more prominent decrease (Figure 4.18).

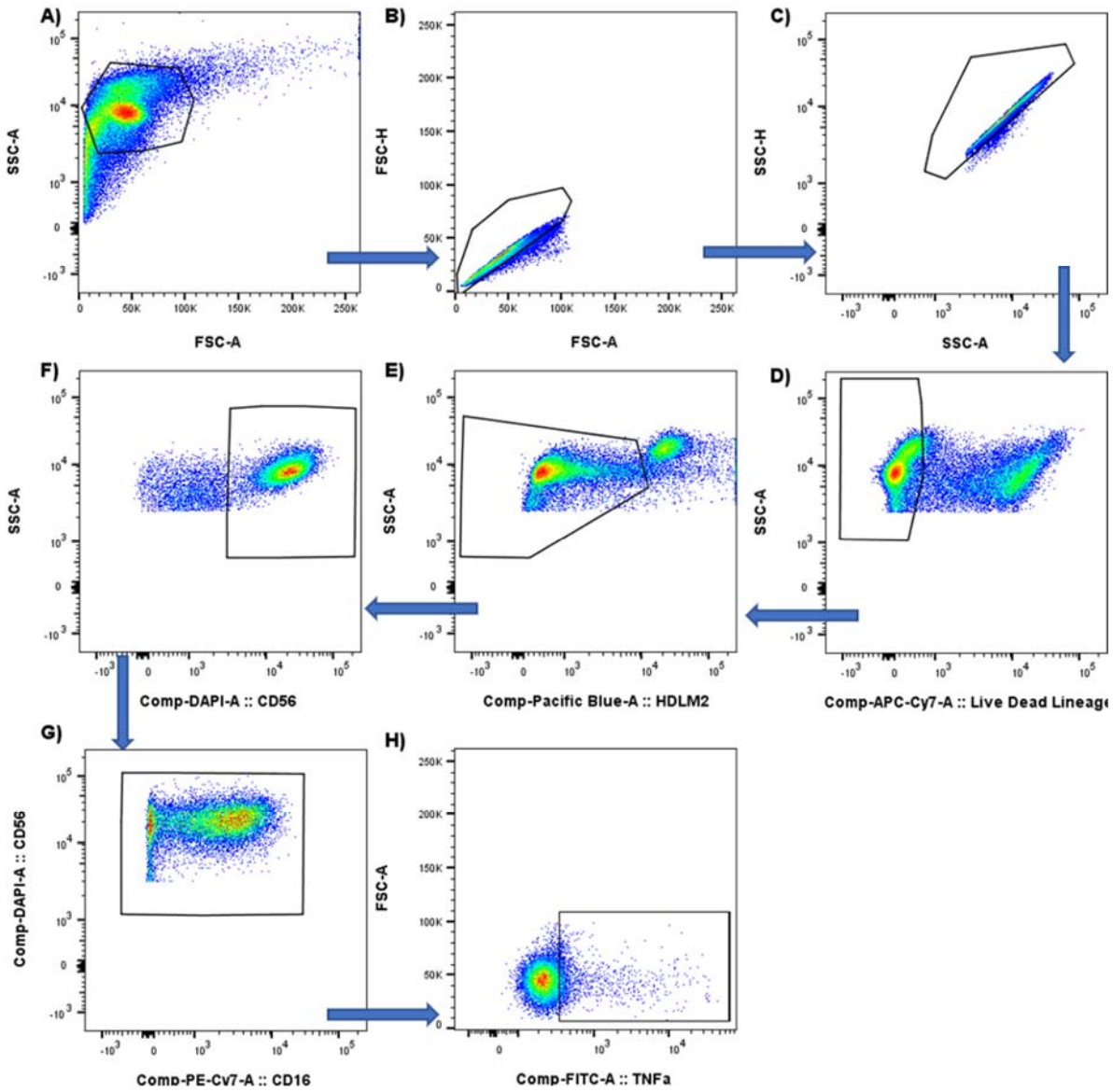

Figure 4.15: Gating strategy for TNFα in NK cells. NK cells were identified from total lymphocytes as shown (A). Then, based on FSC-A/FSC-H (B) and SSC-A/SSC-H (C) scatters single cells were selected for further analysis. Both dead cells and lineage positive cells were removed from analysis by gating on APC-Cy7^{neg-} events (D). Successive gate was applied to exclude target cells stained with CellTrackerViolet from analysis (E). To proceed with NK cell analysis, first CD56+ cells were gated (F) and subsequently CD56+CD16+/- cells (G) which allowed assessment of TNFα expression in the general NK cell subset (H).

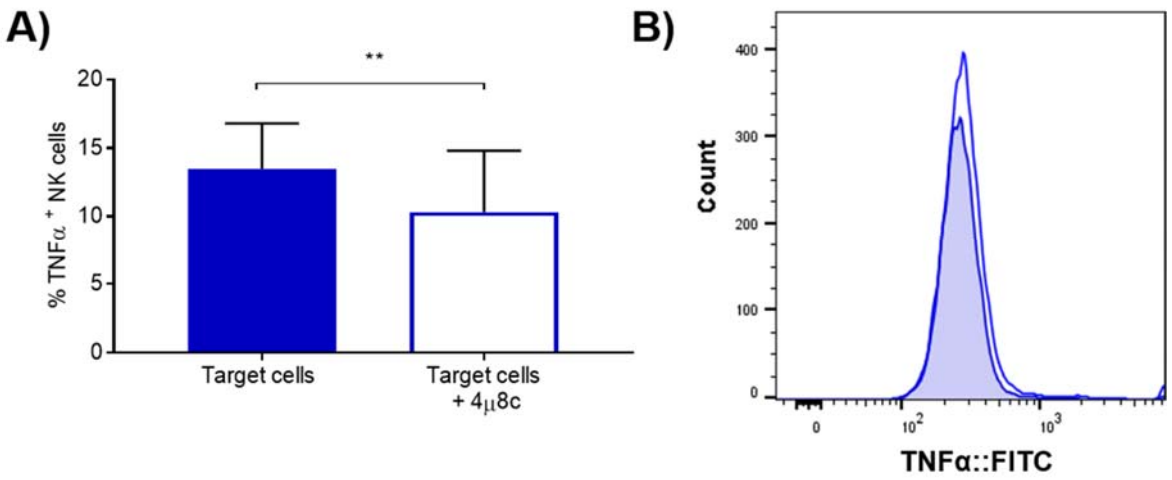

Figure 4.16: In patients with HL, expanded pNK cells with IRE1 blockade display impaired secretion of TNFα. The expanded pNK cells from HL patients were stimulated with HRS cells for 6 hours and then stained intracellularly for TNFα. The percent of $CD3^{-}CD56^{+}$ pNK cells untreated and treated with 60μM of 4μ8c is presented (A). Analysis Student's t-test (n=3), **P<0.01. Representative FACS histogram shows changes in TNFα in untreated (blue line) and 4μ8c treated cells (blue shade) (B).

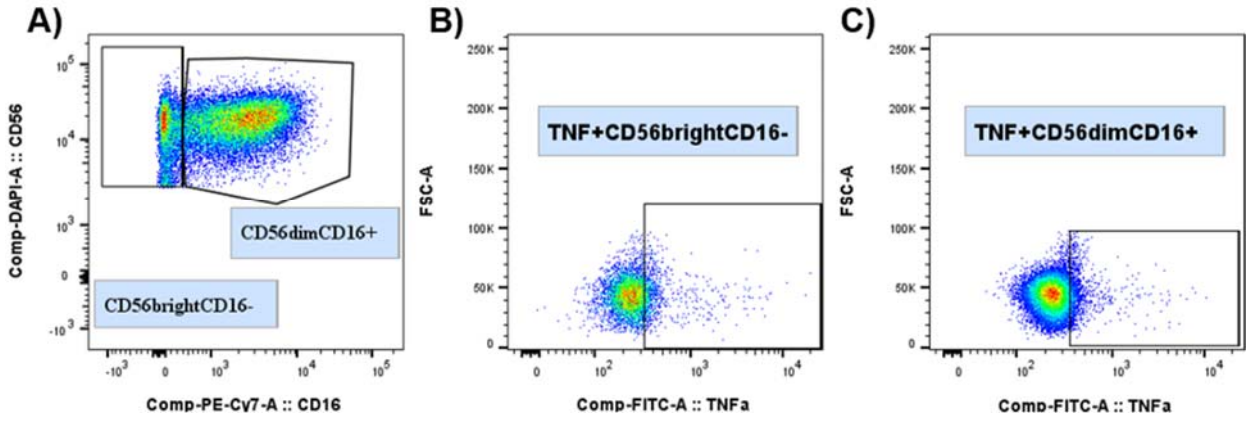

Figure 4.17: Gating strategy of TNFα in distinct NK cell subsets. NK cells were identified from total lymphocytes as shown in Figure 4.15. Then, based on CD56 and CD16 expression NK cells were stratified into two distinct subsets: $CD56^{dim}CD16^{+}$ and $CD56^{bright}CD16^{-}$ for further analysis (A). Successive gate was applied on TNFα+ $CD56^{bright}CD16^{-}$ (B) and TNFα+$CD56^{dim}CD16^{+}$ cells (C) to facilitate analysis of TNFα in different NK cell subsets.

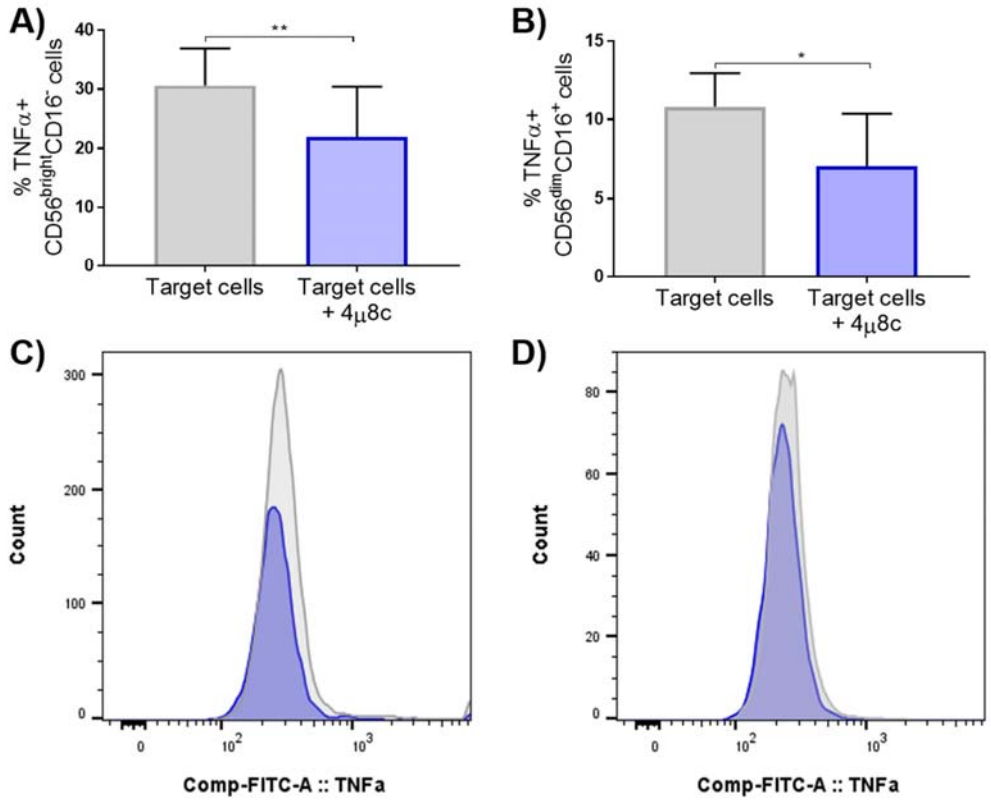

Figure 4.18: In patients with HL, both subsets of expanded pNK cells have impaired secretion of TNFα upon the IRE1 blockade. The expanded pNK cells from HL patients were stimulated with HRS cells for 6 hours and then stained intracellularly for TNFα. The percent of $CD56^{bright}CD16^{-}$ (A) and $CD56^{dim}CD16^{+}$ (B) pNK cells untreated and treated with 60μM of 4μ8c is presented (n=3). Analysis Student's t-test (n=3): **P<0.01, *P<0.05. Representative FACS histogram shows changes in TNFα in untreated (grey shade) and 4μ8c treated (blue shade) $CD56^{bright}CD16^{-}$ (C) or $CD56^{dim}CD16^{+}$ cells (D).

4.3.9 The impact of PD-1 blockade on TNFα secretion by pNK cells

To determine if PD-1 blockade could affect TNFα secretion, expanded pNK cells of HL patients were pre-incubated for 72hrs in the presence of anti-PD-1 antibody (pembrolizumab) or isotype control. Then expanded pNK cells were stimulated with HDLM2 cell line (of HL phenotype) for 6 hours in the presence or absence of 4μ8c and stained for TNFα. Initially, expression of TNFα in the total population of pNK cells was analysed. Upon PD-1 blockade, a trend towards an increase of TNFα expression compared to the isotype control was noted, which was statistically significant (*Target cells* 13.5±3.4%; *α-PD-1* 15.4±4.7%). Results indicate also that PD-1 blockade did partially reverse TNFα secretion in pNK cells with suppressed IRE1-XBP1 pathway activation (*Target cells+4μ8c* 10.3±4.5%; *α-PD-1+4μ8c* 13.2±3.8%).

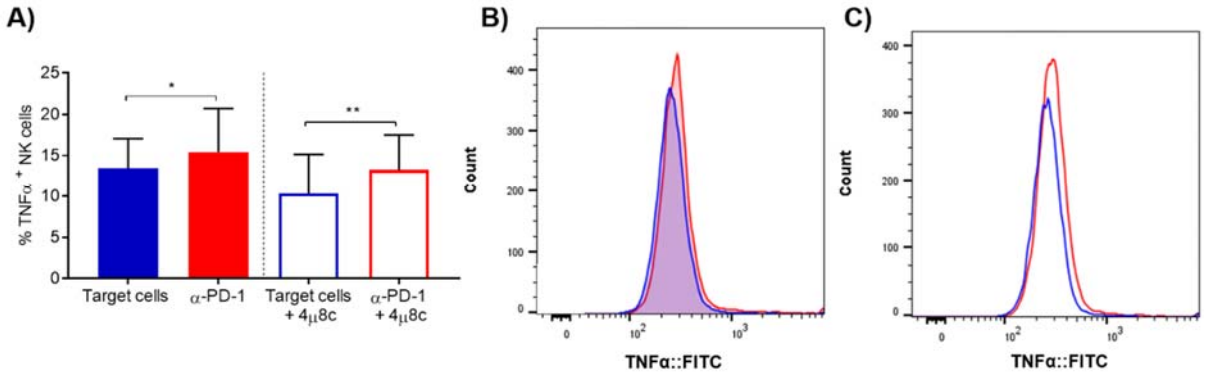

Figure 4.19: PD-1 blockade partially reverses TNFα secretion by pNK cells from patients with HL. Expanded pNK cells from HL patients were stimulated with HRS cells (HDLM-2 cell line) for 6 hours in the presence or absence of PD-1 blockade and/or IRE1 inhibitor 4μ8c. Cells were then stained, fixed, and analysed by flow cytometry to assess TNFα secretion. In the control assays, target cells and primary NK cells were co-incubated with IgG_4 isotype control. PD-1 blockade not only enhanced but also partially reversed TNAα secretion in pNK cells with XBP1s suppression (A). Statistical differences between experimental groups were evaluated by Student's t-test (n=3), **P<0.01, *P<0.05. Representative FACS histograms present changes in TNFα secretion in pNK cells treated with α-PD-1 (red shade) or untreated (target cells - blue shade) (B), and 4μ8c alone (blue line) or combination of α-PD-1 and 4μ8c (red line) (C).

Changes in TNFα secretion upon PD-1 blockade were also examined in different pNK cell subsets. Analysis indicates that application of PD-1 blockade did not enhance TNFα secretion in any of tested pNK cell subsets (Figure 4.20). However, application of PD-1 blockade in pNK cells with suppressed IRE1-XBP1 pathway partially reversed TNFα secretion in both $CD56^{dim}CD16^{+}$ and $CD56^{bright}CD16^{-}$ subsets (Figure 4.20).

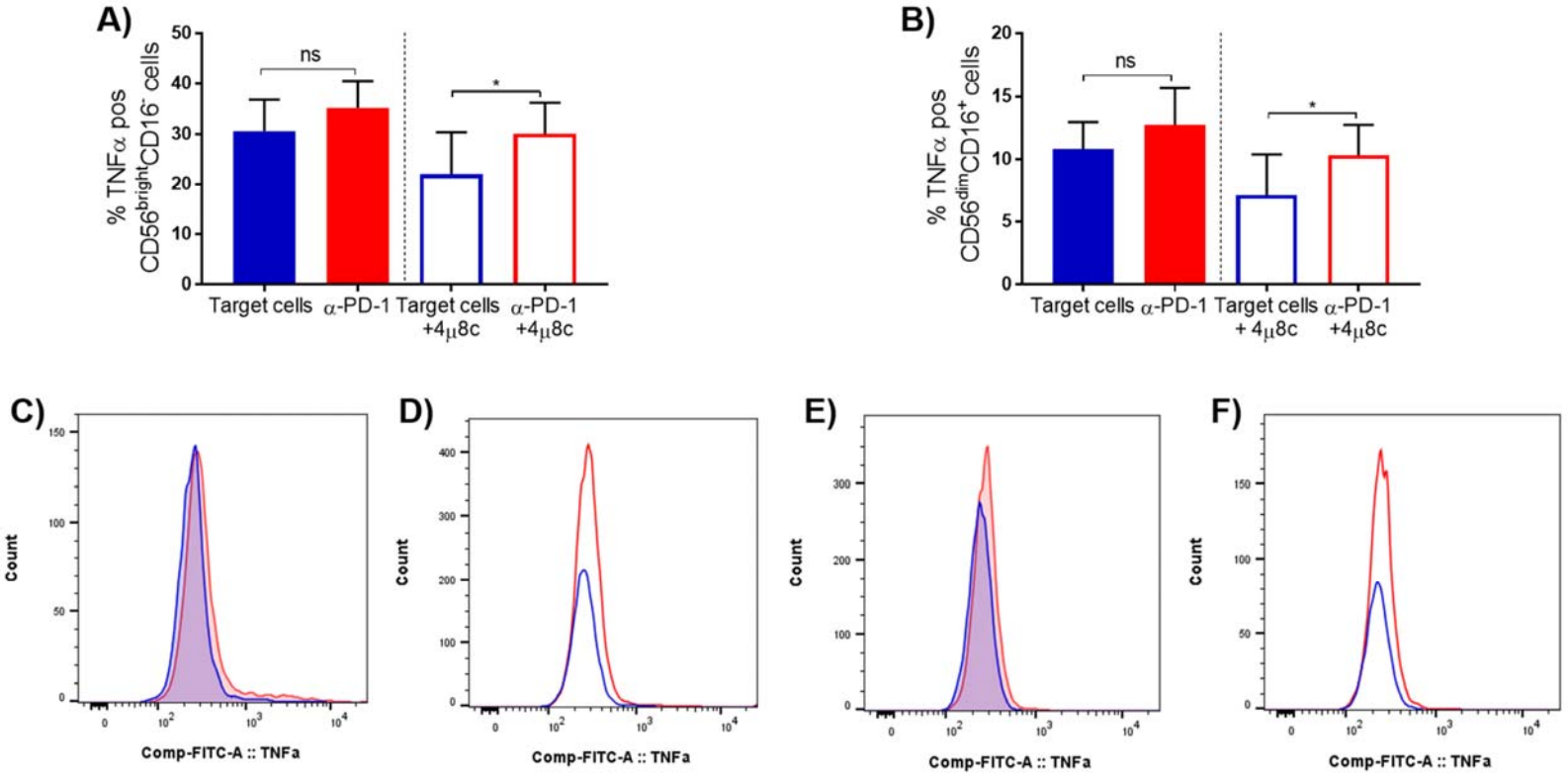

Figure 4.20: PD-1 blockade partially reverses TNFα secretion in both CD56^{bright}CD16^{-} and CD56^{dim}CD16^{+} cells with suppressed IRE1-XBP1 pathway. Expanded pNK cells from HL patients were stimulated with HRS cells (HDLM-2 cell line) for 6 hours in the presence or absence of PD-1 blockade and/or IRE1 inhibitor 4μ8c. Cells were then stained, fixed, and analysed by flow cytometry to assess TNFα secretion. PD-1 blockade or IRE1 inhibition did not induce significant changes in frequency of TNFα^{+}CD56^{bright}CD16^{-} (A) or TNFα^{+}CD56^{dim}CD16^{+} cells (B). Statistical differences between experimental groups were evaluated by Student's t-test (n=3) *P<0.05, ns – not significant. Representative FACS plots present TNFα expression in the CD56^{bright}CD16^{-} (C, D) or the CD56^{dim}CD16^{+} (E, F) cells treated with α-PD-1 (red shade) or isotype control (blue shade) (C, E), and 4μ8c alone (blue line) or combination of α-PD-1 and 4μ8c (red line) (D, F).

4.3.10 Suppression of the IRE1-XBP1 pathway is associated with impaired degranulation

One mechanism of NK cell-mediated killing is through lytic granule release. To interrogate whether the IRE1-XBP1 pathway is involved in degranulation, expanded pNK cells from patients with HL patients were stained for CD107a surface expression. CD107a is present on the surface of NK lytic vesicles consisting of perforin and granzymes. During the process of degranulation, the membrane of the secretory lysosomes fuses with the plasma membrane of the activated NK cell and the lytic granules content is then released at the immunological synapse to induce death of the target cell [154]. Hence, CD107a is one method to assess NK cell degranulation.

To determine whether the IRE1-XBP1 pathway is involved in this process, CD107a antibody was added to pNK cells of HL patients stimulated with HDLM2 target cells in the presence or absence of 4μ8c for 6 hours. Then only cells were analysed for CD107a expression by flow cytometry (Figure 4.22). It was found that inhibition of the IRE1-XBP1 pathway resulted in decreased expression of CD107a following direct cytotoxicity (*Target cells* 73.4±6.7; *Target cells+4μ8c* 55.3±13.7). Addition of 60μM of IRE1 inhibitor caused a ~25% reduction of CD107a expressing $CD3^{-}CD56^{+}$ cells (Figure 4.21).

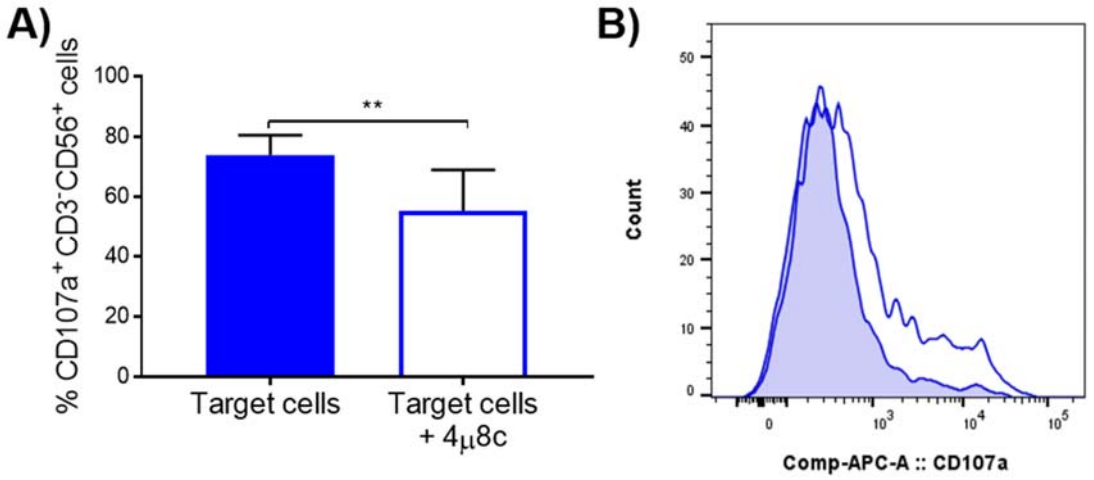

Figure 4.21: In HL, pNK cells with suppressed XBP1s exert impaired degranulation. The expanded pNK cells from HL patients were stimulated with HRS cells for a total of 6 hours and stained for CD107a. The percent of $CD3^{-}CD56^{+}CD16^{+/-}$ pNK cells untreated and treated with 60μM of 4μ8c is presented (A, n=3). Statistical differences between experimental groups were evaluated by Student's t-test (n=3), **P<0.01. Representative FACS histogram shows changes in CD107a in untreated (blue line) and 4μ8c treated cells (blue shade) (B).

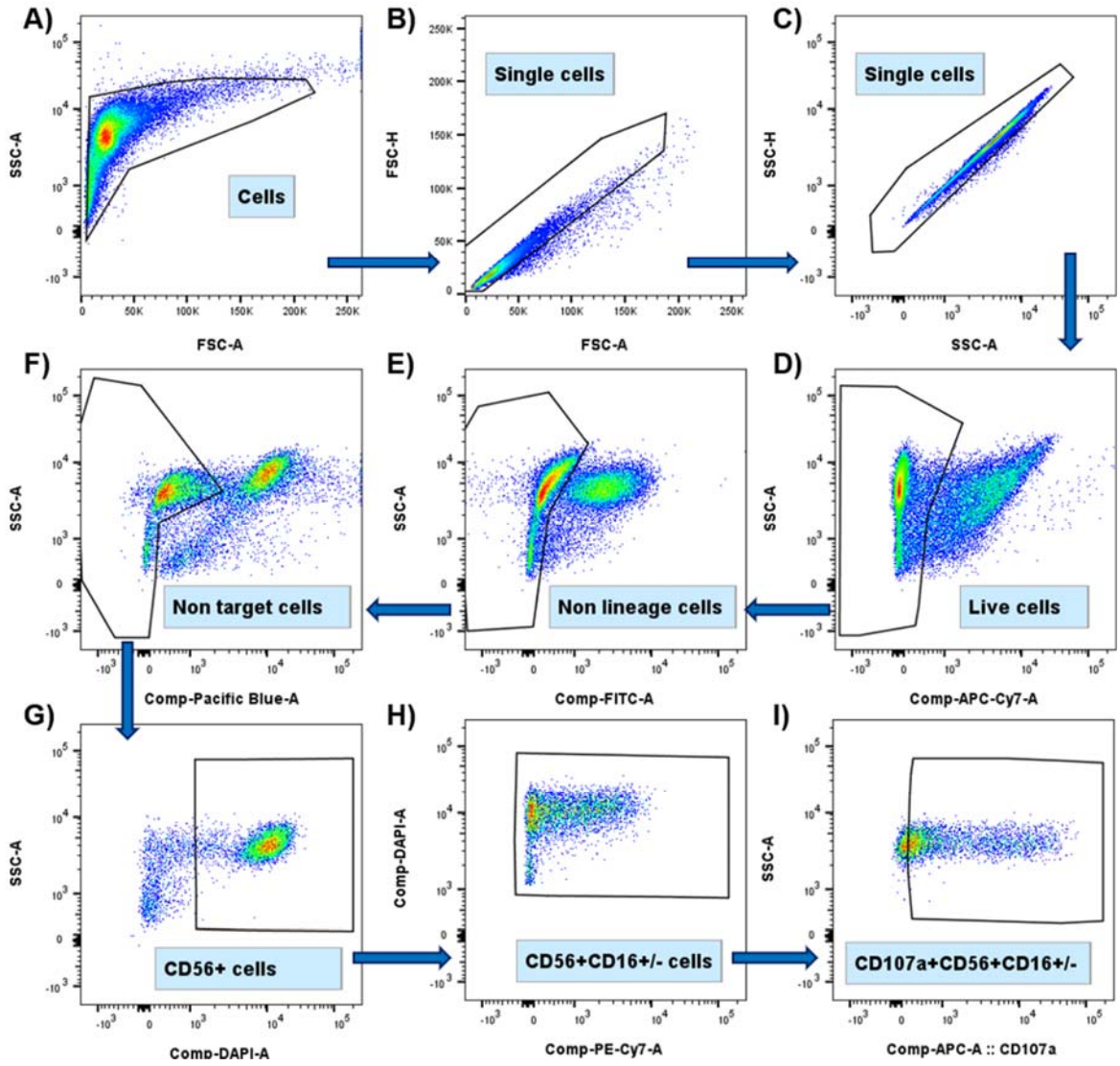

Figure 4.22: Gating strategy of CD107a in NK cell subset. NK cells were identified from total lymphocytes as shown (A). Then, based on FSC-A/FSC-H (B) and SSC-A/SSC-H (C) scatters single cells were selected for further analysis. Dead cells were excluded from analysis by gating on APC-Cy7^{neg-} events (D). Successive gate was applied to exclude non-lineage cells (CD3-CD14-CD19-) (E) and target cells stained with CellTrackerViolet from analysis (F). To proceed with NK cell analysis, CD56+ cells were gated on (G), which allowed to then gate on CD56+CD16-/+ cells (H) and assess CD107a expression in general NK cell population (I).

The CD56^{dim}CD16^{+} subset of NK cells is primarily involved in target cell lysis *in vivo*. Hence, changes in CD107a release were also interrogated in individual subsets of NK cells to determine potential differences between two NK cell subsets following the IRE1 blockade. Upon the IRE1 blockade a significant decrease in CD107a release was observed in both NK cell subsets (Figure 4.24). This data indicates that in HL patients, both NK cell subsets with suppressed IRE1-XBP1 pathway demonstrate a suboptimal degranulation.

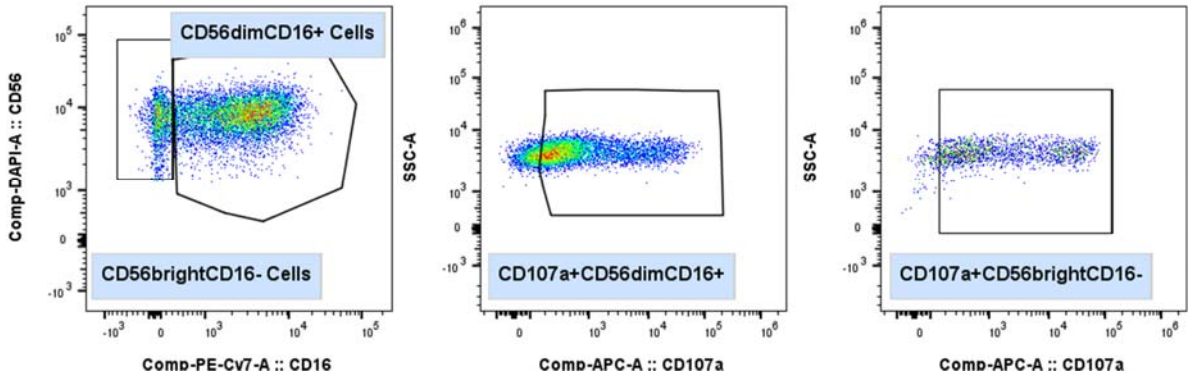

Figure 4.23: Gating strategy of CD107a in distinct NK cell subsets. NK cells were identified from total lymphocytes as shown in Figure 4.22. Then, based on CD56 and CD16 expression NK cells were stratified into two subsets: $CD56^{dim}CD16^{+}$ and $CD56^{bright}CD16^{-}$ (A). Successive gate was applied on CD107a+$CD56^{bright}CD16^{-}$ (B) and CD107a+$CD56^{dim}CD16^{+}$ cells (C) to facilitate analysis of CD107a in different NK cell subsets.

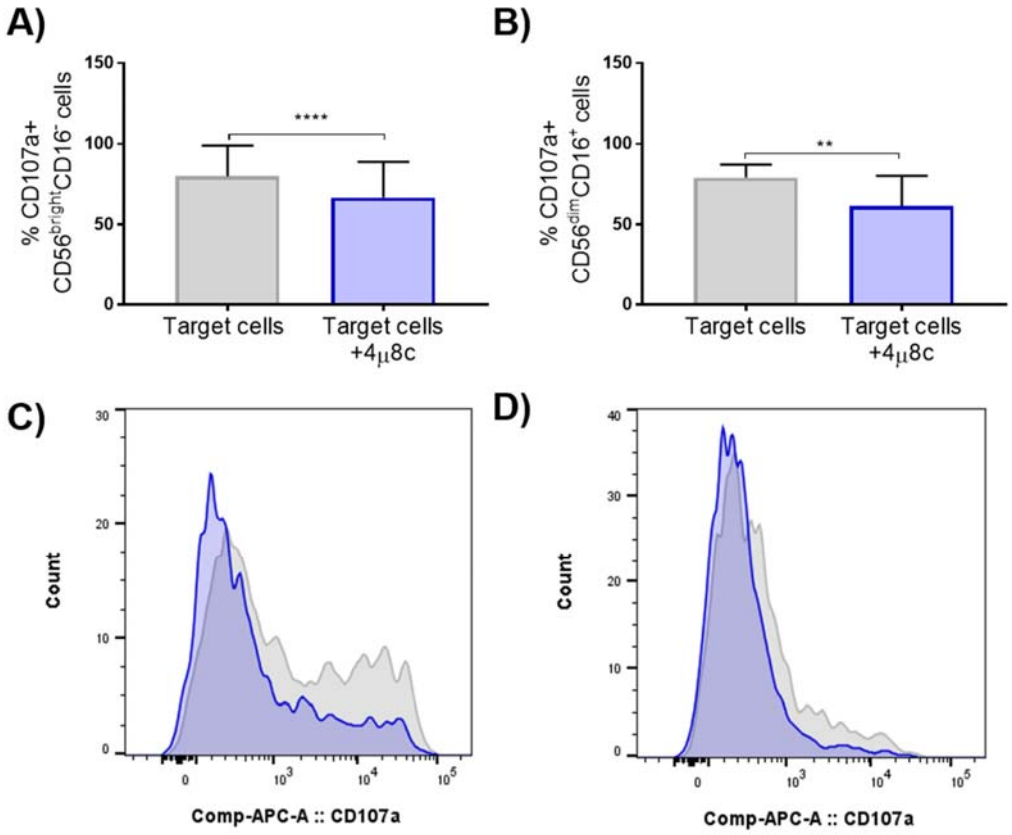

Figure 4.24: In HL, both NK cell subsets display impaired degranulation in the presence of IRE1 blockade. The expanded pNK cells from HL patients were stimulated with HRS cells for a total of 6 hours and stained for CD107a. The percent of $CD56^{bright}CD16^{-}$ (A) and $CD56^{dim}CD16^{+}$ (B) pNK cells untreated or treated with 60μM of 4μ8c is presented (n=3). Statistical differences between experimental groups were evaluated by Student's t-test (n=3), ****P<0.001, **P<0.01. Representative FACS histogram shows changes in CD107a in untreated (grey shade) and 4μ8c treated (blue shade) $CD56^{bright}CD16^{-}$ (C) and $CD56^{dim}CD16^{+}$ (D) cells.

4.3.11 PD-1 blockade does not significantly enhance NK cell degranulation

To determine whether PD-1 blockade could enhance NK cell degranulation, expanded pNK cells from patients with HL were pre-incubated for 72hrs in presence of pembrolizumab or isotype control. Then cells were stimulated with HDLM2 target cells for 6 hours in the presence or absence of 4μ8c, and antibody against CD107a. I observed that neither did PD-1 blockade enhance NK cell degranulation over control nor reversed degranulation of pNK cells with a suppressed IRE1-XBP1 pathway (Figure 4.25). These observations might result from variations across tested patients and limited number of patient samples tested. In the previous study by Vari *et al*, PD-1 blockade was demonstrated to improve degranulation of a sorted subset of the KHYG-1 NK cell line that had uniformly high expression of PD-1. Hence, the level of PD-1 expression may underlie the strength of the PD-1 blockade effectiveness, as well as the greater homogeneity of KHYG-1 cells in contrast to pNK cells.

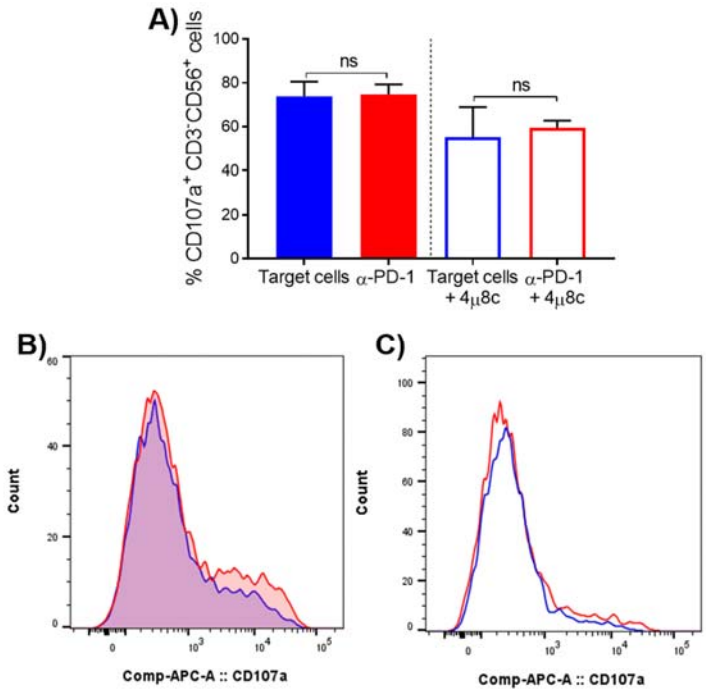

Figure 4.25: PD-1 blockade does not significantly improve degranulation of pNK cells in patients with HL. Expanded pNK cells from HL patients were stimulated with HRS cells (the HDLM-2 cell line) for 6 hours in the presence or absence of PD-1 blockade and/or IRE1 inhibitor 4μ8c. Cells were then stained and analysed by flow cytometry to assess degranulation based on CD107a marker (A). In the control assays, target cells and pNK cells were co-incubated with IgG_4 isotype control. Statistical differences between experimental groups were evaluated by Student's t-test (n=3) ns – not significant (Target cells vs α-PD-1: p= 0.54; Target cells+4μ8c vs. α-PD-1+4μ8c: p= 0.67). Representative FACS histograms present changes in CD107a release in NK cells treated with α-PD-1 (red shade) or isotype control (blue shade) (B), and 4μ8c alone (blue line) or combination of α-PD-1 and 4μ8c (red line) (C).

I also examined changes in CD107a release upon PD-1 blockade in different NK cell subsets. Analysis indicates that neither did application of PD-1 blockade enhance CD107a release in any of tested NK cell subsets nor reversed impaired CD107a release in NK cell subsets with suppressed IRE1-XBP1 pathway (Figure 4.26).

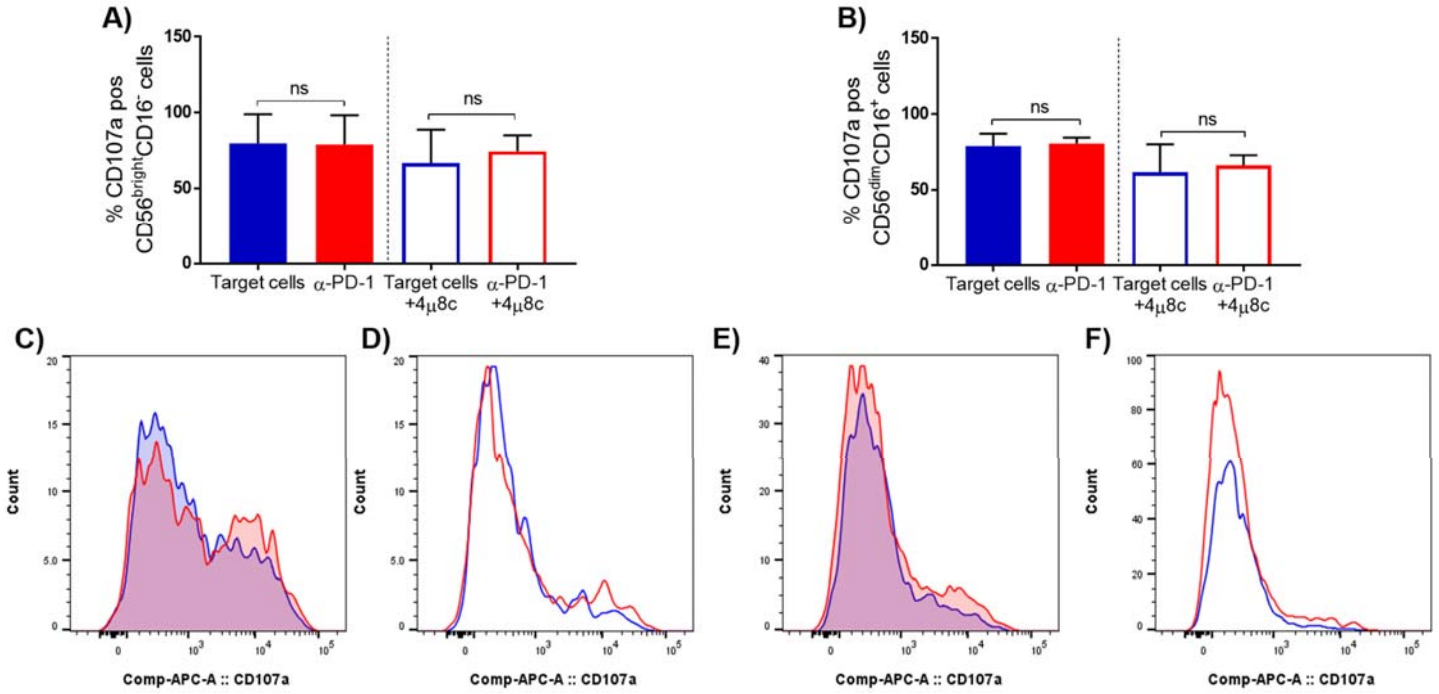

Figure 4.26: PD-1 blockade does not improve degranulation by CD56brightCD16- or CD56dimCD16+ cells in patients with HL. Expanded pNK cells from HL patients were stimulated with HRS cells (the HDLM-2 cell line) for 6 hours in the presence or absence of PD-1 blockade and/or IRE1 inhibitor 4μ8c. Cells were then stained and analysed by flow cytometry to assess degranulation based on CD107a marker (A). In the control assays, target cells and pNK cells were co-incubated with IgG_4 isotype control. Statistical differences between experimental groups were evaluated by Student's t-test (n=3) ns – not significant (A: Target cells vs α-PD-1: p= 0.48; Target cells+4μ8c vs. α-PD-1+4μ8c: p= 0.31. B: Target cells vs α-PD-1: p= 0.43; Target cells+4μ8c vs. α-PD-1+4μ8c: p= 0.74). Representative FACS histograms present changes in CD107a release in the $CD56^{bright}CD16^{-}$ (C, D) or the $CD56^{dim}CD16^{+}$ (E, F) cells treated with α-PD-1 (red shade) or isotype control (blue shade) (C, E), and 4μ8c alone (blue line) or combination of α-PD-1 and 4μ8c (red line) (D, F).

4.3.12 Thapsigargin enhances NK cell degranulation and cytotoxicity

To determine if IRE1 activators may improve effector function of NK cells with suppressed expression of XBP1s I interrogated the effect of TG, a known IRE1 activator, on NK cell-mediated cytotoxicity and degranulation in response to HRS cells. For this, pNK cells from HL patients were incubated with CTV stained HDLM-2 target cells at a 1:1 ratio for 6 hours in the presence of DMSO (control), 60 μM of 4μ8c and/or 100nM of TG.

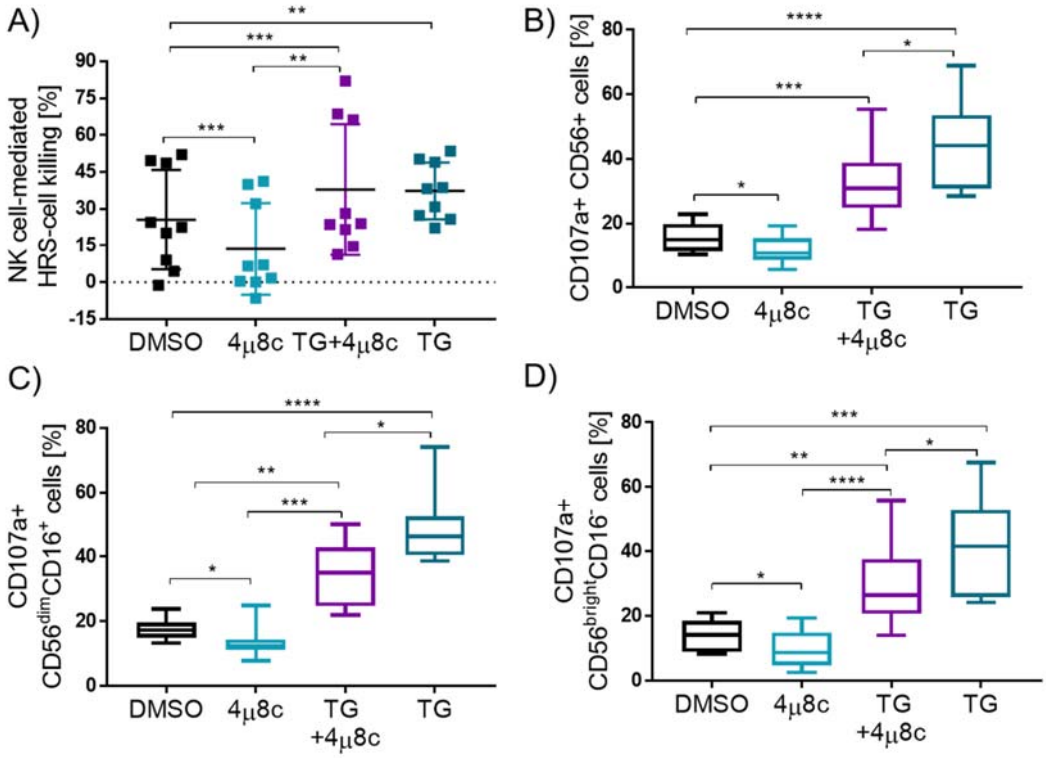

Figure 4.27: Thapsigargin reverses impaired target cell lysis mediated by pNK cells with suppressed expression of XBP1s. pNK cells from patients with HL were stimulated with HDLM-2 target cells for 6 hours in the presence of DMSO, 60μM of 4μ8c and/or 100nM of TG. The ability of pNK cells to lyse target cells was assessed using flow cytometry. The percent of target cell lysis is presented (A). These cells were also stained with CD107a antibody to assess the level of degranulation in CD56+ subset of NK cells (B), $CD56^{dim}CD16^{+}$ (C), or $CD56^{bright}CD16^{-}$ (D).

It was found that addition of 60μM IRE1 inhibitor to pNK cells resulted in a significant reduction in the lysis of HDLM-2 target cells (Figure 4.27.A), it was also reflected in reduced level of degranulation (Figure 4.27.B). In contrast, application of TG to pNK cells resulted in increased cytotoxicity towards HDLM-2 cells that was further supported by enhanced degranulation. Notably, application of TG to pNK cells with suppressed XBP1s expression reversed impaired cytotoxicity and degranulation. In case of degranulation it was also interrogated in different NK cell subsets i.e. $CD56^{bright}CD16^{-}$ (Figure 4.27) and $CD56^{dim}CD16^{+}$ (Figure 4.27), however no significant changes

were observed between these two groups. This analysis indicates that TG is a potent drug that not only enhances NK cell effector function but also reverses the impairment of NK cell function driven by suppressed XBP1s.

4.3.13 Summary of results

The main aim of this chapter was to determine whether the IRE1-XBP1 pathway is dysregulated in NK cells from HL patients following the stimulation with HRS cells. The flow cytometry results demonstrated that XBP1s, an activation marker of the IRE1-XBP1 pathway, is not activated in NK cells following the stimulation with HRS-cells and this observation was restricted to the $CD56^{bright}CD16^{-}$ subset of NK cells. Concomitantly, NK cells with suppressed XBP1s were found to exert impaired migration, immune synapse formation with HRS cells, degranulation, IFNγ and TNFα secretion. Additionally, in depth analysis of distinct NK cell subsets, $CD56^{dim}CD16^{+}$ and $CD56^{bright}CD16^{-}$, revealed that the IRE1 blockade impairs cytotoxicity, degranulation, IFNγ and TNFα secretion in both tested subsets. Notably, application of IRE1 activator, TG, reversed impaired cytotoxicity and degranulation of NK cells.

PD-1 is expressed on a range of immune cells including NK cells, and its expression increases following NK cell stimulation. Due to the proven clinical efficiency of PD-1 blockade in HL, the effect of this checkpoint blockade on NK cell effector function was also interrogated. As demonstrated in the result section of this chapter, PD-1 blockade alone enhances NK cell migration, immune synapse formation, IFNγ and TNFα secretion. In addition, subset analysis revealed that secretion of IFNγ was significantly enhanced in both NK cell subsets. Whereas application of PD-1 blockade in NK cells with suppressed XBP1s partially reversed the immune synapse formation capacity and IFNγ secretion in the $CD56^{bright}CD16^{-}$ but not in the $CD56^{dim}CD16^{+}$ cells. In addition, analysis of NK cell subsets demonstrated that PD-1 blockade partially reversed TNFα secretion and this observation was restricted to both NK cell subsets.

4.4 DISCUSSION

4.4.1 The IRE1-XBP1 pathway is impaired in NK cells from HL patients

In this chapter, I show that NK cells of patients with HL patients exert a dysregulation of IRE1-XBP1 pathway demonstrated by suppressed expression of XBP1s. This observation was restricted to the $CD56^{bright}CD16^{-}$ subset of NK cells. Although the role of IRE1-XBP1 pathway can vary across different cell types and diseases, I show that in NK cells of patients with HL, suppression of the IRE1-XBP1 pathway is associated with a multifaceted impairment of NK cell function, including migration, actin accumulation at the NKIS, degranulation, and IFNγ secretion.

Conventionally, NK cells are subdivided into two distinct subsets: $CD56^{dim}CD16^{+}$ and $CD56^{bright}CD16^{-}$. To determine if the IRE1-XBP1 pathway is dysregulated in the setting of HL I interrogated the expression of the activation marker – XBP1s in these two NK cells subsets. I found that the pathway is not operative in the $CD56^{bright}CD16^{-}$ subset of NK cells compared to healthy controls. Interestingly, in a study of HL, the latter subset of NK cells was found to be expanded and expressed high level of PD-1 [93]. Nevertheless, whether suppression of the IRE1-XBP1 pathway is directly linked to PD-1 overexpression remains to be determined.

Another important aspect of NK cell function is recognition of a target cell and subsequent formation of IS to mount an executive response. In this study, it was noted that NK cells with an IRE1 blockade formed a less stable IS, as manifested by limited actin accumulation at the NKIS. To determine the consequences of this aberration the functional mechanisms that occur following the IS formation i.e. degranulation and cytokine release were also assessed.

I investigated the effect of IRE1 blockade on degranulation assessed by the expression of CD107a, a marker that indicates the NK cell activation status [154]. Notably, a significant reduction in CD107a release in the presence of IRE1 blockade was observed, which suggests that activation of NK cells in patients with HL is impaired. As this assay evaluates the presence of a membrane coating the lytic granules fused with the plasma cell membrane upon the release of the lytic granule content, these data imply that IRE1-XBP1 pathway might be involved in the trafficking of the lytic granules towards the cell membrane. Importantly, application of IRE1 activator (TG) reversed impaired degranulation of NK cells with suppressed XBP1s. In addition, NK cells from HL patients demonstrated also reduced cytotoxicity against HRS-cells in the presence of IRE1 blockade, but application of TG reversed this impairment.

Furthermore, NK cells of HL patients with a suppressed IRE-1-XBP1 pathway, demonstrated a marked decrease in IFNγ and TNFα secretion. Similarly, IRE1 blockade was shown to impair

secretion of IFNβ and TNFα in macrophages or IFNγ in Th1 cells [122] [193]. In contrast, in the study of ovarian cancer upregulation of XBP1s in T cells was associated with decreased expression of IFNγ [126]. It should be emphasized that in this study we investigated IRE1-XBP1 pathway solely in NK cells from the peripheral blood. Further research encompassing tumour infiltrating NK cells is required.

4.4.2 PD-1 blockade enhances NK cell function

PD-1 pathway blockade is a highly promising therapy and has elicited durable anti-tumour responses and long-term remissions in a subset of patients with a broad spectrum of cancers [194] [195] [196] [197]. In health, the expression level of PD-1 on NK cells is limited but its expression increases in a variety of diseases [93] [91] [198]. A recent study of HL demonstrated a marked expansion of the $CD56^{bright}CD16^{-}PD\text{-}1^{+}$ subset, which suggests enhanced sensitivity of NK cells in patients with HL to PD-1 blockade [93]. In the light of this finding, I investigated the effect of pembrolizumab on NK cell effector function.

A previous study of MM showed that PD-1 blockade enhanced immune complex formation between NK cells and MM cells, as well as NK cell migration towards MM cells [91]. In line with these findings, we found that application of PD-1 blockade improved NK cell migration. Additionally, the accumulation of actin at the NKIS, between NK cell and HRS cell, was more pronounced following PD-1 blockade suggesting enhanced immune synapse formation between NK and HRS cells.

To test the downstream events following the NKIS formation, I tested the efficacy of pembrolizumab on NK cell degranulation and cytokine secretion. In a study of NK cells from post-transplant lymphoproliferative disorder (PTLD) patients, a significantly up-regulated PD-1 was associated with functional impairment of NK cells. Moreover, disruption of PD-1/PD-L1 signalling enhanced IFNγ release but did not enhance degranulation examined by CD107a staining [198]. In line with these findings, I also found that PD-1 blockade enhanced IFNγ secretion in NK cells of HL patients, but not NK cell degranulation (CD107a). In contrast, in the study by Vari *et al*., blockade of PD-1 on the PD-1 high subset of NK cells from the KHYG-1 cell line did improve NK cell degranulation evaluated by CD107a staining [93]. This discrepancy may be explained by differences between NK cell line and pNK cells, and the level of PD-1 expression on tested cells, as well as in the experimental approaches.

Interestingly, I did observe significant increase of TNFα secretion upon PD-1 blockade in the total NK cell population. However, interrogation of individual NK cell subsets i.e. $CD56^{dim}CD16^{+}$ and $CD56^{bright}CD16^{-}$ did not reveal any improvement in TNFα secretion upon PD-1 blockade.

Nevertheless, it should be emphasized that the number of samples tested in this study was limited. Therefore, to clarify these findings further investigations into the effect of PD-1 blockade on TNFα secretion are required.

Data presented in this chapter, indicate that further research is needed to clarify the impact of PD-1 blockade on NK cell effector function. Moreover, these findings suggest that blockade of other checkpoint inhibitors, such as LAG-3 or TIM-3, to boost NK cell function should be considered.

4.4.3 The interplay between IRE1-XBP1 pathway and PD-1 in HL

Based on the finding that IRE1-XBP1 pathway is dysregulated in pNK cells in patients with HL, I tested whether PD-1 blockade can reverse the impairment driven by XBP1s suppression. I found that pembrolizumab partially reversed IS formation and IFNγ secretion in NK cells with a suppressed IRE1-XBP1 pathway. This suggests that treatment with PD-1 blocking mAbs may reverse certain pNK cells effector function defects that arise in the context of suppression of the IRE1-XBP1 pathway.

However, I found that pembrolizumab did not reverse impaired degranulation or TNFα secretion in NK cells. Interestingly, analysis of NK cell subsets indicates that PD-1 blockade partially reverses TNFα secretion in both $CD56^{dim}CD16^{+}$ and $CD56^{bright}CD16^{-}$ subsets in the presence of a IRE1-XBP1 pathway inhibitor. Collectively, these results suggest that while PD-1 blockade may influence some aspects of IRE1-XBP1 pathway mediated NK cell dysfunction, others effector functions are not reversed. It should also be highlighted that in this study we did not determine whether IRE1-XBP1 pathway and PD-1/PD-L1/PD-L2 signalling are interconnected. Further investigations into these pathways are required to dissect the molecular mechanisms underpinning the potential interplay between these two pathways, so that appropriate treatment regimens could be implemented to boost the anti-tumour capacity of NK cells in the setting of HL.

4.4.4 Conclusion

In conclusion, in experiments performed on a range of NK cells lines and pNK cells (refer to Chapter 3) I observed that the IRE1-XBP1 pathway in pNK cells of HL patients is involved in NK cell effector function. The pathway is dysregulated in pNK cells of HL patients and this observation was restricted to the $CD3^{-}CD56^{bright}CD16^{-}$ (that is known to be enriched in PD-1). The consequences of this dysregulation were: impaired NKIS formation, degranulation and cytokine secretion. Given that the PD-1 blocking antibody pembrolizumab is a critical component of current treatment strategies in relapsed/refractory HL, we also tested whether it can overcome NK cell impairment mediated by the

IRE1-XBP1 pathway. We found that PD-1 blockade alone can enhance IFNγ secretion and IS formation and partially reverses IRE1-XBP1 pathway mediated NK cell impairment.

CHAPTER 5:

Final Discussion

5.1 INTRODUCTION

NK cells as a key component of innate arm of the immune system are able to lyse malignant cells without previous exposure to their antigens. In contrast to T cells, NK cells attack "non-self" cells within the host and elicit a rapid immune response involving NK cell-mediated cytotoxicity or secretion of regulatory cytokines to recruit the adaptive responses and potentiate the anti-tumour potential of the immune system [10] [23]. That NK cell function is not limited by the MHC-I recognition, exerts broad cytotoxicity and are activated rapidly makes them a unique armament of our immune system. The potential of NK cells to lyse tumour cells has led to intensification of research focusing on development of immunotherapies utilising these cells [199] [200].

Limited knowledge of NK cell biology contributed to the failure of the initial attempts of re-infusion of IL-2 stimulated autologous cells. Subsequently there was some encouraging therapeutic signals seen with alternate approaches including use of KIR-mismatched cell infusions [100] [101]. Notably, a significant role of NK cells in controlling cancer development has been demonstrated by a long-term follow-up study of a large population of healthy cancer-free individuals. After over a decade of surveillance, those with high levels of NK cell cytotoxicity were found to be significantly less likely to develop cancer than those individuals with lower levels of NK cell cytotoxicity [86]. Although NK cells have an impressive capacity to eliminate tumour cells, often the TME develops strategies to disable NK cell surveillance. Amongst others, these strategies may involve upregulation of inhibitory ligands on tumour cells or shedding of ligands for activating receptors to disable NK cell activation [142] [201].

Since dysfunction of the IRE1-XBP1 pathway has been implicated in multiple diseases including cancer I sought to interrogate the role of this pathway in NK cells as well as NK cells from HL patients [202] [203] [204] [175]. In this study, I demonstrate for the first time that the IRE1-XBP1 pathway is required for optimal NK cell function. Notably, activation of this pathway was dysfunctional in NK cells in patients with HL. As such, strategies targeting this pathway to restore NK cell function in HL may be of potential benefit. Following on from recent observations by my laboratory that show that NK cells from patients with HL display a skewed phenotype including expansion of PD-1 expressing $CD56^{bright}CD16^{-}$ cells [93], I went on to test the impact of PD-1 blockade on NK cell activity. Therefore in this chapter, potential therapies targeting not only the IRE1-XBP1 pathway but also PD-1 checkpoint blockade will be discussed.

5.2 *XBP1* SPLICING IN NK CELLS

In a healthy individual, the IRE1-XBP1 pathway operates within the UPR system as a physiological response to ER stress triggered by physiological stimuli such as oxidative stress, glucose depletion and hypoxia. These processes lead to accumulation of misfolded and unfolded proteins in cells which in turn induce IRE1 auto-phosphorylation followed by dimerization and activation of endonuclease activity to splice out a 26-nucleotide intron from *XBP1* mRNA, leadings to generation of XBP1s [205]. This molecule is a potent transcription factor involved in ER stress mitigation by regulation of a range of chaperones, foldases and glycotransferases [204] [184] [170] [206].

However, activation of this pathway has also been associated with immune effector cell function, as well as ER stress mitigation, indicating that this pathway operates outside of the UPR system. For instance, activation of the IRE1-XBP1 pathway is required for the optimal secretion of pro-inflammatory cytokines i.e. TNFα and IFNγ in macrophages, DCs development and survival [122] [123], and differentiation of cells such as eosinophils and B cells [162] [121]. Interestingly, in multiple myeloma, malignant cells exploit the IRE1-XBP1 pathway to successfully persist in the tumour microenvironment [177].

Within this study it was found that following the stimulation of NK cells with blood cancer target cells, either leukaemia or lymphoma, the IRE1-XBP1 pathway was activated as demonstrated by *XBP1* splicing (Figure 1). Investigation of known down-stream targets of XBP1s suggests that within NK cells the IRE1-XBP1 pathway operates in a non-canonical manner i.e. independent of the UPR system. Furthermore, the *XBP1* splicing was successfully inhibited by a small molecule inhibitor, enabling a detailed analysis of NK cell function upon IRE1 blockade. Collectively, it was established that the IRE1-XBP1 pathway is required for optimal NK cell function. Following IRE1-XBP1 pathway blockade, NK cells had impaired migration. While the blockade of IRE1 did not influence the number of conjugates formed between NK cells and HRS cells, it did impact actin polarization at the immune synapse interphase indicating the formation of less stable conjugates. Finally, IRE1 blockade impaired the secretion of both cytokines - TNFα and IFNγ.

Notably, investigations of the IRE1-XBP1 pathway in circulating pNK cells from patients with HL suggest that the pathway is not activated in these cells in response to HRS cells. Of note, this observation was restricted to the $CD56^{bright}CD16^{-}$ subset of pNK cells that my laboratory has previously shown to be expanded in patients with HL [93]. The successful expansion of *ex vivo* pNK cells enabled investigations of the IRE1-XBP1 pathway in pNK cells from HL patients. Similar to the results of *in vitro* studies, it was found that suppression of the pathway was associated with

impaired immune synapse formation and IFNγ secretion. Interestingly, expanded pNK cells demonstrated also impaired release of CD107a, a surrogate marker of NK cell degranulation.

Altogether, these findings highlight the importance of the IRE1-XBP1 pathway not only in NK cells function but also in the context of existing immune evasion mechanisms in HL. Therefore, targeting this pathway might be of potential interest to augment NK cell anti-tumoural function.

5.3 PD-1 BLOCKADE EFFECT ON NK CELL FUNCTION

The rich infiltrate of immune cells in HL is controlled by the malignant cells that promote immunosuppressive environment, and thereby the immune responses are limited. Hence, therapeutic approaches in HL focus not only on targeting the malignant cells but also the cellular interactions in the tumour microenvironment [207] [201] [133]. One mechanism that tumour cells utilise to control the surrounding immune cells is by overexpression of PD-L1/PD-L2 ligands that through interaction with PD-1 receptor inhibit the immune effector function. In health, PD-1/PD-L1/PD-L2 axis restrains the immune system to maintain the tolerance and prevent unwanted overreactions from happening, however malignant cells hijack this pathway to compromise the anti-tumour activity [208]. Hence, disruption of the PD-1/PD-L1/PD-L2 signalling with the PD-1 blocking monoclonal antibodies has become an attractive strategy to harness the immune effector cells anti-tumour potential [208] [191] [209]. These observations have led to multiple clinical trials examining the effectiveness of PD-1 blockade in HL that led to the approval of the PD-1 blockade in HL therapy. Currently, available data indicate that the cure rates of PD-1 blockade in refractive/relapsed cases of HL are 70-80% [192].

So far, the accepted paradigm dictated that the impressive results of PD-1/PD-L1/PD-L2 axis disruption in HL is principally due to the restoration of T cell function. However, recent studies have demonstrated that NK cells also display increased expression of PD-1 in multiple cancer types including HL [93] [91] [210] [211] [212]. This observation suggests that increased expression of PD-1 on NK cells may impose a brake on their anti-tumour activity [213], and that the benefits of the PD-1 blockade might be attributable to restoration of both T cell and NK cell function. Yet little is known about the functional impact of disrupting the PD-1/PD-L1 axis on NK cells. To date, there is limited data from other blood cancers that report that blockade of PD-1 improves NK cell-mediated anti-tumour effects. For example, in MM, following the PD-1 blockade NK cells display enhanced trafficking and conjugate formation [91]. Previous data from my supervisor's laboratory indicates that the high-rate of clinical response to PD-1 blockade observed in HL may in part result from disruption of interactions between PD-1+ NK cells and PD-L1/L2 expressed on Hodgkin Reed-Sternberg cells and TAMs [93].

The results of my study further support the notion that PD-1 is a key checkpoint for NK cell function, and the high efficacy of PD-1 blockade therapy in HL may result from mobilization of NK cells to instigate anti-tumour responses. Firstly, PD-1 blockade on a PD-1 expressing NK cell line enhanced migration. Next, I found that PD-1 blockade improves actin accumulation at the immune synapse interphase leading to formation of more stable immune conjugates, and enhanced secretion of IFNγ but not TNFα or lytic granules (Figure 1).

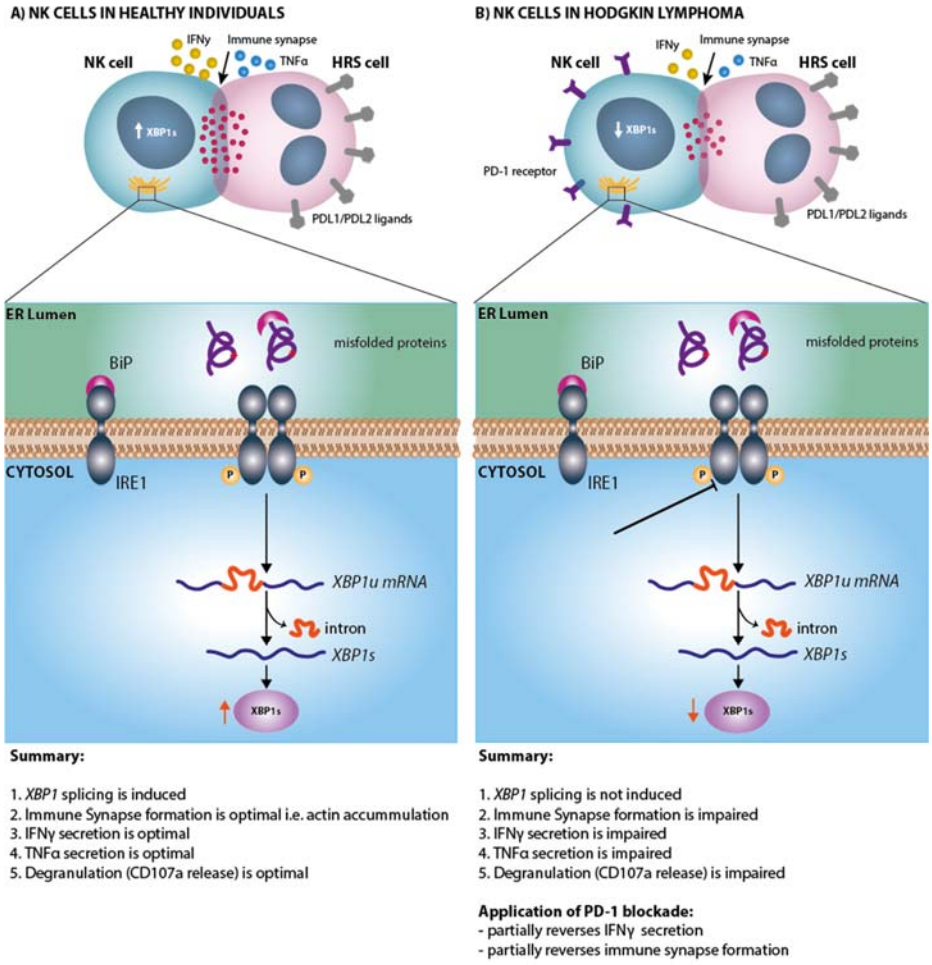

Figure 5.1: The IRE1-XBP1 pathway is required for the optimal NK cell function. In healthy NK cells the IRE1-XBP1 pathway is activated following the stimulation with target cell e.g. HRS cells (A), whereas in NK cells from HL patients the pathway is not activated, and this is restricted to the CD56brightCD16- subset of NK cells (B). The induction of XBP1 splicing is associated with optimal NK cell function i.e. migration, immune synapse formation, cytokine secretion and degranulation. These functions are impaired in NK cells from HL patients, but application of PD-1 blockade partially reverses impaired immune synapse formation and IFNγ secretion. Although PD-1 blockade enhanced NK cell migration, it was unable to reverse the effects of IRE1 blockade on NK cell migration in my experimental system.

5.4 CLINICAL IMPLICATIONS

Checkpoint blockade has led to a renewed focus on understanding the tumour microenvironment. The focus of this research has principally been on understanding the operative immune escape mechanisms by which malignant cells circumvent host T cells. Similarly, advances in immunotherapeutics such as in chimeric antigen receptor (CAR) T cells, and in bispecific T cell engager 'BiTE' antibodies that re-direct host T cell function, have also given prominence to T cell research. By contrast, NK cell research to date has been relatively neglected. However, NK cells is also an important component of host anti-tumoural immunity, and may have potential applicability as cellular immunotherapy, particularly with regard to the treatment of haematological malignancies [92] [214].

There are a number of reasons why NK cells are an attractive area to research host anti-tumoural immunity. Firstly, malignant B cells frequently have aberrant expression of MHC-I molecules making them less likely to be able to be lysed by effector T cells. Paradoxically, cells that lack MHC-I are more susceptible to NK cell lysis (the 'missing self' hypothesis). Next, NK cells have advantages in terms of immunotherapies, including the ability to be pre-generated and available as "off-the-shelf" therapy. CAR NK cells, NK cell lines in which a chimeric antigen receptor has been inserted, are currently in pre-clinical development. As NK cells do not produce IL-6, they are far less likely to induce cytokine release syndrome (CRS) than 'conventional' CAR T cells [215] [216] [217]. NK cell-based therapies are discussed in a greater detail in an earlier chapter (Chapter 1, section 1.4)

In this study, I established that the IRE1-XBP1 pathway is involved in regulating NK cell motility, IS formation and cytokine release. Also, I showed that NK cells from patients with HL have a dysfunctional IRE1-XBP1 pathway that is not activated in response to HRS cells. Further understanding of the pathway dysfunction in NK cells might result in the development of a potential strategy to enhance NK cell function, by targeting the IRE1-XBP1 pathway. One approach would be to develop small molecules, with high specificity (to minimize off-target effects), that target IRE1 RNase activity to augment the *XBP1* splicing. Alternatively, this could be achieved by genetic manipulation e.g. using clustered regularly interspaced short palindromic repeats (CRISPR)/CRISPR associated protein 9 (Cas9) to generate *ex vivo* NK cells with XBP1s overexpression. CRISPR/Cas9 is a robust technology for gene editing that is faster and more accurate than previously used techniques for DNA editing. This system requires two components to mediate gene editing i.e. an enzyme called Cas9 and a guide RNA (gRNA). The gRNA is a short sequence complementary to host's DNA sequence that enables Cas9 to target the specific sequence in the genome [218] [219]. Utilising this approach in HL xenograft mouse model would facilitate *in vivo* study of the IRE1-XBP1 pathway

impact on NK-HRS cells interaction. In xenograft mouse models, existing HL cell lines are engrafted into immunodeficient mice to avoid graft rejection. Importantly, M'Katcher *et al.* established a xenograft model of HL, where NSG mice are engrafted with the L428 cell line, enabling the study of novel candidate drugs [220].

Currently, the NK-92 cell line is the only FDA-approved NK cell line for clinical trials [215] [226]. Recent studies investigating generation of UCB-derived NK cells indicate that these cells might be superior to NK-92 cells as they exert a longer lifespan *in vivo* than NK-92 cells. Indeed, a recent study by Liu *et al.* have shown that UCB-derived NK cells are a good resource to generate CD19-specific CAR NK cells with improved transfection rates and longer lifespan *in vivo* [227]. The latter was achieved by introduction of IL-15 gene to ensure NK cell proliferation and persistence *in vivo* [226, 227]. The use of the NK-92 cell line or UCB-derived NK cells with an operative IRE1-XBP1 pathway would enable infusion of effective NK cells without the need to genetically modify them beforehand. In my study the NK-92 cell line was found to have a functional IRE1-XBP1 pathway, hence infusion of NK-92 cell lines would enable infusion of effective NK cells without the need to genetically enhance this pathway beforehand.

PD-1 blockade is an approved therapy for patients with relapsed/refractory HL. However, there remains minimal data on the role of PD-1 blockade on NK cells in HL. My data demonstrates that PD-1 blockade partially reverses the NK cell impairment caused by dysfunctional IRE1-XBP1 pathway activation. In addition, it would be interesting to delineate the impact of other immune checkpoint blockades such as LAG-3, TIM-3, or TIGIT on NK cell function and examine whether simultaneous targeting of multiple checkpoints amplifies the effect of single agent therapies.

Furthermore, HL is characterised by the presence of TAMs that promote an immunosuppressive microenvironment. Recently it was demonstrated that these cells exert elevated expression of PD-L1 and PD-L2 that may interact with NK cells via PD-1 to further promote immunosuppressive environment [228] [93]. Targeting the IRE1-XBP1 pathway in NK cells from HL may contribute to IFNγ-induced polarization of TAMs away from an M2 'tumour tolerogenic' to a M1 'proinflammatory anti-tumoural' phenotype [229]. Moreover, the broad regulatory effects of IFNγ secreted by NK cells to the TME may further shape hosts' immune responses by inducing maturation of DCs [230]. Notably, mature DCs have increased antigen presentation capacity, hence effectively 'bridging the gap' between the innate and adaptive immune system [231].

5.5 CONCLUSION

Although cure rates are high in HL (~80% in advanced and >90% in early stage disease), because the standard care of treatment has significant short and long-term adverse effects, there is a need to develop less toxic therapies. An immune cell-rich TME and a paucity of malignant cells highlights that targeting immune cells is a viable strategy in HL. Indeed HL is the 'poster child' of PD-1 blockade, with current response rates of relapsed/refractory cases of HL 70-80% [192] [190]. Notably, this includes patients that have relapsed or remained refractory to the prior round of chemotherapy, suggesting that HL has the potential to be one of the first lymphoid malignancies that is treated by a 'chemotherapy-free' immune-mediated regimen.

The frequent loss of MHC-I and elevated expression of PD-L1/PD-L2 ligands on HRS cells renders NK cells a viable strategy in HL [128]. As such, I aimed to investigate the NK cell compartment from patients with HL to determine potential contributions of the IRE1-XBP1 pathway to NK cell dysfunction and explore the potential of PD-1 blockade to restore NK cell functionality. I demonstrate a hitherto unrecognized mechanism underlying NK cell dysfunction in HL i.e. the IRE1-XBP1 pathway suppression that contributes to the impaired migration, immune synapse formation, degranulation, and IFNγ secretion. Interestingly, application of PD-1 blockade, an approved therapeutic in HL, partially restored the impaired immune synapse formation and IFNγ secretion by NK cells. These results suggest that the promising outcomes in HL patients treated with the PD-1 checkpoint blockade may not be only mediated by T cells, but also by NK cells.

List of References

1. Lim, O., et al., *Present and Future of Allogeneic Natural Killer Cell Therapy.* Front Immunol, 2015. **6**: p. 286.
2. Waldhauer, I. and A. Steinle, *NK cells and cancer immunosurveillance.* Oncogene, 2008. **27**(45): p. 5932-43.
3. Cooper, M.A., T.A. Fehniger, and M.A. Caligiuri, *The biology of human natural killer-cell subsets.* Trends Immunol, 2001. **22**(11): p. 633-40.
4. Peng, H. and Z. Tian, *NK cell trafficking in health and autoimmunity:a comprehensive review.* Clin Rev Allergy Immunol, 2014. **47**(2): p. 119-27.
5. Gonzalez, V.D., et al., *Expansion of functionally skewed CD56-negative NK cells in chronic hepatitis C virus infection: correlation with outcome of pegylated IFN-alpha and ribavirin treatment.* J Immunol, 2009. **183**(10): p. 6612-8.
6. Gonzalez, V.D., et al., *Expansion of CD56- NK cells in chronic HCV/HIV-1 co-infection: reversion by antiviral treatment with pegylated IFNalpha and ribavirin.* Clin Immunol, 2008. **128**(1): p. 46-56.
7. Hu, P.F., et al., *Natural killer cell immunodeficiency in HIV disease is manifest by profoundly decreased numbers of CD16+CD56+ cells and expansion of a population of CD16dimCD56- cells with low lytic activity.* J Acquir Immune Defic Syndr Hum Retrovirol, 1995. **10**(3): p. 331-40.
8. Milush, J.M., et al., *CD56negCD16(+) NK cells are activated mature NK cells with impaired effector function during HIV-1 infection.* Retrovirology, 2013. **10**: p. 158.
9. Bjorkstrom, N.K., H.G. Ljunggren, and J.K. Sandberg, *CD56 negative NK cells: origin, function, and role in chronic viral disease.* Trends Immunol, 2010. **31**(11): p. 401-6.
10. Vivier, E., et al., *Functions of natural killer cells.* Nat Immunol, 2008. **9**(5): p. 503-10.
11. Herberman, R.B., et al., *Natural cytotoxic reactivity of mouse lymphoid cells against syngeneic and allogeneic tumors. II. Characterization of effector cells.* Int J Cancer, 1975. **16**(2): p. 230-9.
12. Abel, A.M., et al., *Natural Killer cells: Development, maturation, and clinical utilization.* Front Immunol, 2018. **9**: p. 1869.
13. Bhat, R. and C. Watzl, *Serial killing of tumor cells by human natural killer cells--enhancement by therapeutic antibodies.* PLoS One, 2007. **2**(3): p. e326.
14. Smyth, M.J., et al., *Activation of NK cell cytotoxicity.* Mol Immunol, 2005. **42**(4): p. 501-10.
15. Osinska, I., K. Popko, and U. Demkow, *Perforin: an important player in immune response.* Cent Eur J Immunol, 2014. **39**(1): p. 109-15.
16. Gwalani, L.A. and J.S. Orange, *Single degranulations in NK cells can mediate target cell killing.* J Immunol, 2018. **200**(9): p. 3231-3243.
17. Trapani, J.A., et al., *Localization of granzyme B in the nucleus. A putative role in the mechanism of cytotoxic lymphocyte-mediated apoptosis.* J Biol Chem, 1996. **271**(8): p. 4127-33.
18. Heusel, J.W., et al., *Cytotoxic lymphocytes require granzyme B for the rapid induction of DNA fragmentation and apoptosis in allogeneic target cells.* Cell, 1994. **76**(6): p. 977-87.
19. Khosravi-Far, R. and M.D. Esposti, *Death receptor signals to mitochondria.* Cancer Biol Ther, 2004. **3**(11): p. 1051-7.
20. Trinchieri, G., *Biology of natural killer cells.* Adv Immunol, 1989. **47**: p. 187-376.
21. Lanier, L.L., J.J. Ruitenberg, and J.H. Phillips, *Functional and biochemical analysis of CD16 antigen on natural killer cells and granulocytes.* J Immunol, 1988. **141**(10): p. 3478-85.
22. Wang, W., et al., *Nk cell-mediated antibody-dependent cellular cytotoxicity in cancer immunotherapy.* Front Immunol, 2015. **6**: p. 368.
23. Caligiuri, M.A., *Human natural killer cells.* Blood, 2008. **112**(3): p. 461-9.

24. Martin-Fontecha, A., et al., *Induced recruitment of NK cells to lymph nodes provides IFN-gamma for T(H)1 priming.* Nat Immunol, 2004. **5**(12): p. 1260-5.
25. Higuchi, M., et al., *Membrane tumor necrosis factor-alpha (TNF-alpha) expressed on HTLV-I-infected T cells mediates a costimulatory signal for B cell activation--characterization of membrane TNF-alpha.* Clin Immunol Immunopathol, 1997. **82**(2): p. 133-40.
26. Balkwill, F., *Tumour necrosis factor and cancer.* Nat Rev Cancer, 2009. **9**(5): p. 361-71.
27. Wajant, H., *The role of TNF in cancer.* Results Probl Cell Differ, 2009. **49**: p. 1-15.
28. Chester, C., K. Fritsch, and H.E. Kohrt, *Natural killer cell immunomodulation: Targeting activating, inhibitory, and co-stimulatory receptor signaling for cancer immunotherapy.* Front Immunol, 2015. **6**: p. 601.
29. Campbell, K.S. and J. Hasegawa, *Natural killer cell biology: an update and future directions.* J Allergy Clin Immunol, 2013. **132**(3): p. 536-544.
30. Walzer, T., et al., *Natural killer cell-dendritic cell crosstalk in the initiation of immune responses.* Expert Opin Biol Ther, 2005. **5 Suppl 1**: p. S49-59.
31. Guillerey, C., N.D. Huntington, and M.J. Smyth, *Targeting natural killer cells in cancer immunotherapy.* Nat Immunol, 2016. **17**(9): p. 1025-36.
32. Farag, S.S. and M.A. Caligiuri, *Human natural killer cell development and biology.* Blood Rev, 2006. **20**(3): p. 123-37.
33. Lanier, L.L., *NK cell recognition.* Annu Rev Immunol, 2005. **23**: p. 225-74.
34. Pegram, H.J., et al., *Activating and inhibitory receptors of natural killer cells.* Immunol Cell Biol, 2011. **89**(2): p. 216-24.
35. Radaev, S. and P.D. Sun, *Structure and function of natural killer cell surface receptors.* Annu Rev Biophys Biomol Struct, 2003. **32**: p. 93-114.
36. Ljunggren, H.G. and K. Karre, *In search of the 'missing self': MHC molecules and NK cell recognition.* Immunol Today, 1990. **11**(7): p. 237-44.
37. Cheng, M., et al., *NK cell-based immunotherapy for malignant diseases.* Cell Mol Immunol, 2013. **10**(3): p. 230-52.
38. Draghi, M., et al., *Single-cell analysis of the human NK cell response to missing self and its inhibition by HLA class I.* Blood, 2005. **105**(5): p. 2028-35.
39. Thielens, A., E. Vivier, and F. Romagne, *NK cell MHC class I specific receptors (KIR): from biology to clinical intervention.* Curr Opin Immunol, 2012. **24**(2): p. 239-45.
40. Campbell, K.S. and A.K. Purdy, *Structure/function of human killer cell immunoglobulin-like receptors: lessons from polymorphisms, evolution, crystal structures and mutations.* Immunology, 2011. **132**(3): p. 315-25.
41. Hilton, H.G. and P. Parham, *Missing or altered self: human NK cell receptors that recognize HLA-C.* Immunogenetics, 2017. **69**(8-9): p. 567-579.
42. Morvan, M.G. and L.L. Lanier, *NK cells and cancer: you can teach innate cells new tricks.* Nat Rev Cancer, 2016. **16**(1): p. 7-19.
43. Lopez-Botet, M., et al., *The CD94/NKG2 C-type lectin receptor complex.* Curr Top Microbiol Immunol, 1998. **230**: p. 41-52.
44. Lee, N., et al., *HLA-E is a major ligand for the natural killer inhibitory receptor CD94/NKG2A.* Proc Natl Acad Sci U S A, 1998. **95**(9): p. 5199-204.
45. Borrego, F., et al., *Recognition of human histocompatibility leukocyte antigen (HLA)-E complexed with HLA class I signal sequence-derived peptides by CD94/NKG2 confers protection from natural killer cell-mediated lysis.* J Exp Med, 1998. **187**(5): p. 813-8.
46. Braud, V.M., et al., *HLA-E binds to natural killer cell receptors CD94/NKG2A, B and C.* Nature, 1998. **391**(6669): p. 795-9.
47. Wada, H., et al., *The inhibitory NK cell receptor CD94/NKG2A and the activating receptor CD94/NKG2C bind the top of HLA-E through mostly shared but partly distinct sets of HLA-E residues.* Eur J Immunol, 2004. **34**(1): p. 81-90.
48. Bauer, S., et al., *Activation of NK cells and T cells by NKG2D, a receptor for stress-inducible MICA.* Science, 1999. **285**(5428): p. 727-9.

49. Wu, J., et al., *An activating immunoreceptor complex formed by NKG2D and DAP10.* Science, 1999. **285**(5428): p. 730-2.
50. Billadeau, D.D., et al., *NKG2D-DAP10 triggers human NK cell-mediated killing via a Syk-independent regulatory pathway.* Nat Immunol, 2003. **4**(6): p. 557-64.
51. Bahram, S., *MIC genes: from genetics to biology.* Adv Immunol, 2000. **76**: p. 1-60.
52. Sutherland, C.L., N.J. Chalupny, and D. Cosman, *The UL16-binding proteins, a novel family of MHC class I-related ligands for NKG2D, activate natural killer cell functions.* Immunol Rev, 2001. **181**: p. 185-92.
53. Long, E.O., *Tumor cell recognition by natural killer cells.* Semin Cancer Biol, 2002. **12**(1): p. 57-61.
54. Klimosch, S.N., et al., *Genetically coupled receptor-ligand pair NKp80-AICL enables autonomous control of human NK cell responses.* Blood, 2013. **122**(14): p. 2380-9.
55. Peipp, M., et al., *HER2-specific immunoligands engaging NKp30 or NKp80 trigger NK-cell-mediated lysis of tumor cells and enhance antibody-dependent cell-mediated cytotoxicity.* Oncotarget, 2015. **6**(31): p. 32075-88.
56. Deng, G., et al., *Generation and preclinical characterization of an NKp80-Fc fusion protein for redirected cytolysis of natural killer (NK) cells against leukemia.* J Biol Chem, 2015. **290**(37): p. 22474-84.
57. McQueen, K.L. and P. Parham, *Variable receptors controlling activation and inhibition of NK cells.* Curr Opin Immunol, 2002. **14**(5): p. 615-21.
58. Hudspeth, K., B. Silva-Santos, and D. Mavilio, *Natural cytotoxicity receptors: broader expression patterns and functions in innate and adaptive immune cells.* Front Immunol, 2013. **4**: p. 69.
59. Fuchs, A., et al., *Paradoxic inhibition of human natural interferon-producing cells by the activating receptor NKp44.* Blood, 2005. **106**(6): p. 2076-82.
60. Vitale, M., et al., *Identification of NKp80, a novel triggering molecule expressed by human NK cells.* Eur J Immunol, 2001. **31**(1): p. 233-42.
61. Shemesh, A., et al., *Splice variants of human natural cytotoxicity receptors: novel innate immune checkpoints.* Cancer Immunol Immunother, 2018. **67**(12): p. 1871-1883.
62. Arnon, T.I., G. Markel, and O. Mandelboim, *Tumor and viral recognition by natural killer cells receptors.* Semin Cancer Biol, 2006. **16**(5): p. 348-58.
63. Kruse, P.H., et al., *Natural cytotoxicity receptors and their ligands.* Immunol Cell Biol, 2014. **92**(3): p. 221-9.
64. Sivori, S., et al., *NKp46 is the major triggering receptor involved in the natural cytotoxicity of fresh or cultured human NK cells. Correlation between surface density of NKp46 and natural cytotoxicity against autologous, allogeneic or xenogeneic target cells.* Eur J Immunol, 1999. **29**(5): p. 1656-66.
65. Sivori, S., et al., *p46, a novel natural killer cell-specific surface molecule that mediates cell activation.* J Exp Med, 1997. **186**(7): p. 1129-36.
66. Vitale, M., et al., *NKp44, a novel triggering surface molecule specifically expressed by activated natural killer cells, is involved in non-major histocompatibility complex-restricted tumor cell lysis.* J Exp Med, 1998. **187**(12): p. 2065-72.
67. Pende, D., et al., *Identification and molecular characterization of NKp30, a novel triggering receptor involved in natural cytotoxicity mediated by human natural killer cells.* J Exp Med, 1999. **190**(10): p. 1505-16.
68. Biassoni, R. and M.S. Malnati, *Human Natural Killer Receptors, Co-Receptors, and Their Ligands.* Curr Protoc Immunol, 2018. **121**(1): p. e47.
69. Mace, E.M., *Phosphoinositide-3-Kinase signaling in human Natural Killer cells: New insights from primary immunodeficiency.* Front Immunol, 2018. **9**: p. 445.
70. Mace, E.M., et al., *Cell biological steps and checkpoints in accessing NK cell cytotoxicity.* Immunol Cell Biol, 2014. **92**(3): p. 245-55.

71. Krzewski, K. and J.L. Strominger, *The killer's kiss: the many functions of NK cell immunological synapses.* Curr Opin Cell Biol, 2008. **20**(5): p. 597-605.
72. Topham, N.J. and E.W. Hewitt, *Natural killer cell cytotoxicity: how do they pull the trigger?* Immunology, 2009. **128**(1): p. 7-15.
73. Barber, D.F., M. Faure, and E.O. Long, *LFA-1 contributes an early signal for NK cell cytotoxicity.* J Immunol, 2004. **173**(6): p. 3653-9.
74. Mace, E.M. and J.S. Orange, *New views of the human NK cell immunological synapse: recent advances enabled by super- and high-resolution imaging techniques.* Front Immunol, 2012. **3**: p. 421.
75. Chiesa, S., et al., *Coordination of activating and inhibitory signals in natural killer cells.* Mol Immunol, 2005. **42**(4): p. 477-84.
76. Mace, E.M. and J.S. Orange, *Dual channel STED nanoscopy of lytic granules on actin filaments in natural killer cells.* Commun Integr Biol, 2012. **5**(2): p. 184-6.
77. Brown, A.C., et al., *Remodelling of cortical actin where lytic granules dock at natural killer cell immune synapses revealed by super-resolution microscopy.* PLoS Biol, 2011. **9**(9): p. e1001152.
78. Rak, G.D., et al., *Natural killer cell lytic granule secretion occurs through a pervasive actin network at the immune synapse.* PLoS Biol, 2011. **9**(9): p. e1001151.
79. Krzewski, K. and J.E. Coligan, *Human NK cell lytic granules and regulation of their exocytosis.* Front Immunol, 2012. **3**: p. 335.
80. Sanborn, K.B., et al., *Phosphorylation of the myosin IIA tailpiece regulates single myosin IIA molecule association with lytic granules to promote NK-cell cytotoxicity.* Blood, 2011. **118**(22): p. 5862-71.
81. Sanborn, K.B., et al., *Myosin IIA associates with NK cell lytic granules to enable their interaction with F-actin and function at the immunological synapse.* J Immunol, 2009. **182**(11): p. 6969-84.
82. Voskoboinik, I., M.J. Smyth, and J.A. Trapani, *Perforin-mediated target-cell death and immune homeostasis.* Nat Rev Immunol, 2006. **6**(12): p. 940-52.
83. Orange, J.S., *Formation and function of the lytic NK-cell immunological synapse.* Nat Rev Immunol, 2008. **8**(9): p. 713-25.
84. Yoon, S.R., T.D. Kim, and I. Choi, *Understanding of molecular mechanisms in natural killer cell therapy.* Exp Mol Med, 2015. **47**(e141): p. e141.
85. Mandal, A. and C. Viswanathan, *Natural killer cells: In health and disease.* Hematol Oncol Stem Cell Ther, 2015. **8**(2): p. 47-55.
86. Imai, K., et al., *Natural cytotoxic activity of peripheral-blood lymphocytes and cancer incidence: an 11-year follow-up study of a general population.* Lancet, 2000. **356**(9244): p. 1795-9.
87. Levy, E.M., M.P. Roberti, and J. Mordoh, *Natural killer cells in human cancer: from biological functions to clinical applications.* J Biomed Biotechnol, 2011. **2011**: p. 676198.
88. Salles, G., et al., *Rituximab in B-Cell Hematologic Malignancies: A Review of 20 Years of Clinical Experience.* Adv Ther, 2017. **34**(10): p. 2232-2273.
89. Paul, S. and G. Lal, *The molecular mechanism of Natural Killer cells function and its importance in cancer immunotherapy.* Front Immunol, 2017. **8**: p. 1124.
90. Childs, R.W. and M. Carlsten, *Therapeutic approaches to enhance natural killer cell cytotoxicity against cancer: the force awakens.* Nat Rev Drug Discov, 2015. **14**(7): p. 487-98.
91. Benson, D.M., Jr., et al., *The PD-1/PD-L1 axis modulates the natural killer cell versus multiple myeloma effect: a therapeutic target for CT-011, a novel monoclonal anti-PD-1 antibody.* Blood, 2010. **116**(13): p. 2286-94.
92. Barrow, A.D. and M. Colonna, *Exploiting NK Cell Surveillance Pathways for Cancer Therapy.* Cancers (Basel), 2019. **11**(1).
93. Vari, F., et al., *Immune evasion via PD-1/PD-L1 on NK cells and monocyte/macrophages is more prominent in Hodgkin lymphoma than DLBCL.* Blood, 2018. **131**(16): p. 1809-1819.

94. Vey, N., et al., *A phase 1 trial of the anti-inhibitory KIR mAb IPH2101 for AML in complete remission.* Blood, 2012. **120**(22): p. 4317-23.
95. Benson, D.M., Jr., et al., *A phase 1 trial of the anti-KIR antibody IPH2101 in patients with relapsed/refractory multiple myeloma.* Blood, 2012. **120**(22): p. 4324-33.
96. Al Absi, A., et al., *Actin cytoskeleton remodeling drives breast cancer cell escape from Natural Killer-mediated cytotoxicity.* Cancer Res, 2018. **78**(19): p. 5631-5643.
97. Vey, N., et al., *A phase 1 study of lirilumab (antibody against killer immunoglobulin-like receptor antibody KIR2D; IPH2102) in patients with solid tumors and hematologic malignancies.* Oncotarget, 2018. **9**(25): p. 17675-17688.
98. Geller, M.A. and J.S. Miller, *Use of allogeneic NK cells for cancer immunotherapy.* Immunotherapy, 2011. **3**(12): p. 1445-59.
99. Lanier, L.L., *Natural killer cell receptor signaling.* Curr Opin Immunol, 2003. **15**(3): p. 308-14.
100. Ruggeri, L., et al., *Effectiveness of donor natural killer cell alloreactivity in mismatched hematopoietic transplants.* Science, 2002. **295**(5562): p. 2097-100.
101. Curti, A., et al., *Successful transfer of alloreactive haploidentical KIR ligand-mismatched natural killer cells after infusion in elderly high risk acute myeloid leukemia patients.* Blood, 2011. **118**(12): p. 3273-9.
102. Ruggeri, L., et al., *Role of natural killer cell alloreactivity in HLA-mismatched hematopoietic stem cell transplantation.* Blood, 1999. **94**(1): p. 333-9.
103. Rubnitz, J.E., et al., *NKAML: a pilot study to determine the safety and feasibility of haploidentical natural killer cell transplantation in childhood acute myeloid leukemia.* J Clin Oncol, 2010. **28**(6): p. 955-9.
104. Miller, J.S., et al., *Successful adoptive transfer and in vivo expansion of human haploidentical NK cells in patients with cancer.* Blood, 2005. **105**(8): p. 3051-7.
105. Bachanova, V., et al., *Haploidentical natural killer cells induce remissions in non-Hodgkin lymphoma patients with low levels of immune-suppressor cells.* Cancer Immunol Immunother, 2018. **67**(3): p. 483-494.
106. Liang, S., et al., *Comparison of autogeneic and allogeneic natural killer cells immunotherapy on the clinical outcome of recurrent breast cancer.* Onco Targets Ther, 2017. **10**: p. 4273-4281.
107. Besser, M.J., et al., *Development of allogeneic NK cell adoptive transfer therapy in metastatic melanoma patients: in vitro preclinical optimization studies.* PLoS One, 2013. **8**(3): p. e57922.
108. Romee, R., et al., *Cytokine activation induces human memory-like NK cells.* Blood, 2012. **120**(24): p. 4751-60.
109. Hetz, C., *The unfolded protein response: controlling cell fate decisions under ER stress and beyond.* Nat Rev Mol Cell Biol, 2012. **13**(2): p. 89-102.
110. Wu, R., et al., *Involvement of the IRE1alpha-XBP1 pathway and XBP1s-dependent transcriptional reprogramming in metabolic diseases.* DNA Cell Biol, 2015. **34**(1): p. 6-18.
111. Walter, P. and D. Ron, *The unfolded protein response: from stress pathway to homeostatic regulation.* Science, 2011. **334**(6059): p. 1081-6.
112. Urano, F., A. Bertolotti, and D. Ron, *IRE1 and efferent signaling from the endoplasmic reticulum.* J Cell Sci, 2000. **113 Pt 21**: p. 3697-702.
113. Tirasophon, W., A.A. Welihinda, and R.J. Kaufman, *A stress response pathway from the endoplasmic reticulum to the nucleus requires a novel bifunctional protein kinase/endoribonuclease (Ire1p) in mammalian cells.* Genes Dev, 1998. **12**(12): p. 1812-24.
114. Bertolotti, A., et al., *Dynamic interaction of BiP and ER stress transducers in the unfolded-protein response.* Nat Cell Biol, 2000. **2**(6): p. 326-32.
115. Zhou, J., et al., *The crystal structure of human IRE1 luminal domain reveals a conserved dimerization interface required for activation of the unfolded protein response.* Proc Natl Acad Sci U S A, 2006. **103**(39): p. 14343-8.

116. Kimata, Y., et al., *Two regulatory steps of ER-stress sensor Ire1 involving its cluster formation and interaction with unfolded proteins.* J Cell Biol, 2007. **179**(1): p. 75-86.
117. Calfon, M., et al., *IRE1 couples endoplasmic reticulum load to secretory capacity by processing the XBP-1 mRNA.* Nature, 2002. **415**(6867): p. 92-6.
118. Lee, K., et al., *IRE1-mediated unconventional mRNA splicing and S2P-mediated ATF6 cleavage merge to regulate XBP1 in signaling the unfolded protein response.* Genes Dev, 2002. **16**(4): p. 452-66.
119. Yoshida, H., et al., *XBP1 mRNA is induced by ATF6 and spliced by IRE1 in response to ER stress to produce a highly active transcription factor.* Cell, 2001. **107**(7): p. 881-91.
120. Iwakoshi, N.N., et al., *Plasma cell differentiation and the unfolded protein response intersect at the transcription factor XBP-1.* Nat Immunol, 2003. **4**(4): p. 321-9.
121. Reimold, A.M., et al., *Plasma cell differentiation requires the transcription factor XBP-1.* Nature, 2001. **412**(6844): p. 300-7.
122. Martinon, F., et al., *TLR activation of the transcription factor XBP1 regulates innate immune responses in macrophages.* Nat Immunol, 2010. **11**(5): p. 411-8.
123. Iwakoshi, N.N., M. Pypaert, and L.H. Glimcher, *The transcription factor XBP-1 is essential for the development and survival of dendritic cells.* J Exp Med, 2007. **204**(10): p. 2267-75.
124. Cubillos-Ruiz, J.R., et al., *ER stress sensor XBP1 controls anti-tumor immunity by disrupting dendritic cell homeostasis.* Cell, 2015. **161**(7): p. 1527-38.
125. Kamimura, D. and M.J. Bevan, *Endoplasmic reticulum stress regulator XBP-1 contributes to effector CD8+ T cell differentiation during acute infection.* J Immunol, 2008. **181**(8): p. 5433-41.
126. Song, M., et al., *IRE1alpha-XBP1 controls T cell function in ovarian cancer by regulating mitochondrial activity.* Nature, 2018. **562**(7727): p. 423-428.
127. Matsuki, E. and A. Younes, *Lymphomagenesis in Hodgkin lymphoma.* Semin Cancer Biol, 2015. **34**: p. 14-21.
128. Kuppers, R., *The biology of Hodgkin's lymphoma.* Nat Rev Cancer, 2009. **9**(1): p. 15-27.
129. Kuppers, R., A. Engert, and M.L. Hansmann, *Hodgkin lymphoma.* J Clin Invest, 2012. **122**(10): p. 3439-47.
130. Kaseb, H. and H.M. Babiker, *Cancer, Lymphoma, Hodgkin*, in *StatPearls*. 2018, StatPearls Publishing

StatPearls Publishing LLC.: Treasure Island (FL).
131. Steidl, C., J.M. Connors, and R.D. Gascoyne, *Molecular pathogenesis of Hodgkin's lymphoma: increasing evidence of the importance of the microenvironment.* J Clin Oncol, 2011. **29**(14): p. 1812-26.
132. Mathas, S., S. Hartmann, and R. Kuppers, *Hodgkin lymphoma: Pathology and biology.* Semin Hematol, 2016. **53**(3): p. 139-47.
133. Cirillo, M., et al., *The translational science of hodgkin lymphoma.* Br J Haematol, 2019. **184**(1): p. 30-44.
134. Meti, N., K. Esfahani, and N.A. Johnson, *The role of immune checkpoint inhibitors in Classical Hodgkin Lymphoma.* Cancers (Basel), 2018. **10**(6).
135. Liu, W.R. and M.A. Shipp, *Signaling pathways and immune evasion mechanisms in classical Hodgkin lymphoma.* Hematology Am Soc Hematol Educ Program, 2017. **2017**(1): p. 310-316.
136. Aldinucci, D., et al., *Interactions between tissue fibroblasts in lymph nodes and Hodgkin/Reed-Sternberg cells.* Leuk Lymphoma, 2004. **45**(9): p. 1731-9.
137. Viel, S., et al., *TGF-beta inhibits the activation and functions of NK cells by repressing the mTOR pathway.* Sci Signal, 2016. **9**(415): p. ra19.
138. Mathas, S., et al., *c-FLIP mediates resistance of Hodgkin/Reed-Sternberg cells to death receptor-induced apoptosis.* J Exp Med, 2004. **199**(8): p. 1041-52.

139. Gandhi, M.K., et al., *Galectin-1 mediated suppression of Epstein-Barr virus specific T-cell immunity in classic Hodgkin lymphoma.* Blood, 2007. **110**(4): p. 1326-9.
140. Renner, C. and F. Stenner, *Cancer immunotherapy and the immune response in Hodgkin Lymphoma.* Front Oncol, 2018. **8**: p. 193.
141. Juszczynski, P., et al., *The AP1-dependent secretion of galectin-1 by Reed Sternberg cells fosters immune privilege in classical Hodgkin lymphoma.* Proc Natl Acad Sci U S A, 2007. **104**(32): p. 13134-9.
142. Menter, T. and A. Tzankov, *Mechanisms of Immune Evasion and Immune Modulation by Lymphoma Cells.* Front Oncol, 2018. **8**: p. 54.
143. Roemer, M.G., et al., *Classical Hodgkin Lymphoma with Reduced beta2M/MHC Class I Expression Is Associated with Inferior Outcome Independent of 9p24.1 Status.* Cancer Immunol Res, 2016. **4**(11): p. 910-916.
144. Roemer, M.G.M., et al., *Major Histocompatibility Complex Class II and Programmed Death Ligand 1 Expression Predict Outcome After Programmed Death 1 Blockade in Classic Hodgkin Lymphoma.* J Clin Oncol, 2018. **36**(10): p. 942-950.
145. Engert, A. and A. Younes, *Hodgkin Lymphoma: A Comprehensive Overview. Hematologic Malignancies.* Springer International Publishing 2015, 2015.
146. Diepstra, A., et al., *HLA-G protein expression as a potential immune escape mechanism in classical Hodgkin's lymphoma.* Tissue Antigens, 2008. **71**(3): p. 219-26.
147. Caocci, G., et al., *HLA-G expression and role in advanced-stage classical Hodgkin lymphoma.* Eur J Histochem, 2016. **60**(2): p. 2606.
148. Zocchi, M.R., et al., *High ERp5/ADAM10 expression in lymph node microenvironment and impaired NKG2D ligands recognition in Hodgkin lymphomas.* Blood, 2012. **119**(6): p. 1479-89.
149. Zhang, Y., et al., *Common cytological and cytogenetic features of Epstein-Barr virus (EBV)-positive natural killer (NK) cells and cell lines derived from patients with nasal T/NK-cell lymphomas, chronic active EBV infection and hydroa vacciniforme-like eruptions.* Br J Haematol, 2003. **121**(5): p. 805-14.
150. Cross, B.C., et al., *The molecular basis for selective inhibition of unconventional mRNA splicing by an IRE1-binding small molecule.* Proc Natl Acad Sci U S A, 2012. **109**(15): p. E869-78.
151. Denmeade, S.R. and J.T. Isaacs, *The SERCA pump as a therapeutic target: making a "smart bomb" for prostate cancer.* Cancer Biol Ther, 2005. **4**(1): p. 14-22.
152. Hiramatsu, N., et al., *Real-time detection and continuous monitoring of ER stress in vitro and in vivo by ES-TRAP: evidence for systemic, transient ER stress during endotoxemia.* Nucleic Acids Res, 2006. **34**(13): p. e93.
153. Maly, J. and L. Alinari, *Pembrolizumab in classical Hodgkin's lymphoma.* Eur J Haematol, 2016. **97**(3): p. 219-27.
154. Alter, G., J.M. Malenfant, and M. Altfeld, *CD107a as a functional marker for the identification of natural killer cell activity.* J Immunol Methods, 2004. **294**(1-2): p. 15-22.
155. Campbell, K.S., *NK cell methods*. 2 ed. Springer protocols, ed. J.M. Walker. 2010, New York: Humana Press.
156. Fais, S. and W. Malorni, *Leukocyte uropod formation and membrane/cytoskeleton linkage in immune interactions.* J Leukoc Biol, 2003. **73**(5): p. 556-63.
157. Springer, T.A. and M.L. Dustin, *Integrin inside-out signaling and the immunological synapse.* Curr Opin Cell Biol, 2012. **24**(1): p. 107-15.
158. Raemer, P.C., K. Kohl, and C. Watzl, *Statins inhibit NK-cell cytotoxicity by interfering with LFA-1-mediated conjugate formation.* Eur J Immunol, 2009. **39**(6): p. 1456-65.
159. Mace, E.M., et al., *A dual role for talin in NK cell cytotoxicity: activation of LFA-1-mediated cell adhesion and polarization of NK cells.* J Immunol, 2009. **182**(2): p. 948-56.
160. Mace, E.M., et al., *Elucidation of the integrin LFA-1-mediated signaling pathway of actin polarization in natural killer cells.* Blood, 2010. **116**(8): p. 1272-9.

161. Osman, M.S., D.N. Burshtyn, and K.P. Kane, *Activating Ly-49 receptors regulate LFA-1-mediated adhesion by NK cells.* J Immunol, 2007. **178**(3): p. 1261-7.
162. Bettigole, S.E., et al., *The transcription factor XBP1 is selectively required for eosinophil differentiation.* Nat Immunol, 2015. **16**(8): p. 829-37.
163. Lozzio, B.B. and C.B. Lozzio, *Properties and usefulness of the original K-562 human myelogenous leukemia cell line.* Leuk Res, 1979. **3**(6): p. 363-70.
164. Yagita, M., et al., *A novel natural killer cell line (KHYG-1) from a patient with aggressive natural killer cell leukemia carrying a p53 point mutation.* Leukemia, 2000. **14**(5): p. 922-30.
165. Gong, J.H., G. Maki, and H.G. Klingemann, *Characterization of a human cell line (NK-92) with phenotypical and functional characteristics of activated natural killer cells.* Leukemia, 1994. **8**(4): p. 652-8.
166. Tornroos, H., H. Hagerstrand, and C. Lindqvist, *Culturing the Human Natural Killer Cell Line NK-92 in Interleukin-2 and Interleukin-15 - Implications for Clinical Trials.* Anticancer Res, 2019. **39**(1): p. 107-112.
167. Zhang, C., et al., *Chimeric Antigen Receptor-Engineered NK-92 Cells: An Off-the-Shelf Cellular Therapeutic for Targeted Elimination of Cancer Cells and Induction of Protective Antitumor Immunity.* Front Immunol, 2017. **8**: p. 533.
168. Portal, E.S.S.B.R. *KM-H2 cell line*. 2011 [cited 2019 16 Apr]; Available from: https://web.expasy.org/cellosaurus/CVCL_1330.
169. Acosta-Alvear, D., et al., *XBP1 controls diverse cell type- and condition-specific transcriptional regulatory networks.* Mol Cell, 2007. **27**(1): p. 53-66.
170. Lee, A.H., N.N. Iwakoshi, and L.H. Glimcher, *XBP-1 regulates a subset of endoplasmic reticulum resident chaperone genes in the unfolded protein response.* Mol Cell Biol, 2003. **23**(21): p. 7448-59.
171. Tsai, Y.C. and A.M. Weissman, *The Unfolded Protein Response, Degradation from Endoplasmic Reticulum and Cancer.* Genes Cancer, 2010. **1**(7): p. 764-778.
172. Medel, B., et al., *IRE1alpha Activation in Bone Marrow-Derived Dendritic Cells Modulates Innate Recognition of Melanoma Cells and Favors CD8(+) T Cell Priming.* Front Immunol, 2018. **9**: p. 3050.
173. Zhang, L., et al., *IRE1 inhibition perturbs the unfolded protein response in a pancreatic beta-cell line expressing mutant proinsulin, but does not sensitize the cells to apoptosis.* BMC Cell Biol, 2014. **15**: p. 29.
174. Strasser, A., P.J. Jost, and S. Nagata, *The many roles of FAS receptor signaling in the immune system.* Immunity, 2009. **30**(2): p. 180-92.
175. Mimura, N., et al., *Blockade of XBP1 splicing by inhibition of IRE1alpha is a promising therapeutic option in multiple myeloma.* Blood, 2012. **119**(24): p. 5772-81.
176. Papandreou, I., et al., *Identification of an Ire1alpha endonuclease specific inhibitor with cytotoxic activity against human multiple myeloma.* Blood, 2011. **117**(4): p. 1311-4.
177. Gambella, M., et al., *High XBP1 expression is a marker of better outcome in multiple myeloma patients treated with bortezomib.* Haematologica, 2014. **99**(2): p. e14-6.
178. Shaffer, A.L., et al., *XBP1, downstream of Blimp-1, expands the secretory apparatus and other organelles, and increases protein synthesis in plasma cell differentiation.* Immunity, 2004. **21**(1): p. 81-93.
179. Berrou, J., et al., *Natural killer cell function, an important target for infection and tumor protection, is impaired in type 2 diabetes.* PLoS One, 2013. **8**(4): p. e62418.
180. Stewart, C., et al., *Regulation of IRE1alpha by the small molecule inhibitor 4mu8c in hepatoma cells.* Endoplasmic Reticulum Stress Dis, 2017. **4**(1): p. 1-10.
181. Kemp, K.L., et al., *The serine-threonine kinase inositol-requiring enzyme 1alpha (IRE1alpha) promotes IL-4 production in T helper cells.* J Biol Chem, 2013. **288**(46): p. 33272-82.
182. Yang, J., et al., *The interaction between XBP1 and eNOS contributes to endothelial cell migration.* Exp Cell Res, 2018. **363**(2): p. 262-270.

183. Dejeans, N., et al., *Autocrine control of glioma cells adhesion and migration through IRE1alpha-mediated cleavage of SPARC mRNA.* J Cell Sci, 2012. **125**(Pt 18): p. 4278-87.
184. Glimcher, L.H., *XBP1: the last two decades.* Ann Rheum Dis, 2010. **69 Suppl 1**: p. i67-71.
185. Maestre, L., et al., *Expression pattern of XBP1(S) in human B-cell lymphomas.* Haematologica, 2009. **94**(3): p. 419-22.
186. Bujisic, B., et al., *Impairment of both IRE1 expression and XBP1 activation is a hallmark of GCB DLBCL and contributes to tumor growth.* Blood, 2017. **129**(17): p. 2420-2428.
187. Merryman, R.W., et al., *Checkpoint blockade in Hodgkin and non-Hodgkin lymphoma.* Blood Adv, 2017. **1**(26): p. 2643-2654.
188. Wang, Y., et al., *Advances in CD30- and PD-1-targeted therapies for classical Hodgkin lymphoma.* J Hematol Oncol, 2018. **11**(1): p. 57.
189. Beldi-Ferchiou, A., et al., *PD-1 mediates functional exhaustion of activated NK cells in patients with Kaposi sarcoma.* Oncotarget, 2016. **7**(45): p. 72961-72977.
190. Brockelmann, P.J. and A. Engert, *Checkpoint Inhibition in Hodgkin Lymphoma - a Review.* Oncol Res Treat, 2017. **40**(11): p. 654-660.
191. Armand, P., et al., *Programmed Death-1 Blockade With Pembrolizumab in Patients With Classical Hodgkin Lymphoma After Brentuximab Vedotin Failure.* J Clin Oncol, 2016. **34**(31): p. 3733-3739.
192. Chen, R., et al., *Phase II Study of the Efficacy and Safety of Pembrolizumab for Relapsed/Refractory Classic Hodgkin Lymphoma.* J Clin Oncol, 2017. **35**(19): p. 2125-2132.
193. Pramanik, J., et al., *Genome-wide analyses reveal the IRE1a-XBP1 pathway promotes T helper cell differentiation by resolving secretory stress and accelerating proliferation.* Genome Med, 2018. **10**(1): p. 76.
194. Xu, J.X., et al., *FDA Approval Summary: Nivolumab in Advanced Renal Cell Carcinoma After Anti-Angiogenic Therapy and Exploratory Predictive Biomarker Analysis.* Oncologist, 2017. **22**(3): p. 311-317.
195. Xia, L., Y. Liu, and Y. Wang, *PD-1/PD-L1 Blockade Therapy in Advanced Non-Small-Cell Lung Cancer: Current Status and Future Directions.* Oncologist, 2019. **24**(Suppl 1): p. S31-s41.
196. Bhatnagar, V., et al., *FDA Approval Summary: Daratumumab for Treatment of Multiple Myeloma After One Prior Therapy.* Oncologist, 2017. **22**(11): p. 1347-1353.
197. Narayan, V., et al., *Pembrolizumab monotherapy versus chemotherapy for treatment of advanced urothelial carcinoma with disease progression during or following platinum-containing chemotherapy. A Cochrane Rapid Review.* Cochrane Database Syst Rev, 2018. **7**: p. Cd012838.
198. Wiesmayr, S., et al., *Decreased NKp46 and NKG2D and elevated PD-1 are associated with altered NK-cell function in pediatric transplant patients with PTLD.* Eur J Immunol, 2012. **42**(2): p. 541-50.
199. Chiossone, L., et al., *Natural killer cells and other innate lymphoid cells in cancer.* Nat Rev Immunol, 2018. **18**(11): p. 671-688.
200. Rezvani, K., et al., *Engineering Natural Killer Cells for Cancer Immunotherapy.* Mol Ther, 2017. **25**(8): p. 1769-1781.
201. Wein, F., et al., *Complex Immune Evasion Strategies in Classical Hodgkin Lymphoma.* Cancer Immunol Res, 2017. **5**(12): p. 1122-1132.
202. Chen, C. and X. Zhang, *IRE1alpha-XBP1 pathway promotes melanoma progression by regulating IL-6/STAT3 signaling.* J Transl Med, 2017. **15**(1): p. 42.
203. Kharabi Masouleh, B., et al., *Mechanistic rationale for targeting the unfolded protein response in pre-B acute lymphoblastic leukemia.* Proc Natl Acad Sci U S A, 2014. **111**(21): p. E2219-28.
204. Chen, X., et al., *XBP1 promotes triple-negative breast cancer by controlling the HIF1[agr] pathway.* Nature, 2014. **508**(7494): p. 103-107.

205. Chalmers, F., et al., *The multiple roles of the unfolded protein response regulator IRE1alpha in cancer.* Mol Carcinog, 2019.
206. Uemura, A., et al., *Unconventional splicing of XBP1 mRNA occurs in the cytoplasm during the mammalian unfolded protein response.* J Cell Sci, 2009. **122**(Pt 16): p. 2877-86.
207. Aldinucci, D., C. Borghese, and N. Casagrande, *Formation of the Immunosuppressive Microenvironment of Classic Hodgkin Lymphoma and Therapeutic Approaches to Counter It.* Int J Mol Sci, 2019. **20**(10).
208. Allen, P.B. and L.I. Gordon, *PD-1 blockade in Hodgkin's lymphoma: learning new tricks from an old teacher.* Expert Rev Hematol, 2016. **9**(10): p. 939-49.
209. Ok, C.Y. and K.H. Young, *Checkpoint inhibitors in hematological malignancies.* J Hematol Oncol, 2017. **10**(1): p. 103.
210. Hsu, J., et al., *Contribution of NK cells to immunotherapy mediated by PD-1/PD-L1 blockade.* J Clin Invest, 2018. **128**(10): p. 4654-4668.
211. Pesce, S., et al., *Identification of a subset of human natural killer cells expressing high levels of programmed death 1: A phenotypic and functional characterization.* J Allergy Clin Immunol, 2017. **139**(1): p. 335-346.e3.
212. Liu, Y., et al., *Increased expression of programmed cell death protein 1 on NK cells inhibits NK-cell-mediated anti-tumor function and indicates poor prognosis in digestive cancers.* Oncogene, 2017. **36**(44): p. 6143-6153.
213. Mariotti, F.R., et al., *PD-1 in human NK cells: evidence of cytoplasmic mRNA and protein expression.* Oncoimmunology, 2019. **8**(3): p. 1557030.
214. Hu, W., et al., *Cancer Immunotherapy Based on Natural Killer Cells: Current Progress and New Opportunities.* Front Immunol, 2019. **10**: p. 1205.
215. Zhang, J., H. Zheng, and Y. Diao, *Natural Killer Cells and Current Applications of Chimeric Antigen Receptor-Modified NK-92 Cells in Tumor Immunotherapy.* Int J Mol Sci, 2019. **20**(2).
216. Lopez-Lastra, S. and J.P. Di Santo, *Modeling Natural Killer Cell Targeted Immunotherapies.* Front Immunol, 2017. **8**: p. 370.
217. Freund-Brown, J., L. Chirino, and T. Kambayashi, *Strategies to enhance NK cell function for the treatment of tumors and infections.* Crit Rev Immunol, 2018. **38**(2): p. 105-130.
218. Gupta, R.M. and K. Musunuru, *Expanding the genetic editing tool kit: ZFNs, TALENs, and CRISPR-Cas9.* J Clin Invest, 2014. **124**(10): p. 4154-61.
219. Hsu, P.D., E.S. Lander, and F. Zhang, *Development and applications of CRISPR-Cas9 for genome engineering.* Cell, 2014. **157**(6): p. 1262-78.
220. M'Kacher, R., et al., *Establishment and Characterization of a Reliable Xenograft Model of Hodgkin Lymphoma Suitable for the Study of Tumor Origin and the Design of New Therapies.* Cancers (Basel), 2018. **10**(11).
221. Lai, Y., et al., *Current status and perspectives of patient-derived xenograft models in cancer research.* J Hematol Oncol, 2017. **10**(1): p. 106.
222. von Kalle, C., et al., *Growth of Hodgkin cell lines in severely combined immunodeficient mice.* Int J Cancer, 1992. **52**(6): p. 887-91.
223. Mark, A., et al., *Characteristic mTOR activity in Hodgkin-lymphomas offers a potential therapeutic target in high risk disease--a combined tissue microarray, in vitro and in vivo study.* BMC Cancer, 2013. **13**: p. 250.
224. Ju, W., et al., *Augmented efficacy of brentuximab vedotin combined with ruxolitinib and/or Navitoclax in a murine model of human Hodgkin's lymphoma.* Proc Natl Acad Sci U S A, 2016. **113**(6): p. 1624-9.
225. Locatelli, S.L., et al., *Perifosine and sorafenib combination induces mitochondrial cell death and antitumor effects in NOD/SCID mice with Hodgkin lymphoma cell line xenografts.* Leukemia, 2013. **27**(8): p. 1677-87.
226. Hu, Y., Z. Tian, and C. Zhang, *Natural Killer Cell-Based Immunotherapy for Cancer: Advances and Prospects.* Engineering, 2019. **5**(1): p. 106-114.

227. Liu, E., et al., *Cord blood NK cells engineered to express IL-15 and a CD19-targeted CAR show long-term persistence and potent antitumor activity.* Leukemia, 2017. **32**: p. 520.
228. Steidl, C., et al., *Tumor-associated macrophages and survival in classic Hodgkin's lymphoma.* N Engl J Med, 2010. **362**(10): p. 875-85.
229. Hu, X., et al., *IFN-gamma-primed macrophages exhibit increased CCR2-dependent migration and altered IFN-gamma responses mediated by Stat1.* J Immunol, 2005. **175**(6): p. 3637-47.
230. Frasca, L., et al., *IFN-gamma arms human dendritic cells to perform multiple effector functions.* J Immunol, 2008. **180**(3): p. 1471-81.
231. Castiello, L., et al., *Monocyte-derived DC maturation strategies and related pathways: a transcriptional view.* Cancer Immunol Immunother, 2011. **60**(4): p. 457-66.

Appendix 1. Ethics approval letter

THE UNIVERSITY OF QUEENSLAND
AUSTRALIA

Human Ethics Research Office

Cumbrae-Stewart Building #72
The University of Queensland
St Lucia, QLD 4072

CRICOS PROVIDER NUMBER 00025B

1 December 2016

Prof Maher Gandhi
UQ Diamantina Institute

Dear Prof Gandhi,

Clearance Number: 2014001002 / HREC/07/QPAH/035
Project Title: "Biomarkers as Tools to Assist Clinical Outcome in Patients with Lymphomas - 09/11/2016 - AMENDMENT"

Following administrative review of the human research ethics approval from Metro South Human Research Ethics Committee, I am pleased to advise that, as the University of Queensland's authorised delegate for the University of Queensland's Human Research Ethics Committees A & B, approval is granted for this project.

The approved documents include:

Document	Version	Date
Metro South Human Research Ethics Committee Approval Form	n/a	14/06/2016
Notification of Amendment MSF49 in respect to request for extension of Ethics to 31/12/2019 and update to the personnel: Removal of personnel: Ms Gemma Bond, William Nicol, Kacey O'Rourke and Mrs Pauline Crooks Addition of personnel: Gayathri Thillaiyampalam, Karolina Bednarska, Marina Mathew, Santiyagu Savarimuth Francis, Alexandre Cristino, Yasmin Harvey, Simone Birch, Phil Law (previously added)	n/a	08/06/16

This project has been approved to 31st December 2019.

We would like to take this opportunity to remind you that, should any modifications be made to this project, they will need to be approved by the lead human research ethics committee prior to being forwarded to the University of Queensland's human ethics office for administrative review and approval.

Address. Human Research Ethics Office
Cumbrae-Stewart Building #72
The University of Queensland
St Lucia, QLD 4072
E humanethics@research.uq.edu.au
W www.uq.edu.au/research/integrity-compliance/human-ethics

THE UNIVERSITY OF QUEENSLAND
AUSTRALIA

Human Ethics Research Office

Cumbrae-Stewart Building #72
The University of Queensland
St Lucia, QLD 4072

CRICOS PROVIDER NUMBER 00025B

Please keep a copy of this document for your records.

Yours truly,

Nicole Shively

Nicole Shively
Deputy Director, Research Management Office
Research Ethics Operations
The University of Queensland